GREEN ROOFS AS A CLIMATE CHANGE ADAPTATION STRATEGY IN CITIES: EVALUATION OF GREENHOUSE GAS EMISSIONS, SUBSTRATE TEMPERATURES, AND WATER BALANCE IN NORTHEASTERN ITALY

by

ALEXANDRA M. LUGO-ARROYO

(Under the Direction of Aaron Thompson)

ABSTRACT

This work aimed to evaluate the potential of blue-green roofs (GRs) to serve as a climate change adaptation strategy in cities by evaluating three ecosystem services (reduction of greenhouse gas emissions, cooling of the microclimate, and stormwater management) were affected by design and management factors. We compared daytime GHG emissions (CO_2, CH_4, and N_2O), daily substrate temperatures, and the water balance of 48 GR mesocosms in northeastern Italy during two monitoring periods. Four plant species (*Sedum* spp., cold season grasses, warm season grasses, or wildflowers), two substrate depths (8 or 14 cm), and two irrigation levels (1 or 2 L m^{-2} day^{-1}) were evaluated, for a total of 16 treatments with 3 replicates. Our results suggest that deeper substrate depths provided greater thermal benefits and water retention, plant species was the most important consideration for GHGs and water balance, and irrigation levels were only important during the hottest months.

INDEX WORDS: green roofs, greenhouse, ecosystem services, climate change, carbon dioxide, methane, nitrous oxide, water balance, substrate temperatures

GREEN ROOFS AS A CLIMATE CHANGE ADAPTATION STRATEGY IN CITIES: EVALUATION OF GREENHOUSE GAS EMISSIONS, SUBSTRATE TEMPERATURES, AND WATER BALANCE IN NORTHEASTERN ITALY

by

ALEXANDRA M. LUGO-ARROYO

BS, University of Puerto Rico Mayagüez, 2021

MS, University of Padova, Italy, 2023

A Thesis Submitted to the Graduate Faculty of The University of Georgia in Partial Fulfillment of the Requirements for the Degree

MASTER OF SCIENCE

ATHENS, GEORGIA

2023

GREEN ROOFS AS A CLIMATE CHANGE ADAPTATION STRATEGY IN CITIES:

EVALUATION OF GREENHOUSE GAS EMISSIONS, SUBSTRATE TEMPERATURES,

AND WATER BALANCE IN NORTHEASTERN ITALY

by

ALEXANDRA M. LUGO-ARROYO

Major Professor: Aaron Thompson
Committee: Dorcas Franklin
Maurizio Borin

Electronic Version Approved:

Ron Walcott
Vice Provost for Graduate Education and Dean of the Graduate School
The University of Georgia
December 2023

DEDICATION

I am dedicating this thesis to the two forces that kept me moving forward through the hardest and most difficult parts of this process: my cat, Cristobal, and my friends. More specifically, I would like to dedicate this work to all my life-long friends back home who cheered me on (even though there was an ocean separating us) and to the new friends I made across the world that helped me make my home away from home. Without my cat's ceaseless demands for affection, and my friends' constant encouragement and understanding, I would not have been able to complete this work. Thanks for being my biggest cheerleaders.

ACKNOWLEDGEMENTS

This work was made possible and supported by the Dual MS program in Crop and Soil Sciences with an emphasis on Sustainable Agriculture between the University of Georgia (USA) and the University of Padova (Italy). Foremost, I would like to thank my advisors and mentors—Dr. Carmelo Maucieri, Dr. Aaron Thompson, Dr. Giampaolo Zanin, Dr. Maurizio Borin, and Dr. Dorcas Franklin—for the invaluable academic guidance and support and without whom this thesis would not have been possible. Special thanks to Dr. Nicola dal Ferro, Dr. Miguel Cabrera, and Dr. Francesco Morari for all their help navigating the administrative parts of this degree program. I would also like to extend my sincere thanks to the students and *borsisti*—Michele Zanon, Francesco Morbidini, and Leonardo Ferin—for all their patience and help with my field work. I would also like to recognize the farm staff at the experimental site for their constant availability and guidance.

Lastly, I would be remiss in not mentioning my friends, cat, and family who gave me relentless motivation and moral support throughout this entire process. Many thanks once again to everyone mentioned. Everything that went into completing this work—from the coursework, the proposal, data collection, and putting together this thesis—would not have been possible without each and every person mentioned here.

TABLE OF CONTENTS

APPENDICES

LIST OF TABLES

Page

LIST OF FIGURES

CHAPTER 1

INTRODUCTION

The broad aim of this work was to assess different green roof solutions as a potential climate change adaptation strategy in urban environments. Specifically, our objective was to evaluate how three selected ecosystem services [reduction of greenhouse gas (GHG) emissions (CO_2, CH_4, and N_2O), cooling of the microclimate, and stormwater management] were affected by three selected design and management parameters (plant species choice, substrate depth, and irrigation level) in extensive green roof (GR) mesocosms in northeastern Italy in two different monitoring seasons.

Chapter 2: Literature review

The second chapter of this thesis begins by providing a theoretical background. It begins with a brief overview stating the importance of this study and then goes into detail on the definitions, concepts, and processes, as well as the knowledge gaps, that are relevant to this study.

Chapter 3: Diurnal greenhouse gas emissions and substrate temperatures from blue-green roofs in northeastern Italy during a dry-hot season

This chapter details the results from our dry-hot summer monitoring period from June – September 2022. Daytime GHG emissions and substrate temperatures were measured from 48 GR mesocosms in northeastern Italy during a dry-hot summer season with atypical meteorological conditions with the aim of evaluating how these ecosystem services were affected by plant species choice, substrate depth, and irrigation practices during a period of marked plant-stress.

Chapter 4: Diurnal greenhouse gas emissions, substrate temperatures, and water balance from green roofs in northeastern Italy

This chapter goes over the results from an entire year as our monitoring season (April 2022 to April 2023). Daytime GHG emissions and substrate temperatures were monitored for 48 GR mesocosms in northeastern Italy during a spring, summer, fall, and winter season. Additionally, a simple water balance was calculated for each of the seasons and on a yearly cumulative basis. The aim was to evaluate how these ecosystem services were affected by plant species, substrate depth, and irrigation practices throughout different seasons and meteorological conditions.

Chapter 5: Conclusions

This thesis closes by restating the most important conclusions and insights obtained from our study to determine if the GR solutions evaluated can potentially be a successful climate change adaptation strategy for urban environments.

CHAPTER 2

LITERATURE REVIEW

OVERVIEW

The negative impacts of climate change are made worse by increasing urbanization, where the exponential increase in urban land cover is accompanied by a decrease in natural land cover (Shafique et al., 2018). However, there is an opportunity for science to link climate change adaptation in cities with sustainable urban development through the implementation of green infrastructures (Sanchez Rodriguez et al., 2018; Manso et al., 2021). This is especially relevant in European and other developed countries, given that their urban population has been continuously increasing since 1950 and is projected to more than double in 2030 (Cohen, 2006). Green roofs (GR)—a type of green infrastructure—have been highlighted as having a crucial role in sustainable urban development by providing multiple economic, social, and, most notably, ecosystem services in cities (Francis & Jensen, 2017). This project will focus on evaluating how three selected ecosystem services (reduction of GHGs, cooling of the microclimate, and stormwater management) are affected by plant species choice, substrate depth, and irrigation regime in an experimental green roof mesocosm system at the University of Padova Experimental Farm in Padova, Italy.

BACKGROUND

The central region of the Veneto province in Italy comprises four territorial areas that experienced marked economic and social growth during the Industrial era, collectively known as the “Italian economic locomotive”—namely, Padova, Treviso, Venice, and Vicenza (Fregolent & Tonin, 2016). This pulse of socioeconomic growth was accompanied by an intense period of urbanization and land conversion, with an average increase in developed land of over 130% between 1997 and 2007 and, together with Lombardy, constituting the region with the highest rate of soil loss (increasing 10% between 1950 and 2013) in the country (Fregolent & Tonin, 2016). The city of Padova (Figure 2.1) provides an interesting case study given its mixture of highly urbanized areas intermixed with agricultural landscapes, promoted primarily by the historic and continued cultivation of the Po River Valley in northeastern Italy (Biagi et al., 1993; Borin et al., 1997). Land use conversion—both to agricultural land and urban infrastructure—is projected to be the second most important contributor of greenhouse gas emissions in the future, preceded by fossil fuel combustion, which is also a relevant consequence of urbanization (Grimmond, 2007; Han & Zhu, 2020). Other consequences of urbanization are warmer temperatures, increased flooding and runoff, and increased air pollution (Oberndorfer et al., 2007). Evaluating the possible role green roofs (GRs) might play in mitigating the negative consequences of urbanization and land use change in Padova, Italy and quantifying the ecosystem services they offer could provide data to consider them as a part of climate change adaptation and sustainable urban development plan in this continuously bustling socioeconomic hub. Literature has established that green infrastructure, particularly GRs, could represent a successful strategy to alleviate some of the pressures of climate change in urban environments (Oberndorfer et al., 2007, Francis & Jensen, 2017; Shafique et al., 2018; Langemeyer et al., 2020; Manso et al., 2021). Given that roofs comprise approximately 25% of overall urban surfaces areas, GRs represent a significant opportunity to mitigate climate change in cities without building extensive infrastructure (Nguyen Le Trung et al., 2018).

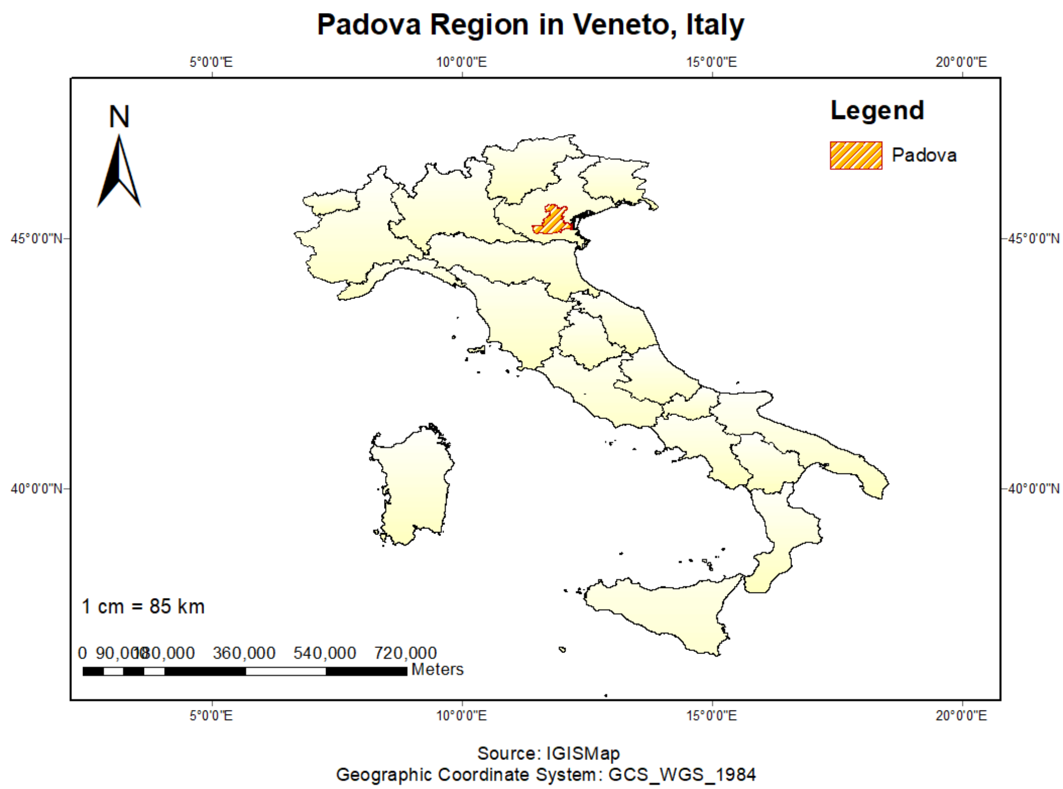

Figure 2.1 Map of Italy with Padova province shown in orange. Map made with ArcMap 10.8.1 software.

Green roofs are also known in the literature as vegetated roofs, cool roofs, eco roofs, roof gardens, or living roofs, and are broadly defined as roofs populated with vegetation and a growing substrate (Shafique et al., 2018). Their components may vary slightly according to national construction standards and availability of materials, but they typically follow the same general structure. According to the Italian design, management, and construction standards for GRs and roof gardens defined in UNI 11235, GRs are comprised of a vegetation layer, a growth substrate layer, a filter fabric, a drainage element, a protection layer, a root barrier, an insulation layer, and a water proofing membrane all layered on top of the roof deck (Nguyen Le Trung et al., 2018).

Green roofs can be further categorized into types, based on the vegetation used, the management intensity, and the depth of the substrate. Green roofs are classified as extensive, semi-intensive, or intensive systems (Table 2.1) (Shafique et al., 2018). The focus of this study will be on extensive GR systems. Their minimal maintenance and the wide variety of succulent and herbaceous species that can be grown on extensive GRs make them an attractive and relatively simple system to implement on a larger scale to move towards sustainably developing urban areas. Green roofs provide a wide variety of economic, social, and ecosystem services that are conducive towards sustainable urban development, such as stormwater management, reduced Urban Heat Island (UHI) effect, decreasing energy consumption of buildings, provision of space for food production, increased biodiversity, decreased air pollution, and increased aesthetic value (Francis & Jensen, 2017; Shafique et al., 2018). Among the ecosystem services, the mitigation of the UHI effect and the potential for stormwater management are particularly emphasized in the literature (Oberndorfer et al., 2007; Alexandri & Jones, 2008; Mechelen et al., 2015; Starry et al., 2016; Sánchez & Reames, 2019; Liu et al., 2021).

Table 2.1: Description of green roof types. Management level, substrate depths (cm), and vegetation types used are shown for each green roof type. Adapted from Langemeyer et al., 2020.

Type	Management level	Substrate depth (cm)	Vegetation type
Intensive	High	30 – 100	Large shrubs and small trees
Semi-intensive	Intermediate	15 – 30	Shrubs, ornamentals, and grasses
Extensive	Low	8 – 15	Succulents, perennial herbs, or grasses

The UHI refers to the warming effect that urban infrastructure has on the climate of a region, causing a significant rise in average temperatures (Alexandri & Jones, 2008). These higher temperatures, or the formation of these *urban heat islands*, are caused by the low albedo of urban infrastructure, which absorbs and re-emits most of the sunlight as heat with little to no reflectance and transfers an appreciable amount to the building, increasing cooling costs (Francis & Jensen, 2017; Sanchez & Reames, 2019). Green roofs can reduce the UHI effect, via evapotranspiration—effectively cooling the surrounding microenvironment—and, to a slightly lesser degree, by using materials in their construction that have a higher albedo than typical roofs (Oberndorfer et al., 2007). Reduction of the UHI effect is well established for GRs. A model-based study of temperature decreases after implementing GRs found that in each of the nine cities distributed globally under consideration there was a decrease in asphalt surface temperature, roof surface temperature, and air temperature (Alexandri & Jones, 2008). The same study found that these thermal benefits were more significant in the hotter regions (Alexandri & Jones, 2008).

Better stormwater management that can decrease flooding potential and runoff in urban landscapes is another well-researched and proven benefit of GR infrastructure. Urbanization increases flooding and runoff mainly because it shifts land area from previously pervious surfaces, such as vegetation and soil cover, to highly impervious and less porous surfaces, such as pavements, rooftops, and sidewalks (Grimmond, 2007; Starry et al., 2016; Liu et al., 2021). This increase in flooding potential and runoff due to an abundance of impervious urban infrastructure is likely to worsen due to the increasing frequency of more intense climatic precipitation events as a consequence of climate change (Liu et al., 2021). In developed cities, rooftops comprise anywhere from 40 – 50% of a city's total impervious surfaces (Shafique et al., 2018). Therefore, rooftops represent an ideal space for the implementation of green infrastructure.

Recently, the potential of GRs to reduce and mitigate GHG emissions from cities has garnered attention (Mihalakakou et al., 2023). It is important to note that GRs can serve as either a source or sink of greenhouse gas emissions, depending primarily on the accumulation and decomposition of organic matter in the system, substrate depth, irrigation, and vegetation characteristics (Halim et al., 2022). They have been hypothesized to counterbalance CO_2 emissions, by acting as potential sink through plant photosynthesis (Ismail et al., 2019; Teemusk et al., 2019). Green roofs can also function as a potential source for CH_4, particularly in extensive systems populated with low evapotranspiration plants, such as *Sedum*, due to the increased in substrate moisture, which can potentially lead to anoxic conditions (Halim et al., 2021). Conversely, they have also been found to function as sink for CH_4 under strongly oxic conditions in very well drained substrates of both shallow and deep depth (Halim et al., 2021). Moreover, fertilization and management of urban green areas have been found to be sources of N_2O and CO_2 (Teemusk et al., 2019). There is a substantial knowledge gap regarding nitrogen cycling in GRs and their substrates. Although little is known about microbial communities in GR substrates, nitrogen losses from these systems may be primarily through conversion of readily retained NH_4^+ to readily leached NO_3^-, which might be prevalent in readily drained systems, such as GRs (Dusza et al., 2017; Mitchell et al., 2018). These highly drained GRs are also conducive towards leaching of dissolved organic carbon (Dusza et al., 2017). N_2O losses have also been measured from urban green spaces following fertilization and management. (Mitchell et al., 2018; Teemusk et al., 2019). N_2O losses can occur from partial or incomplete denitrification, an anoxic process that is favored under the same high moisture conditions as CH_4

production detailed previously (Mitchell et al., 2018). However, the extent of this can vary depending on the consistency of the anaerobic conditions present in the system (Welter & Fisher, 2016). Since GRs are typically fast draining with shallow substrates, losses of greenhouse gases from anaerobic pathways are expected to be minor (Mitchell et al., 2018). The linkage between abiotic and biotic factors of the design and management of GRs (substrate depth, moisture conditions, and plant species) and GHG fluxes (Figure 2.2) highlights the need to close the carbon and nitrogen cycle in green roofs to maximize the ecosystem services of green roofs, maintain their long-term fertility, and avoid the release of eutrophic polluted water (Mitchell et al., 2018).

An important collective benefit of GRs is that they represent an opportunity to both *develop* climate change adaptation through sustainable urban development of new buildings and to *integrate* climate change adaptation trough the retrofitting of existing buildings. However, the benefits and services green roofs can provide depend strongly on their design and management. Important considerations are plant species choice, substrate depth, and irrigation practices (Li & Yeung, 2014; Van Mechelen et al., 2015; Dusza et al., 2017; Teemusk et al., 2019; Halim et al., 2021;).

Substrate depth is known to influence water retention which, in turn, affects GHG emissions, stormwater retention and runoff, and temperature by controlling evapotranspiration (Li & Yeung, 2014; Mitchell et al., 2018; Halim et al., 2022). Although extensive GRs are designed to function under minimal management intensity and to be mainly dependent on precipitation, irrigation may be necessary during the hot summer months or in periods of drought brough by the projected seasonal variations in precipitation driven by climate change (Van Mechelen et al., 2015).

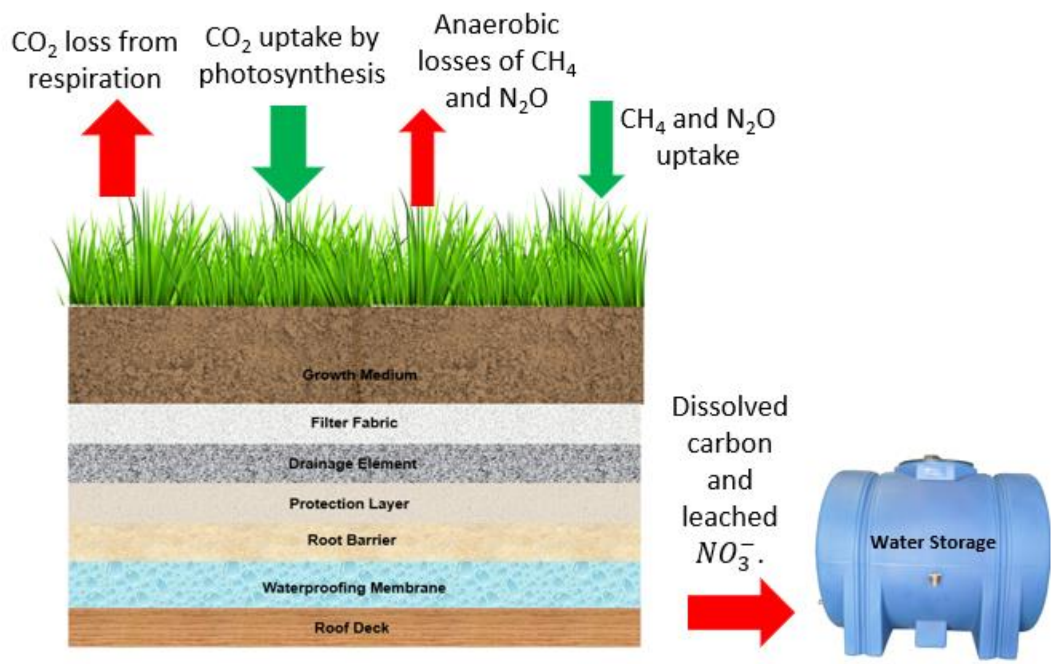

Figure 2.2 Greenhouse gas fluxes under consideration from an extensive green roof system. The arrow thickness represents the relative contribution in terms of magnitude.

Irrigation can affect substrate water retention, as moist substrates retain less water during rain events, decreasing stormwater management, and affecting the remaining ecosystem services by controlling moisture (Van Mechelen et al., 2015). Moreover, irrigation is considered unsustainable in regions with water scarcity and when the water used is potable or saline (Van Mechelen et al., 2015). There is a wide literature gap regarding the use of sustainable irrigation on extensive GR systems. There is also another knowledge gap regarding the effect of plant species on nutrient and water cycles. However, some studies have found that plant species can affect evapotranspiration, and consequently, temperature, and water retention, which in turn affects the remaining ecosystem services (Li & Yeung, 2014; Dusza et al., 2017). Plant characteristics that might influence this are the rooting depth and thickness, and the type of photosynthetic cycling (e.g., CAM, facultative CAM, C3, etc.), both of which directly affect evapotranspiration (Dusza et al., 2017; Halim et al., 2021).

This project will focus on evaluating how the three described ecosystem services associated with GRs—namely, the reduction of GHG emissions (CO_2, CH_4, and N_2O), cooling of the microclimate, and stormwater management—are affected by plant species choice, substrate depth, and irrigation regime during two monitoring periods (a hot dry summer season and an entire year).

REFERENCES

Alexandri, E., & Jones, P. (2008). Temperature decreases in an urban canyon due to green walls and green roofs in diverse climates. *Building and Environment*, *43*(4), 480–493. https://doi.org/10.1016/j.buildenv.2006.10.055

Biagi, P., Cremaschi, M., & Nisbet, R. (1993). Soil exploitation and early agriculture in northern Italy. *The Holocene*, *3*(2), 164–168. https://doi.org/10.1177/095968369300300208

Borin, M., Menini, C., & Sartori, L. (1997). Effects of tillage systems on energy and carbon balance in north-eastern Italy. *Soil and Tillage Research*, *40*(3–4), 209–226. https://doi.org/10.1016/S0167-1987(96)01057-4

Cheng, B., Li, J., Tam, V. W. Y., Yang, M., & Chen, D. (2020). A BIM-LCA Approach for Estimating the Greenhouse Gas Emissions of Large-Scale Public Buildings: A Case Study. *Sustainability*, *12*(2), 685. https://doi.org/10.3390/su12020685

Cohen, B. (2006). Urbanization in developing countries: Current trends, future projections, and key challenges for sustainability. *Technology in Society*, *28*(1–2), 63–80. https://doi.org/10.1016/j.techsoc.2005.10.005

Dusza, Y., Barot, S., Kraepiel, Y., Lata, J.-C., Abbadie, L., & Raynaud, X. (2017). Multifunctionality is affected by interactions between green roof plant species, substrate depth, and substrate type. *Ecology and Evolution*, *7*(7), 2357–2369. https://doi.org/10.1002/ece3.2691

Francis, L. F. M., & Jensen, M. B. (2017). Benefits of green roofs: A systematic review of the evidence for three ecosystem services. *Urban Forestry & Urban Greening*, *28*, 167–176. https://doi.org/10.1016/j.ufug.2017.10.015

Fregolent, L., & Tonin, S. (2016). Local Public Spending and Urban Sprawl: Analysis of This Relationship in the Veneto Region of Italy. *Journal of Urban Planning and Development*, *142*(3), 05016001. https://doi.org/10.1061/(ASCE)UP.1943-5444.0000318

Grimmond, S. (2007). Urbanization and Global Environmental Change: Local Effects of Urban Warming. *The Geographical Journal*, *173*(1), 83–88. http://www.jstor.org/stable/30113496

Halim, M. A., Vantellingen, J., Gorgolewski, A. S., Rose, W. K., Drake, J. A. P., Margolis, L., & Thomas, S. C. (2021). Greenhouse gases and green roofs: Carbon dioxide and methane fluxes in relation to substrate characteristics. *Urban Ecosystems*. https://doi.org/10.1007/s11252-021-01166-8

Heijungs, R., Huppes, G., & Guinée, J. B. (2010). Life cycle assessment and sustainability analysis of products, materials, and technologies. Toward a scientific framework for sustainability life cycle analysis. *Polymer Degradation and Stability*, *95*(3), 422–428. https://doi.org/10.1016/j.polymdegradstab.2009.11.010

Ismail, W. Z. W., Abdullah, M. N., & Asmoni, M. (2019). *A REVIEW OF METHODS FOR ESTIMATING CARBON SEQUESTRATION AT INTENSIVE GREEN ROOFS*. *13*(1), 10.

Langemeyer, J., Wedgwood, D., McPhearson, T., Baró, F., Madsen, A. L., & Barton, D. N. (2020). Creating urban green infrastructure where it is needed – A spatial ecosystem service-based decision analysis of green roofs in Barcelona. *Science of The Total Environment*, *707*, 135487. https://doi.org/10.1016/j.scitotenv.2019.135487

Liu, W., Engel, B. A., & Feng, Q. (2021). Modelling the hydrological responses of green roofs under different substrate designs and rainfall characteristics using a simple water balance model. *Journal of Hydrology*, *602*, 126786. https://doi.org/10.1016/j.jhydrol.2021.126786

Manso, M., Teotónio, I., Silva, C. M., & Cruz, C. O. (2021). Green roof and green wall benefits and costs: A review of the quantitative evidence. *Renewable and Sustainable Energy Reviews*, *135*, 110111. https://doi.org/10.1016/j.rser.2020.110111

Mihalakakou, G., Souliotis, M., Papadaki, M., Menounou, P., Dimopoulos, P., Kolokotsa, D., Paravantis, J. A., Tsangrassoulis, A., Panaras, G., Giannakopoulos, E., & Papaefthimiou, S. (2023). Green roofs as a nature-based solution for improving urban sustainability: Progress and perspectives. *Renewable and Sustainable Energy Reviews*, *180*, 113306. https://doi.org/10.1016/j.rser.2023.113306

Mitchell, M. E., Hamilton, T. L., Uebel-Niemeier, C., Hopfensperger, K. N., & Buffam, I. (2018). Nitrogen cycling players and processes in green roof ecosystems. *Applied Soil Ecology*, *132*, 114–125. https://doi.org/10.1016/j.apsoil.2018.08.007

Nguyen Le Trung, Mahnoor Khawaja, Elahe Beyranvand, Bucchi, D., Akashdeep Singh, & Alam, A. A. (2018). *Approaching a zero-energy building in integrated building design by using green roof and double skin façade as major energy saving strategies*. https://doi.org/10.13140/RG.2.2.10839.32163

Oberndorfer, E., Lundholm, J., Bass, B., Coffman, R. R., Doshi, H., Dunnett, N., Gaffin, S., Köhler, M., Liu, K. K. Y., & Rowe, B. (2007). Green Roofs as Urban Ecosystems: Ecological Structures, Functions, and Services. *BioScience*, *57*(10), 823–833. https://doi.org/10.1641/B571005

Sánchez Rodríguez, R., Ürge-Vorsatz, D., & Barau, A. S. (2018). Sustainable Development Goals and climate change adaptation in cities. *Nature Climate Change*, *8*(3), 181–183. https://doi.org/10.1038/s41558-018-0098-9

Sanchez, L., & Reames, T. G. (2019). Cooling Detroit: A socio-spatial analysis of equity in green roofs as an urban heat island mitigation strategy. *Urban Forestry & Urban Greening*, *44*, 126331. https://doi.org/10.1016/j.ufug.2019.04.014

Shafique, M., Kim, R., & Rafiq, M. (2018). Green roof benefits, opportunities, and challenges – A review. *Renewable and Sustainable Energy Reviews*, *90*, 757–773. https://doi.org/10.1016/j.rser.2018.04.006

Starry, O., Lea-Cox, J., Ristvey, A., & Cohan, S. (2016). Parameterizing a Water-Balance Model for Predicting Stormwater Runoff from Green Roofs. *Journal of Hydrologic Engineering*, *21*(12), 04016046. https://doi.org/10.1061/(ASCE)HE.1943-5584.0001443

Teemusk, A., Kull, A., Kanal, A., & Mander, Ü. (2019). Environmental factors affecting greenhouse gas fluxes of green roofs in temperate zone. *Science of The Total Environment*, *694*, 133699. https://doi.org/10.1016/j.scitotenv.2019.133699

Van Mechelen, C., Dutoit, T., & Hermy, M. (2015). Adapting green roof irrigation practices for a sustainable future: A review. *Sustainable Cities and Society*, *19*, 74–90. https://doi.org/10.1016/j.scs.2015.07.007

Welter, J. R., & Fisher, S. G. (2016). The influence of storm characteristics on hydrological connectivity in intermittent channel networks: Implications for nitrogen transport and denitrification. *Freshwater Biology*, *61*(8), 1214–1227. https://doi.org/10.1111/fwb.12734

CHAPTER 3

DIURNAL GREENHOUSE GAS EMIISIONS AND SUBSTRATE TEMPERATURES FROM BLUE-GREEN ROOFS IN NORTHEASTERN ITALY DURING A DRY-HOT SUMMER SEASON[1]

[1] Lugo-Arroyo et al. Published to Scientia Horticulturae, 10/14/2023.

ABSTRACT

Covering building rooftops with vegetation [green roofs (GR)] holds promise for lowering building temperatures, reducing stormwater runoff, and providing other ecosystem services, but it is unclear how this will impact greenhouse gas (GHG) emissions. The latter may also be influenced by vegetation type, substrate depth, and irrigation regime. We sought to test this by comparing daytime GHG emissions (CO_2, CH_4, and N_2O) and daily substrate temperatures in 48 GR microcosms in northeastern Italy during a dry-hot summer season (June to September 2022). Four vegetation types (*Sedum* spp., cold season grasses, warm season grasses, or wildflowers), two substrate depths (8 or 14 cm), and two irrigation levels (1 or 2 L m^{-2} day^{-1}) were evaluated, for a total of 16 treatments with 3 replicates each. We found that vegetation type had a significant effect on temperature [average temperature of 24.8 ºC (*Sedum* spp.) vs 25.5 ºC (warm season grasses)] and CO_2, CH_4, and N_2O emissions. While all plant species had net CO_2 emissions (median values from 147 to 671 mg m^{-2} h^{-1}) and net N_2O uptake (median values from -0.06 to -0.28 mg mg^{-2} h^{-1}), CH_4 flux had negative values (capture) only in mesocosms with wildflowers (-0.07 mg m^{-2} h^{-1}) and other treatments had median CH_4 emissions of 0.09 mg m^{-2} h^{-1}. Substrate depth significantly affected CO_2 and N_2O fluxes with deeper substrates leading to higher CO_2 emissions (+ 60.7%) and greater N_2O uptake (+ 30.8%). Irrigation level only significantly influenced N_2O fluxes with 2 mm irrigation resulting in higher fluxes (-0.20 mg m^{-2} h^{-1}) than 1 m irrigation (-0.09 mg m^{-2} h^{-1}). Our study suggests that under heat induced plant-stress conditions, GRs can improve N_2O and CH_4 capture but might increase CO_2 emissions, given that the carbon accumulated in the substrate in previous years is being respired and less photosynthesis is occurring. This suggests that plant species choice and substrate depth can significantly alter emissions and are thus important design parameters.

INTRODUCTION

The effects of the ongoing climate change crisis are becoming increasingly visible, with phenomena like land change and urbanization exacerbating challenges such as greenhouse gas (GHG) emissions (carbon dioxide, CO_2; methane, CH_4; nitrous oxide, N_2O), habitat fragmentation, and water scarcity (Van Mechelen et al., 2015; Teemusk et al., 2019; Han & Zhu, 2020). Projections estimate that by 2030 the urban population may rise 60% overall and, in developed countries, reach up to 87%, which will further intensify these negative effects (Shafique et al., 2018; Manso et al., 2021). However, there is an opportunity to link sustainable urban development with climate change adaptation (Manso et al., 2021). Studies have signaled green roofs (GRs)—defined as roofs with substrate and a vegetated surface—as a possible climate change adaptation strategy in cities, highlighting their environmental benefits—or ecosystem services—, such as reduction in GHG emissions, carbon sequestration, thermal regulation, and reduction of the Urban Heat Island (UHI) effect, stormwater management, and increased biodiversity (Oberndorfer et al., 2007; Shafique et al., 2018; Manso et al., 2021; Halim et al., 2022).

Blue-green roofs are GRs that enhance the stormwater management capacity, although they are often used interchangeably (Andanæs et al., 2018). The main difference is that blue-green roofs have an additional storage layer that can temporarily store drained water, while conventional GRs depend solely on the existing retention capacity of the substrate and canopy of the vegetation used (Andanæs et al., 2021). The GRs used in this study are blue-green roofs, but they will be referred throughout as GRs for brevity.

Given that rooftops comprise approximately 25% of overall urban surface areas, GRs represent a significant opportunity to mitigate climate change in cities without building extensive infrastructure (Nguyen Le Trung et al., 2014). In other words, they represent an opportunity to both *implement* climate change adaptation as green infrastructure in new buildings and to *integrate* climate change adaptation through the retrofitting of existing buildings. However, there is a need to quantify these ecosystem services and assess how they are affected by the choice of design, components, and management. Important design elements are plant species choice, substrate depth, and irrigation practices—all of which are interrelated (Li & Yeung, 2014; Van Mechelen et al., 2015; Dusza et al., 2017; Teemusk et al., 2019; Halim et al., 2022).

In this regard, GRs can serve as either a source or sink of GHGs, depending primarily on the accumulation and decomposition of organic matter in the system, substrate depth, irrigation, and plant characteristics (Halim et al., 2022). Green roofs have been hypothesized to counterbalance CO_2 emissions by acting as a potential sink through plant photosynthesis (Mitchell et al., 2018; Teemusk et al., 2019). They may also act as a potential source for CH_4, particularly in extensive systems populated with plant species characterized by low evapotranspiration rates, such as *Sedum* spp., due to increased moisture conditions and, consequently, anoxic conditions (Halim et al., 2022). Conversely, they have also been found to act as a sink for CH_4 under strongly oxic conditions in very well drained substrates of both shallow and deep depth (Halim et al., 2022). Moreover, fertilization and management of urban green areas can be sources of N_2O and CO_2 (Teemusk et al., 2019). Nitrogen losses from these systems may be primarily through conversion of readily retained NH_4^+ to readily leached NO_3^-, which can be prevalent in readily drained systems like GRs (Dusza et al., 2017; Mitchell et al., 2018). Losses of N_2O can also occur from incomplete denitrification, an anoxic process favored under the same high moisture conditions as CH_4 production detailed previously (Mitchell et al., 2018). Given that GRs are typically fast draining with shallow substrates, losses of GHGs from anaerobic pathways are expected to be minor (Mitchell et al., 2018).

As already mentioned, plant species, substrate depth, and irrigation are key elements in affecting the GHGs cycle in GRs. Substrate depth influences water retention which, in turn, affects GHG emissions, stormwater retention and runoff, and temperature by controlling evapotranspiration (Li & Yeung, 2014; Mitchell et al., 2018; Halim et al., 2022). Although extensive GRs are designed to function under minimal management and to be mainly dependent on rainfall, irrigation may be necessary during the hot summer months or in periods of drought (Van Mechelen et al., 2015) Irrigation can affect substrate water retention, as moist substrates retain less water during rain events, decreasing stormwater management, and affecting the remaining ecosystem services by controlling moisture (Van Mechelen et al., 2015). However, the use of irrigation for GRs has ethical considerations and can be considered unsustainable in regions with water scarcity and when the water used is potable or saline (Van Mechelen et al., 2015).

The main objective of this study is to evaluate the effect of plant species choice, substrate depth, and irrigation level on GHG emissions and substrate temperatures of extensive GR systems. For this, we evaluated 48 mesocosms of an extensive GR during a dry summer season—specifically, June to September 2022—in northeast Italy.

MATERIALS AND METHODS

Experimental design

The study site is located at the University of Padova Experimental Farm "L. Toniolo" located in Legnaro, Padova, Italy (45° 21' 5.82" N, 11° 57' 2.44" E). Forty-eight microcosms were studied in a split plot experiment, with irrigation in the whole plot and the vegetation type and substrate treatments used as subplots arranged in a completely randomized 4×2×2 factorial design and three replicates. The experimental variables are: 4 types of vegetation (*Sedum* mixture (Se), cold season grasses (CG), warm season grasses (WG), or wildflowers (WF)), 2 substrate depths (8 cm or 14 cm), and irrigation regime (1 L m^{-2} day^{-1} or 2 L m^{-2} day^{-1}).Sedum treatment was a mix of 9 species/varieties among which the most represented, during the experiment, were *S. album*, *S. kamtschaticum* and *S. reflexum*. ; CG was 10% *Poa pratensis* 'Nublue Plus' and 90% *Festuca arundinacea* 'Rhambler' by weight and WG was *Cynodon dactylon* 'Paul 1'; Wildflower treatment was a mix grass and forb species. The year of establishment, four grass species *(Lolium perenne, Poa pratensis, Festuca rubra* subsp. *rubra* and *Festuca ovina)* and 36 forb species were identified. However, at the time of the experiment, the grasses were the most represented while forbs were strongly reduced (species number reduced to about 12, with *Calendula officinalis*, *Coreopsis grandiflora*, *Coreopsis tinctoria*, *Cota tinctoria*, *Erysimum sp.* and *Leucanthemum vulgaris* being the most represented). The microcosms were established in June 2020 and the monitored period ranged between June and September 2022. Irrigation was manually applied using calibrated watering cans, with of one - two times per week depending on rain events (Table 3.1).

Greenhouse gas (GHG) flux and temperature measurements

The GHG (CO_2, CH_4, and N_2O) fluxes for each mesocosm were measured using a portable Fourier Transform Infrared Spectroscopy (FTIR) analyzer by Gasmet Technologies (The Gasmet^{TM} DX4040) using a static non-stationary chamber technique once a week. A PVC collar (200 mm un diameter) was fitted into the center of each mesocosm one month before monitoring was initiated. A custom-made cylindrical flux chamber was used to measure the GHG fluxes.

Table 3.1 Distribution of water inputs (irrigation and rainfall) received per green roof mesocosm and cumulative rainfall for the sampling season (June to September 2022).

Irrigation level (L m^{-2} day^{-1})	**Total irrigation applied (L m^{-2})**	**Cumulative rainfall (L m^{-2})**	**Total water input (L m^{-2})**
1	72	250.6	322.6
2	144		394.6

It was lined with wind machines on the inside of the cylinder (which served to homogenize the air) and contained a rubber sheathed aperture in the middle, where the portable FTIR analyzer sensor probe was introduced. The cylindrical flux chamber was fitted over the PVC collar in each sampling area. The GHG concentration within the chamber was monitored for 5 minutes per unit, which allowed the values to stabilize, and yielded an average of 10 – 15 measurements per mesocosm.

Sampling began at 8:00 and finished between 13:30 – 14:30. The portable FTIR analyzer was calibrated before and purged after each use with N_2 according to the manufacturer's manual. The data collected was then used to calculate the fluxes, according to the following formula given by Maucieri et al. (2016), where *V* and *A* are the volume and area of the flux chamber, *c* is the concentration measured, and *t* is the time step.

$$\text{GHGs (mg m}^{-2}\text{ h}^{-1}) = \frac{V}{A} \times \frac{dc}{dt}$$

The global warming potential (GWP) of each treatment was calculated with the following formula, using the coefficients established in the IPCC report (2013):

$$\text{GWP (CO}_2\text{ eq. mg m}^{-2}\text{ h}^{-1}) = CO_2 + (CH_4 \times 34) + (N_2O \times 298)$$

Temperature measurements were taken using a handheld soil thermometer at a depth of approximately 3 cm from the bottom of the substrate. Measurements were taken and recorded at a frequency of 3 times per day once a week. The measurements were made in the morning (8:00 – 9:00), at midday (12:00 – 13:00), and in the evening (17:00 – 18:00).

Statistical analysis

All statistical analysis was conducted in R 4.2.2 software. Greenhouse gas data were not normally distributed; therefore, the Kruskal-Wallis test was used to evaluate the median responses of the effect of vegetation species on each GHG flux and GWP and Mann-Whitney test was used to evaluate the effect of substrate depth and irrigation on GHG fluxes and GWP. Given significance, Dunn's test with Bonferroni's adjustment post-hoc comparisons were done. All data were visualized with boxplots. The temperature data were normally distributed. To study the influence of plant species, substrate depth and irrigation level on substrate temperature data, 3-way ANOVA was conducted. Correlations between emissions and GWP with temperatures were assessed using Spearman's Correlation test.

RESULTS

Meteorological data

The meteorological data from June to September 2022 (Figure 3.1a and Figure 3.1b) were obtained from a weather station managed by the Regional Agency for the Prevention and Environmental Protection of Veneto (ARPA Veneto, by its Italian acronym) (https://wwworld.arpa.veneto.it) and located at a distance of 500 m from the experimental site. The average solar radiation for the season was 22.4 MJ m^{-2} and the average wind speed was 1.7 m s^{-1}. The temperature during the season steadily increased, reaching its peak in July, and then started decreasing in September. The minimum average temperatures were 18.4 ºC in June, 19.8 ºC in July, 18.9 ºC in August, and 14.6 ºC in September. The maximum average temperatures were 30.1 ºC in June, 32.0 ºC in July, 30.4 ºC in August, and 24.6 ºC in September. The temperatures overall averaged 24.5 ºC in June, 26.2 ºC in July, 24.6 ºC in August, and 19.3 ºC in September.

Precipitation was afflicted by unusually dry weather. The cumulative rainfall during the sampling season was 250.6 L m^{-2} (Table 3.1), very close to the long term value of 263 L m^{-2} (1994 – 2022). Although the cumulative rainfall averages are similar, the monitoring season was characterized by intense dryness in June and July (Figure 3.2).

(a)

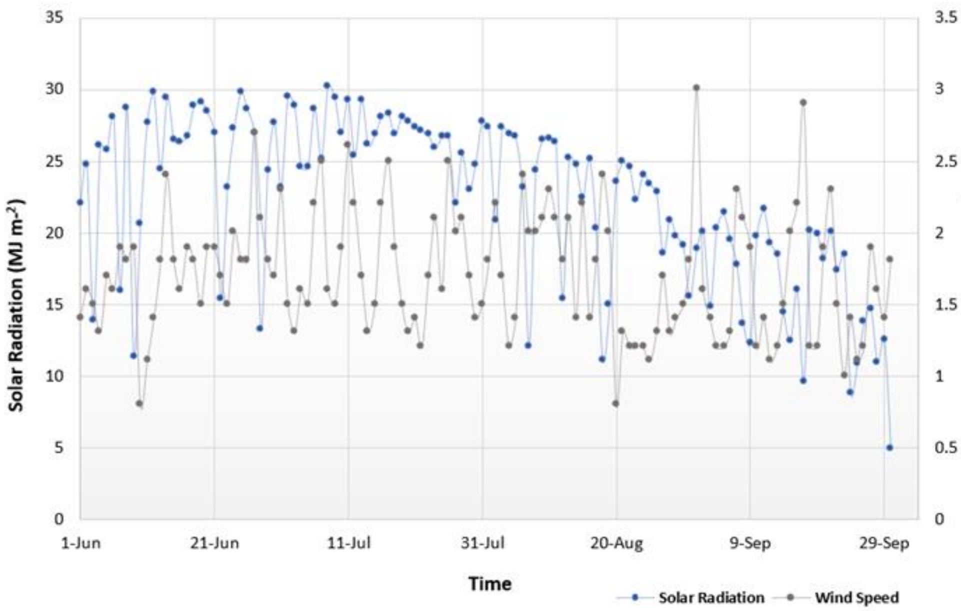

(b)

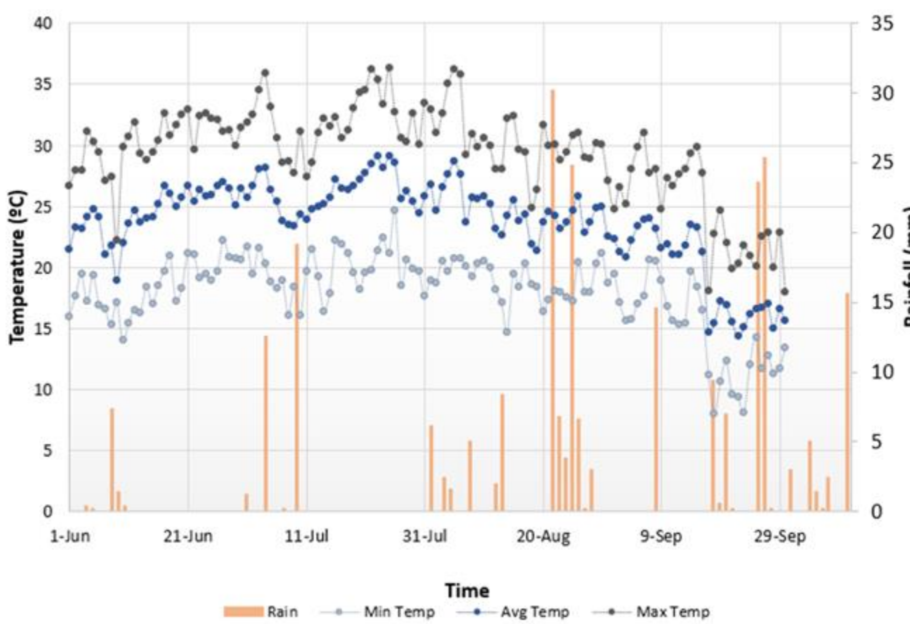

Figure 3.1 (a) Daily average solar radiation (MJ m^{-2}) and wind speed (m s^{-1}) and (b) daily minimum, average, and maximum temperatures (ºC) and daily rainfall (mm) for the summer season (June to September 2022).

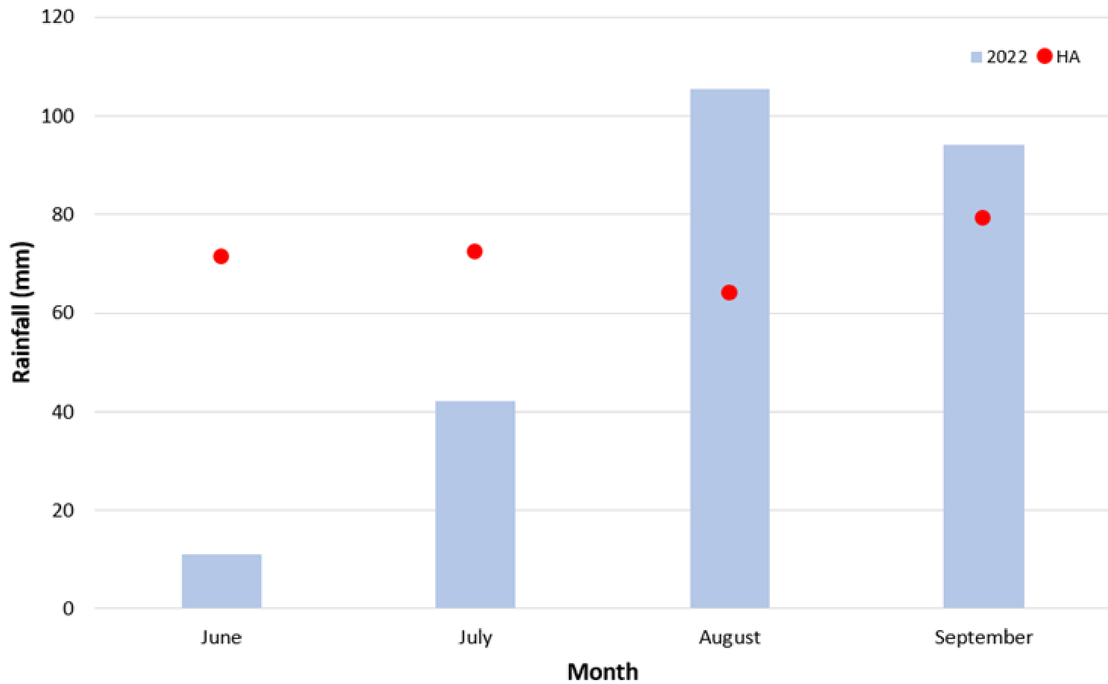

Figure 3.2 Monthly distribution of the rainfall (mm) received in 2022 compared to the historic average (HA) during the summer months.

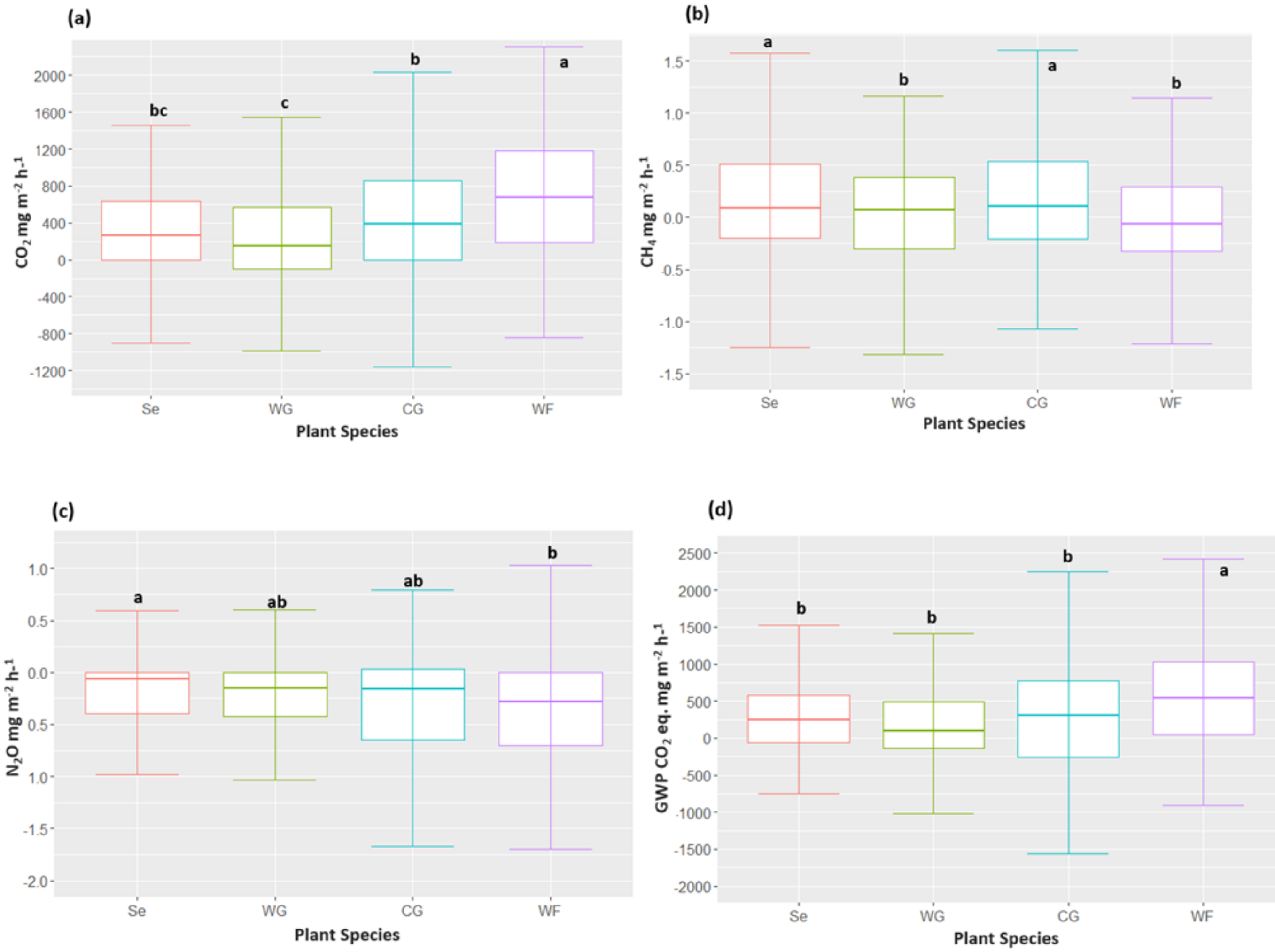

Figure 3.3 Effect of vegetation type (Sedum spp., Se; warm season grasses, WG; cold season grasses, CG; and wildflowers, WF) in green roof microcosms on (a) CO_2, (b) CH_4, (c) N_2O, and (d) global warming potential (GWP) fluxes. Significant differences between treatments are denoted by lowercase letters.

Greenhouse gas (GHG) flux and global warming potential (GWP)

The Kruskal-Wallis test for the effect of vegetation types on GHG fluxes and GWP was significant for all gases—namely, CO_2 ($p < 0.001$), CH_4 ($p < 0.01$), and N_2O ($p < 0.05$), as well as GWP ($p < 0.001$) (Figure 3.3). All vegetation treatments were net emitters of CO_2, with median values of 147 mg m^{-2} day^{-1} (WG), 268 mg m^{-2} day^{-1} (Se), 384 mg m^{-2} day^{-1} (CG), and 671 mg m^{-2} day^{-1} (WF).

Fluxes of CH_4 were low and close to 0, with positive median values for WG (0.068 mg m^{-2} day^{-1}), Se (0.097 mg m^{-2} day^{-1}), and CG (0.11 mg m^{-2} day^{-1}); and a negative median value for WF (-0.66 mg m^{-2} day^{-1}). Only WF differed significantly from Se and CG, with no other significant differences between treatment means. All treatments were net sinks of N_2O, with median values of -0.15 mg m^{-2} day^{-1} (WG), -0.16 mg m^{-2} day^{-1} (CG), -0.28 mg m^{-2} day^{-1} (WF), and -6.34×10^{-2} mg m^{-2} day^{-1} (Se). The only significant differences between treatments were between Se and WF. All treatments had a positive GWP, with median values of 102 CO_2 eq. mg m^{-2} day^{-1} (WG), 241 CO_2 eq. mg m^{-2} day-1 (Se), 314 CO_2 eq. mg m^{-2} day^{-1} (CG), and 564 CO_2 eq. mg m^{-2} day^{-1} (WF). Wildflower (WF) treatment mean was significantly different from all other treatments, while all other pairwise comparisons were not significantly different from one another.

The Mann-Whitney test for the effect of substrate depth on GHG fluxes and GWP was significant for CO_2 ($p < 0.01$) and N_2O ($p < 0.05$) but was not significant for CH_4 or GWP (Figure 3.4). Both substrate depths yielded a net emission of CO_2, with positive median values of 266 mg m^{-2} h^{-1} (8 cm) and 428 mg m^{-2} h^{-1} (14 cm). Notably, both were net sinks of N_2O, with negative median values of -0.13 mg m^{-2} h^{-1} (8 cm) and -0.17 mg m^{-2} h^{-1} (14 cm).

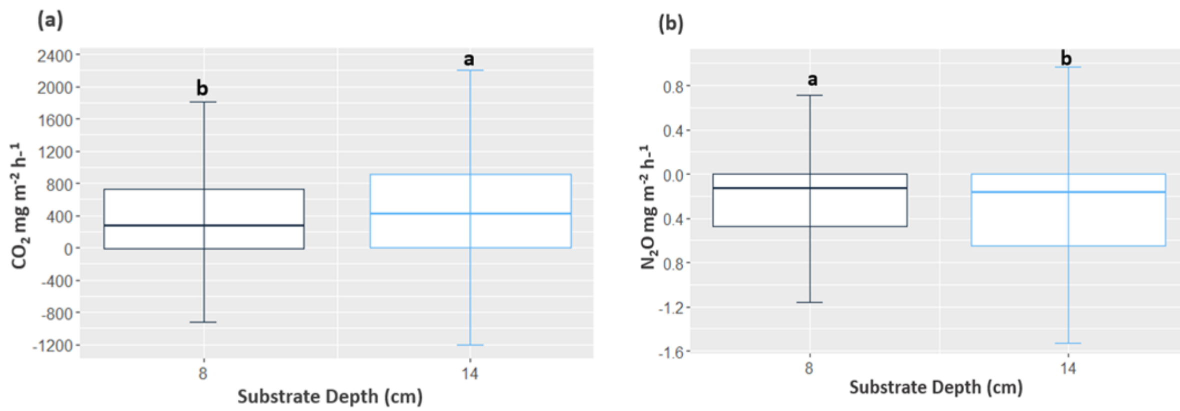

Figure 3.4 Effect of substrate depth (8 or 14 cm) in green roof microcosms on (a) CO_2 and (b) N_2O fluxes. Significant differences between the treatments are denoted by lowercase letters.

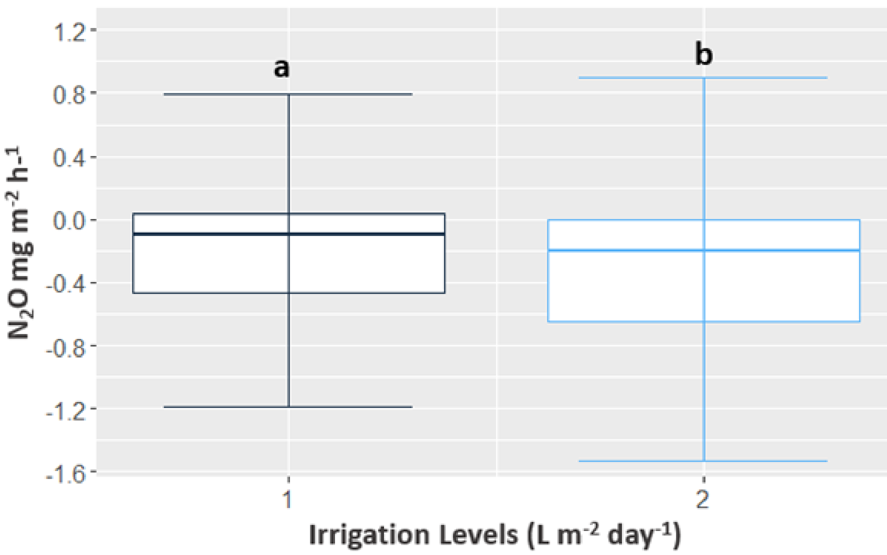

Figure 3.5 Effect of irrigation level (1 or 2 L m^{-2} day^{-1}) in green roof microcosms on N_2O fluxes. Significant differences between the treatments are denoted by lowercase letters.

On average of the substrate depth, CH_4 median flux value was 0.07 mg mg^{-2} h^{-1} and GWP median flux value was 273 CO_2 eq. mg m^{-2} h^{-1}. The Mann-Whitney test for the effect of irrigation on GHG fluxes and GWO yielded significant results only for N_2O ($p < 0.01$) (Figure 3.5). Both irrigation treatments were also net sinks for N_2O, with negative median values -0.09 mg m^{-2} h^{-1} (1 L m^{-2} day^{-1}) and -0.20 L m^{-2} day^{-1} (2 L m^{-2} day^{-1}). On average for irrigation level, median values were 340 mg m^{-2} day^{-1} (CO_2), 0.07 mg m^{-2} h^{-1} (CH_4), 284 CO_2 eq. mg m^{-2} h^{-1} (GWP).

Substrate temperatures

For June data, results showed a significant effect of substrate depth for both morning ($p < 0.001$) and evening temperatures ($p < 0.05$) (Figure 3.6). The average temperatures were 21.8 ºC (8 cm) and 23.1 ºC (14 cm) during the morning and 29.9 ºC (8 cm) and 28.8 ºC (14 cm) during the evening. There were no other significant results. The data for July yielded significant results for substrate depth for morning ($p < 0.001$), midday ($p < 0.01$), and evening ($p < 0.001$) temperatures (Figure 3.6). The average temperatures for each depth were 22.9 ºC (8 cm) and 24.9 ºC (14 cm) in the morning, 26.4 ºC (8 cm) and 27.2 ºC (14 cm) at midday, and 33.0 ºC (8 cm) and 31.4 ºC (14 cm) in the evening. Irrigation treatments were also significant as a control for morning ($p < 0.05$) and midday ($p < 0.01$) temperatures (Figure 3.7). The temperatures for each irrigation level averaged 22.1 ºC (1 L m^{-2} day^{-1}) and 21.8 ºC (2 L m^{-2} day^{-1}) in the morning and 23.7 ºC (1 L m^{-2} day^{-1}) and 24.1 ºC (2 L m^{-2} day^{-1}) at midday. For evening temperatures, the plant species was also significant ($p < 0.001$), with average temperatures of 31.0 ºC (WF), 32.0 ºC (CG), 32.5 ºC (Se), and 33.5 ºC (WG) (Figure 3.8).

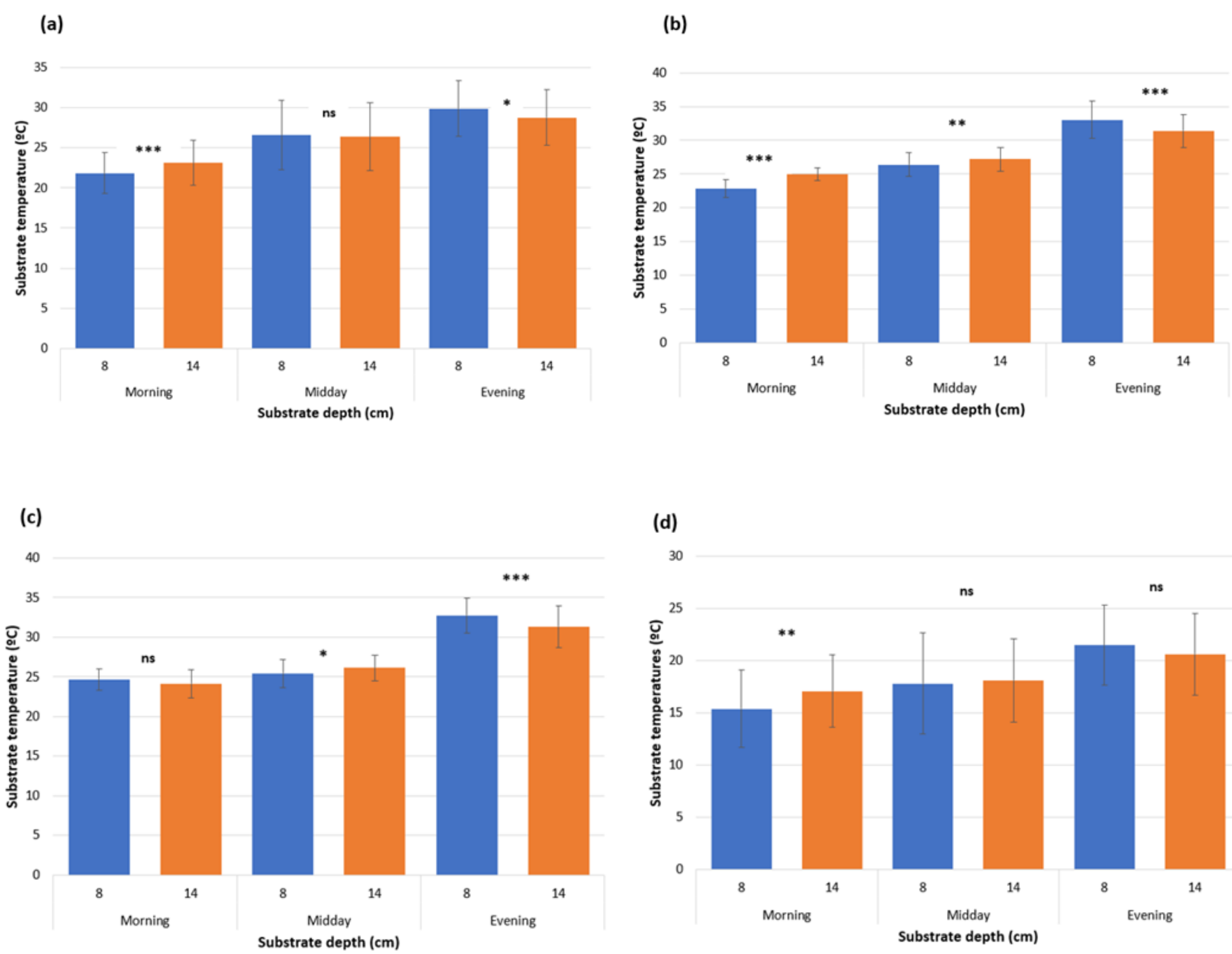

Figure 3.6 Average morning, midday, and evening substrate temperatures by depth (8 or 14 cm) in green roof microcosms in (a) June, (b) July, (c) August, and (d) September. Significant differences between the two substrate depths are denoted with asterisks (* = $p < 0.05$, ** = $p < 0.01$, *** = $p < 0.001$, ns = no significance). Error bars represent the standard deviation of each treatment.

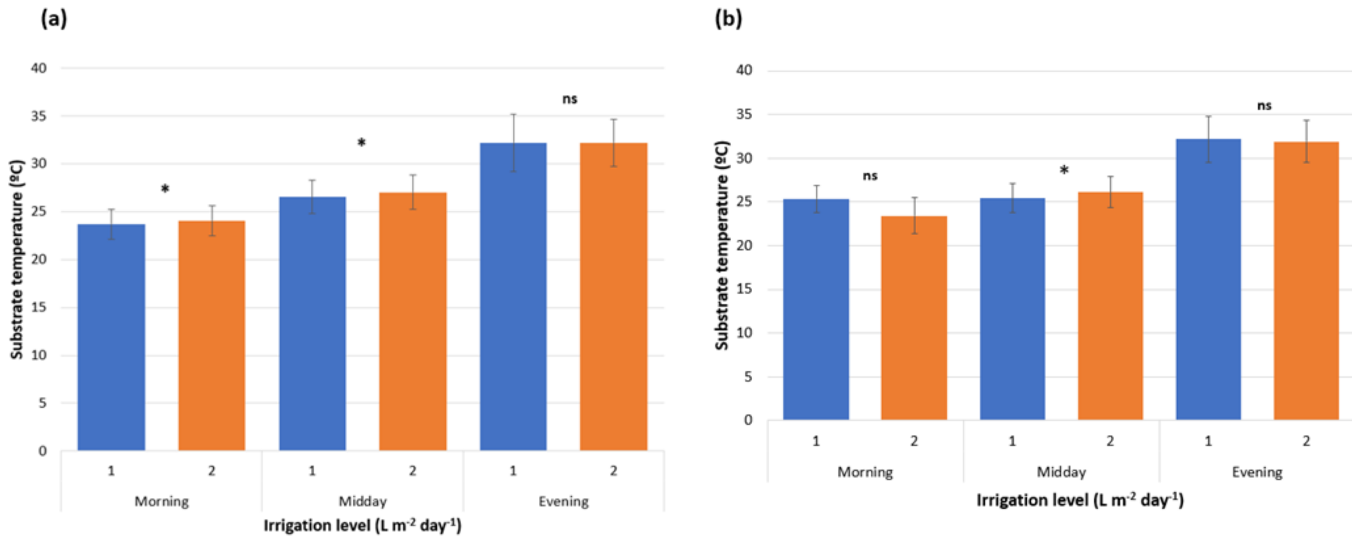

Figure 3.7 Average morning, midday, and evening substrate temperatures by irrigation level (1 or 2 L m^{-2} day^{-1}) in green roof microcosms in (a) July and (b) August. Significant differences between the two substrate depths are denoted with asterisks (* = $p < 0.05$, ** = $p < 0.01$, *** = $p < 0.001$, ns = no significance). Error bars represent the standard deviation of each treatment.

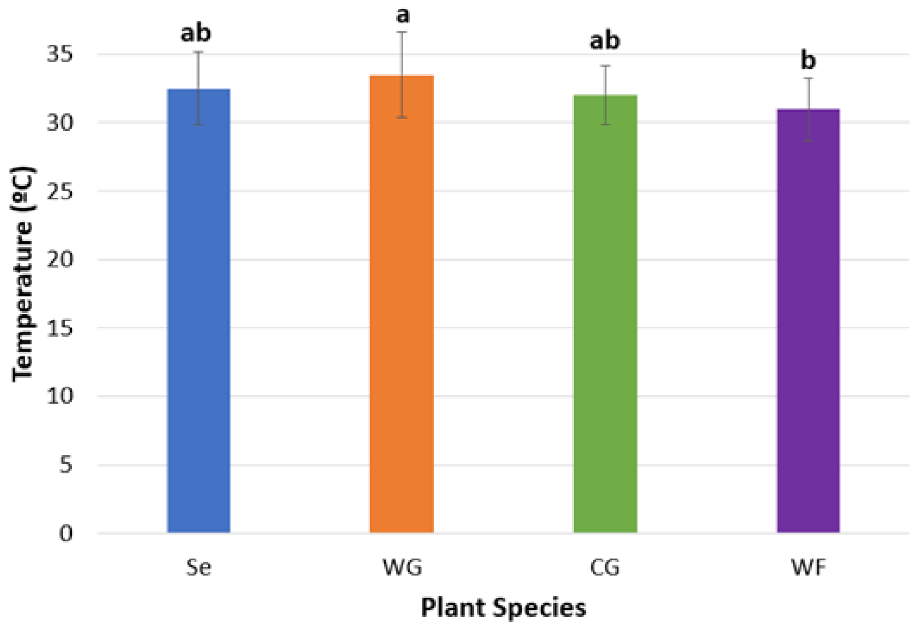

Figure 3.8 Effect of vegetation type (Sedum spp., Se; warm season grasses, WG; cold season grasses, CG; and wildflowers, WF) in green roof microcosms on evening substrate temperatures in July. Significant differences between treatments are denoted by lowercase letters. Error bars represent the standard deviations of each treatment.

Tukey's HSD yielded that only WF differed significantly from WG, with no other significant differences among treatments. There was a significant interaction term between substrate depth and plant species for midday temperatures ($p < 0.01$). For the month of August, there was a significant relationship with substrate depth for midday ($p < 0.05$) and evening ($p < 0.001$) temperatures (Figure 3.6). Average temperatures for each depth in August were 25.4 ºC (8 cm) and 26.1 ºC (14 cm) at midday and 32.7 ºC (8 cm) and 31.3 ºC (14 cm) in the evening. Moreover, irrigation was significant for midday temperatures ($p < 0.05$), with temperatures averaging 25.4 ºC (1 L m^{-2} day^{-1}) and 26.1 ºC (2 L m^{-2} day^{-1}) (Figure 3.7).

In September, the only significant factor was substrate depth for morning temperatures ($p < 0.001$), with average temperatures of 15.4 ºC (8 cm) and 17.1 ºC (14 cm) (Figure 3.6).

The difference between maximum and minimum temperatures observed for each substrate depth was 8.1 ºC (8 cm) and 5.7 ºC (14 cm) in June, 10.2 ºC (8 cm) and 6.5 ºC (14 cm) in July, 8.1 ºC (8 cm) and 7.2 ºC (14 cm) in August, and 6.1 ºC (8 cm) and 3.5 ºC (14 cm) in September.

Correlation between GHG fluxes and GWP with substrate temperatures

Fluxes of CO_2 showed a positive correlation ($p < 0.001$) with both morning (Spearman R = 0.20) and midday (Spearman R = 0.18) substrate temperatures. There was no significant correlation between CO_2 fluxes and evening temperatures. Likewise, CH_4 showed a positive correlation with all temperatures taken—morning (Spearman R = 0.15, $p < 0.01$), midday (Spearman R = 0.16, $p < 0.001$), and evening (Spearman R = 0.16, $p < 0.001$). Also, N_2O fluxes had a strongly significant negative correlation with all temperatures ($p < 0.001$)—morning (Spearman R = -0.28), midday (Spearman R = -0.19), and evening (Spearman R = -0.28). Global warming potential (GWP) yielded no correlation with evening temperatures but a positive correlation with morning (Spearman $R = 0.12$, $p < 0.05$) and midday (Spearman R = 0. 13, $p = 0.0001$) temperatures.

DISCUSSION

During our summer sampling season, hotter than average temperatures and irregular rainfall distribution diminished the role of vegetation for CO_2 uptake through photosynthesis. Due to substantial drought stress, a sizable portion of plant cover in the mesocosms was dying or dead regardless of irrigation applied. This means that respiration was a much greater contributor to CO_2 fluxes across treatments than photosynthesis and, consequently, resulted in higher than expected CO_2 efflux from our green roof (GR) systems.

Effect of vegetation species on greenhouse gas (GHG) fluxes and global warming potential (GWP)

Overall, we measured net CO_2 emission during the daytime, meaning that both autotrophic and heterotrophic respiration were higher than the photosynthesis rate. The high respiration and CO_2 efflux was probably caused by increased degradation of the organic matter that was accumulated during previous seasons. Notably, water stress due to dryness of our monitoring season was not compensated for by the irrigation, which was a limiting factor for plant growth. In particular, we observed a decrease in biomass early on in the summer, and the death of some plants (particularly affected were CG and WF, where 70%, green canopy cover dropped down to 35% and 40%, respectively).This highly influenced the GHG emissions given that the plants were probably releasing the carbon accumulated previously in their biomass instead of sequestering carbon to grow. In spite of this, there were some negative values present in all vegetation types suggesting that, under some conditions and even with stress-induced senescence, GRs can serve as a CO_2 sink. Studies suggest that *Sedum* spp. is among the least effective in reducing GHG emissions and propose grass species as the more effective choice (Shafique et al., 2018). In contrast, our results show that *Sedum* spp. (Se) treatments did not differ significantly from other grass species treatments (WG and CG). Moreover, wildflower (WF) treatments had a significantly higher CO_2 emission rate than *Sedum* spp. Wildflower treatments had an efflux approximately 2.5 times higher than *Sedum* spp. Thus, our results imply that *Sedum* spp. was a significantly smaller net source of CO_2 than WF, in contrast to some studies. However, the higher release values of WF treatments could also be due to the fact that WF mesocosms generally had higher biomass in the previous 2 years of growth (data not shown) and given that the positive values of CO_2 could also be due to the oxidation of organic carbon stored in the substrate with the growth of the plants in previous years, which lead to higher efflux. Conversely, the lower emission of *Sedum* spp. could be due to both their reduced biomass relative to other plant species and their better adaptation to extreme conditions.

The research on the effect of vegetation on GHG fluxes in GRs has mostly been centered around *Sedum* spp. and a limited range of herbaceous and flowering plants and their CO_2 sequestration potential (Charoenkit & Yiemwattana, 2016; Vijayaraghavan, 2016). A review of studies looking at CO_2 sequestration have found that GRs emit less CO_2 than their natural controls (Charoenkit & Yiemwattana, 2016), but another found that—specifically for *Sedum* spp.—carbon sequestration was found to be only a secondary benefit and recommended the use of other species (Agra et al., 2017). This inconsistency with the literature could be due to variations in meteorological variables, substrate characteristics and local differences given that a considerable amount of studies are done in temperate climates typical of North America, whereas our study sire has a humid subtropical climate.

The main controls for CO_2 emissions are signaled to be temperature and moisture (Teemusk et al., 2019). Since plant species was not statistically significant across temperatures in our study, we can assume that moisture played a greater role in regulating CO_2 emissions across treatments. Teemusk et al. (2019) found a negative correlation between CO_2 fluxes and substrate moisture—i.e., less moisture content leads to higher CO_2 fluxes—due to the role of substrate moisture in regulating the organic matter cycle and promoting microbial activity, but only when moisture is the limiting factor to plant growth. Based on this, our dry monitoring season could have intensified the effect of moisture as a control for CO_2 emissions and, in conjunction with overall decreasing plant biomass caused by drought stress, increased CO_2 efflux. It is important to note that the water we supplied during the experimental period was aimed to reduce and not to avoid the drought stress in order to maximize the rainwater retention capacity of GRs.

For CH_4 fluxes, we measured that all treatments served as a net, albeit small, source of CH_4, except for WF which was a net sink. The main control for CH_4 emission or consumption in GRs has been signaled to be moisture—where high moisture and anoxic conditions lead to emissions while low moisture and aerobic conditions are conducive to consumption (Halim et al., 2022). Drought resistant plant species with low evapotranspiration rates, such as *Sedum* spp. and some cold season grasses can have low CO_2 fluxes, but also produce CH_4 due to a retention of high soil moisture (Braun et al., 2022; Halim et al., 2022). This directly supports our results as we found that WF (sink) differed significantly only from *Sedum* spp. and CG (sources). The context of our dry monitoring season could have intensified these results, where, potentially, drought resistant plant species—such as *Sedum* spp. treatments—could have had markedly low evapotranspiration rates.

Interestingly, our study found that for all vegetation types, the microcosms were a net sink of N_2O. Given the dryness of our summer season, this can be attributed to reduced water inputs, leading to a possible limitation of water content in the substrate, which has been highlighted as a main driver for N_2O emissions because it regulates oxygen availability to soil microbes (Bateman & Baggs 2005; Butterbach-Bahal et al., 2013). The difference between N_2O emission or capture in GRs due to biotic factors—such as plant species—is mainly attributed to plant-microbe-substrate interactions and evapotranspiration rates depending on type of photosynthetic cycling, which fall outside of the scope of this study (Dusza et al., 2017; Mitchell et al., 2018; Halim et al., 2022). However, in general, previous studies have signaled that GRs do not have significant fluxes of N_2O (Mitchell et al., 2018; Teemusk et al., 2019). Again, only WF and *Sedum* spp. differed significantly, which follows the same reasoning as with differences between *Sedum* spp. and WF treatment means on CH_4 fluxes, considering the main driver for both fluxes is assumed to be moisture content. Previous studies of CH_4 and N_2O fluxes from GRs have primarily evaluated the effect of substrate characteristics and meteorological parameters on these fluxes, and not vegetation type (Teemusk et al., 2019; Halim et al., 2022).

Our results show that WF had the highest GWP, which can be attributed to the fact that WF microcosms also showed the highest CO_2 flux, which is the largest magnitude that contributes when calculating GWP. Moreover, GWP differing across plant species is due to the fact the vegetation type fluxes differed significantly for each individual flux.

Effect of substrate depth on GHG fluxes and GWP

Our study found that deeper depths resulted in higher CO_2 fluxes, with no significant effect on CH_4. Previous studies have highlighted substrate depth as a major driver for modulating the ecosystem services GRs provide, particularly in reducing GHG emissions through its control on water retention (Li & Yeung, 2014; Dusza et al., 2017; Halim et al., 2022). Halim et al. (2022) found that the main effects of substrate depth were significant for CO_2 fluxes in GRs but not for CH_4 fluxes, where increasing depth resulted in higher CO_2 efflux rates. These studies strengthen our findings. The relationship between carbon cycling and substrate depth has been attributed to the capacity for accumulation of organic matter in the substrate, particularly notable in extensive GR systems over time, where theoretically each 1% substrate organic matter content increase would lead to a net storage of 500 g C m^{-2} for a 10 cm substrate layer (Buffam & Mitchell, 2015). Halim et al. (2022) highlighted that deeper substrate, and higher organic matter, would have a considerably higher CO_2 efflux. Unfortunately, we have no data on organic matter content for these treatments, but our 14 cm-depth microcosms are likely to have higher values because of both higher initial input and higher plant biomass accumulation for their greater support to plant growth.

Remarkably, our study also found that deeper substrate depths corresponded to a larger N_2O sink. There is a general lack of studies looking at the effect of substrate depth on N_2O fluxes. However, the literature highlights that substrate depth can influence the N cycling dynamics of GRs by altering hydrology, substrate moisture and temperature, microbial habitat, and the amount of leachable material (Buffam & Mitchell, 2015). Most N losses from GR systems are thought to be in the form of dissolved N, given that they are typically well drained systems prone to leaching losses—especially in the form of NO_3-N^- (Mitchell et al., 2018). In general, previous studies have found that GRs were net emitters of N_2O, with low fluxes that were highly variable in time (Mitchell, 2017; Mitchell et al., 2018; Teemusk et al., 2019). As cited previously, moisture is a main driver of N_2O emissions. Our dry sampling season could have led to a limitation of water content in the substrate, favoring N_2O uptake over emission.

Although Mitchell et al. (2018) found that their treatments were net emitters, there were some negative values for N_2O fluxes, supporting our finding that GRs can potentially serve as N_2O sinks under certain conditions.

Effect of irrigation on GHG fluxes and GWP

Our study found that irrigation only significantly affected N_2O fluxes, where all treatments were net sinks. There is a lack of studies that focus on the effect of irrigation on N_2O fluxes. However, a study on an urban lawn system—which can be compared to an extensive GR system—found that decreasing moisture resulted in smaller N_2O emissions (Livesley et al., 2010). Our dry season highlighted this condition and resulted in N_2O sinks across all treatments. We found that higher irrigation levels led to greater N_2O sinks, which could indicate that a higher level of irrigation in dry conditions could positively affect this GR ecosystem service.

Effect of substrate depth on substrate temperature

We found that depth was a significant factor for substrate temperatures in all months, although whether the shallow or deeper substrate corresponded to the higher temperature varied. Reyes et al. (2016) and Eksi et al. (2017) both found that increasing depth affected substrate temperature oscillations, where shallower substrate depths observed more extreme minimum and maximum temperatures than deeper substrates. This was especially prevalent during the summer sampling season, where shallower substrate depths dried faster and produced higher temperature fluctuations (Eski et al., 2017). This phenomenon could have been intensified during our particularly dry summer sampling season. Moreover, Nardini et. al. (2012) has signaled GR substrate depths between 12 cm and 20 cm can have a dampening effect over air temperature in the summer, further supporting our results.

Effect of vegetation type and irrigation level on substrate temperature

Vegetation type significantly affected evening temperatures in July but did not cause significant differences for any other time periods. Warm season grasses (WG), the treatment with the highest evening temperature, differed significantly from wildflowers (WF), the treatment with the lowest temperature. A study evaluating evapotranspiration rates on grasses found that, when water is limited, transpiration rates for cool season grasses are higher than for warm season grasses (Romero & Dukes, 2016). However, since a significant effect was only observed in the hottest month during the time of day with the highest temperatures, it could suggest that vegetation type becomes an important driver for substrate temperature beyond a considerably high temperature and water deficit threshold. Literature emphasizes that the magnitude of evapotranspiration influence depends on daily meteorological conditions, such as solar radiation, ambient temperature, relative humidity, and substrate moisture (Hargreaves, 1973; Eksi et al., 2017).

Similarly, a significant effect of irrigation was exerted only during the two hottest months of the season, namely July and August. A review on sustainable irrigation practices for extensive GR systems signaled that in Mediterranean regions with dry, hot summers irrigation is necessary for their success as well as the achievement of thermal regulation benefits (Van Mechelen et al., 2015). This supports our finding that irrigation only significantly affected temperatures during the driest and hottest months, indicating its effect could be triggered only after a certain threshold value. August, although with high levels of precipitation, still had consistent and considerably high temperatures, which could have maintained a dry microclimate in the microcosms. In contrast, September had a similar amount of precipitation to August but with markedly lower temperatures, with no significant effect of irrigation, sustaining our reasoning. Previous studies have demonstrated that, after irrigation, both vegetation and substrate temperature decreased compared to ambient temperature because irrigation increased daily evapotranspiration rates of extensive GRs (Chagolla-Aranda et al., 2017; Kaiser et al., 2019). However, a different study showed that increasing the irrigation supply did not decrease the substrate temperature on days that had over 50 ºC air temperature (Reyes et al., 2016).

Interaction effects between substrate depth and plant species

Interestingly, there was a significant interaction between substrate depth and species in July, for the midday temperatures. A previous study has shown that water retention in GR systems (which can influence evapotranspiration and, consequently, substrate temperatures) was significantly affected by the interaction between vegetation type, substrate depth, and substrate type; however, results were highly variable and yielded complex interactions that could result in trade-off between ecosystem services (Dusza et al., 2017).

Correlation between GHG fluxes and substrate temperatures

CO_2, CH_4, and GWP were positively correlated with substrate temperatures, while N_2O was negatively correlated. Halim et al. (2022) found an exponential relationship between substrate temperatures and CO_2 fluxes and an increase of CH_4 efflux with increasing temperatures. This suggests that substrate temperatures can serve as a predictor of CH_4 and CO_2 fluxes, where higher temperatures will correspond to higher efflux in both cases. But, Teemusk et al. (2019) also found a positive correlation of CO_2 with temperature, but a negative relationship between CH_4 fluxes and temperature. Halim et al. (2022) and Teemusk et al. (2019) both monitored CH_4 fluxes from GR systems with different types of substrates and their correlation with substrate temperatures. Notably, Halim et al. (2022) found that, although the substrates with high organic matter content and no irrigation were a significant CH_4 sink similar to Teemusk et al. (2019), there was significant CH_4 efflux from GRs with substrates low in organic matter and that were previously irrigated. The differences in substrate characteristics and management regime could have led to substrate temperature being a predictor of CH_4 fluxes in our study and Halim et al. (2022), in contrast to Teemusk et al. (2019).

There is also a lack of studies looking at GWP in the context of its relationship to substrate temperatures. However, since CO_2 and CH_4 are, in general, of a higher magnitude than N_2O fluxes in GR systems, we can assume that GWP's correlation with substrate temperatures is mostly determined by the correlation of CO_2 and CH_4 with substrate temperature. Teemusk et al. (2019) found no significant correlation between N_2O fluxes and any meteorological parameters, including temperature. However, the dryness of our monitoring season could have intensified the effect of temperature as a predictor for N_2O fluxes. Potentially, higher temperatures can further decrease the moisture content of the substrate, which is the largest determinant in N_2O uptake or emissions.

Limitations and future research

Our results stem from a very atypical and particular dry summer season relative to normal expected rainfall—specifically, in the first two months of the sampling season—and temperatures of the study area. This means that the replicability of these results is ascribed to these conditions. Further research measuring evapotranspiration rates across vegetation species, substrate moisture content, and organic matter content can serve to better elucidate interactions between the biotic and abiotic components of GRs and their effect on ecosystem services.

CONCLUSIONS

Although our results are circumscribed to one atypical summer season, they suggest that GRs' ecosystem services are significantly affected by meteorological conditions, vegetation type, substrate depth, and irrigation regime. Surprisingly we found that GRs had a positive GWP due to GRs acting as a significant CO_2 source and, albeit smaller, sinks of CH_4 and N_2O. This behavior was mainly due to the atypical summer meteorological conditions that determined a dramatic plants stress, resulting in the death of some plant. Sedum species, the species most resistant to both thermal and water stress among those tested, resulted in the lowest CO_2 fluxes and GWP. Although wildflower (WF) treatments outperformed *Sedum* spp. in N_2O and CH_4 capture, it had more than double the CO_2 emissions. Higher irrigation levels, during the monitored atypical summer season increased the GR's ability to function as a N_2O sink. With regards to substrate depth, deeper substrate depths, during an atypical summer season emitted more CO_2 due to the major stock accumulated in the previous years. Similarly, substrate depth was the main control for substrate temperatures, where deeper depths can provide more thermal insulation. However, irrigation level and vegetation type were significant controls only in the hottest and driest months of the monitoring season. This means that these parameters can be useful considerations in dry, hot climates in order to maximize the thermal benefits from GRs.

Overall, these factors can lead to complex interactions that can result in trade-offs between ecosystem services. To deepen our knowledge on GRs as a nature-based solution for climate change adaptation in cities, the effect of seasonality should be assessed to evaluate how GRs perform and how design and management parameters affect this performance throughout an entire year. The design, component choice, and management practices of GRs for optimization of their potential ecosystem services needs to be counterbalanced with practical considerations, such as building weight limits, relative costs, management intensity, and—in the case of irrigation regime—ethical concerns in water-scarce regions. GRs can serve as a potential strategy for climate change mitigation in cities, however, their application needs to be guided by the scientific considerations that govern the ecosystem services—and their interactions with biotic and abiotic factors of GRs—that they are designed to provide.

REFERENCES

Agra, H., Klein, T., Vasl, A., Shalom, H., Kadas, G., & Blaustein, L. (2017). Sedum-dominated green-roofs in a semi-arid region increase CO_2 concentrations during the dry season. *Science of The Total Environment, 584–585*, 1147–1151. https://doi.org/10.1016/j.scitotenv.2017.01.176

Andenæs, E., Kvande, T., Muthanna, T., & Lohne, J. (2018). Performance of Blue-Green Roofs in Cold Climates: A Scoping Review. *Buildings, 8*(4), 55. https://doi.org/10.3390/buildings8040055

Andenæs, E., Time, B., Muthanna, T., Asphaug, S., & Kvande, T. (2021). Risk Reduction Framework for Blue-Green Roofs. *Buildings, 11*(5), 185. https://doi.org/10.3390/buildings11050185

Bateman, E. J., & Baggs, E. M. (2005). Contributions of nitrification and denitrification to N_2O emissions from soils at different water-filled pore space. *Biology and Fertility of Soils, 41*(6), 379–388. https://doi.org/10.1007/s00374-005-0858-3

Braun, R. C., Bremer, D. J., Ebdon, J. S., Fry, J. D., & Patton, A. J. (2022). Review of cool-season turfgrass water use and requirements: II. Responses to drought stress. *Crop Science, 62*(5), 1685-1701.

Buffam, I., & Mitchell, M. E. (2015). Nutrient cycling in green roof ecosystems. *Green roof ecosystems*, 107-137.

Butterbach-Bahl, K., Baggs, E. M., Dannenmann, M., Kiese, R., & Zechmeister-Boltenstern, S. (2013). Nitrous oxide emissions from soils: How well do we understand the processes and their controls? *Philosophical Transactions of the Royal Society B: Biological Sciences, 368*(1621), 20130122. https://doi.org/10.1098/rstb.2013.0122

Chagolla-Aranda, M. A., Simá, E., Xamán, J., Álvarez, G., Hernández-Pérez, I., & Téllez-Velázquez, E. (2017). Effect of irrigation on the experimental thermal performance of a green roof in a semi-warm climate in Mexico. *Energy and Buildings*, *154*, 232–243. https://doi.org/10.1016/j.enbuild.2017.08.082

Charoenkit, S., & Yiemwattana, S. (2016). Living walls and their contribution to improved thermal comfort and carbon emission reduction: A review. *Building and Environment*, *105*, 82–94. https://doi.org/10.1016/j.buildenv.2016.05.031

Dusza, Y., Barot, S., Kraepiel, Y., Lata, J.-C., Abbadie, L., & Raynaud, X. (2017). Multifunctionality is affected by interactions between green roof plant species, substrate depth, and substrate type. *Ecology and Evolution*, *7*(7), 2357–2369. https://doi.org/10.1002/ece3.2691

Eksi, M., Rowe, D. B., Wichman, I. S., & Andresen, J. A. (2017). Effect of substrate depth, vegetation type, and season on green roof thermal properties. *Energy and Buildings*, *145*, 174-187.

Halim, M. A., Vantellingen, J., Gorgolewski, A. S., Rose, W. K., Drake, J. A. P., Margolis, L., & Thomas, S. C. (2022). Greenhouse gases and green roofs: Carbon dioxide and methane fluxes in relation to substrate characteristics. *Urban Ecosystems*. https://doi.org/10.1007/s11252-021-01166-8

Han, M., & Zhu, B. (2020). Changes in soil greenhouse gas fluxes by land use change from primary forest. *Global Change Biology*, *26*(4), 2656–2667. https://doi.org/10.1111/gcb.14993

IPCC (2013). Climate Change 2013: The physical science basis. Contribution of Working Group I to the Fifth Assessment Report. Intergovernmental Panel on Climate Change [Stocker, T.F., D. Qin, G.-K. Plattner, M. Tignor, S.K. Allen, J. Boschung, A. Nauels, Y. Xia, V. Bex and P.M. Midgley (eds.)]. Cambridge University Press, Cambridge, United Kingdom and New York, NY, USA, 1535 pp.

Kaiser, D., Köhler, M., Schmidt, M., & Wolff, F. (2019). Increasing Evapotranspiration on Extensive Green Roofs by Changing Substrate Depths, Construction, and Additional Irrigation. *Buildings*, *9*(7), 173. https://doi.org/10.3390/buildings9070173

Le Trung, N., Khawaja, M., Beyranvand, E., Bucchi, D., Singh, A.,& Alam, A.A. (2018). *Approaching a nearly zero-energy building in integrated building design by using green roof and double skin façade as major energy saving strategies*: 1-12. https://doi.org/10.13140/RG.2.2.10839.32163

Li, W. C., & Yeung, K. K. A. (2014). A comprehensive study of green roof performance from environmental perspective. *International Journal of Sustainable Built Environment*, *3*(1), 127–134. https://doi.org/10.1016/j.ijsbe.2014.05.001

Livesley, S. J., Dougherty, B. J., Smith, A. J., Navaud, D., Wylie, L. J., & Arndt, S. K. (2010). Soil-atmosphere exchange of carbon dioxide, methane and nitrous oxide in urban garden systems: Impact of irrigation, fertilizer and mulch. *Urban Ecosystems*, *13*(3), 273–293. https://doi.org/10.1007/s11252-009-0119-6

Manso, M., Teotónio, I., Silva, C. M., & Cruz, C. O. (2021). Green roof and green wall benefits and costs: A review of the quantitative evidence. *Renewable and Sustainable Energy Reviews*, *135*, 110111. https://doi.org/10.1016/j.rser.2020.110111

Maucieri, C., Mietto, A., Barbera, A. C., & Borin, M. (2016). Treatment performance and greenhouse gas emission of a pilot hybrid constructed wetland system treating digestate liquid fraction. *Ecological Engineering*, *94*, 406–417. https://doi.org/10.1016/j.ecoleng.2016.05.062

Mitchell, M. E. (2017). *Nutrient Cycling Dynamics and Succession in Green Roof Ecosystems* (Doctoral dissertation, University of Cincinnati). https://search.proquest.com/docview/2124444033/abstract/E4AA6731BEB94BFEPQ/1.

Mitchell, M. E., Hamilton, T. L., Uebel-Niemeier, C., Hopfensperger, K. N., & Buffam, I. (2018). Nitrogen cycling players and processes in green roof ecosystems. *Applied Soil Ecology*, *132*, 114–125. https://doi.org/10.1016/j.apsoil.2018.08.007

Nardini, A., Andri, S., & Crasso, M. (2012). Influence of substrate depth and vegetation type on temperature and water runoff mitigation by extensive green roofs: Shrubs versus herbaceous plants. *Urban Ecosystems*, *15*(3), 697–708. https://doi.org/10.1007/s11252-011-0220-5

Oberndorfer, E., Lundholm, J., Bass, B., Coffman, R. R., Doshi, H., Dunnett, N., Gaffin, S., Köhler, M., Liu, K. K. Y., & Rowe, B. (2007). Green Roofs as Urban Ecosystems: Ecological Structures, Functions, and Services. *BioScience*, *57*(10), 823–833. https://doi.org/10.1641/B571005

Reyes, R., Bustamante, W., Gironás, J., Pastén, P. A., Rojas, V., Suárez, F., ... & Bonilla, C. A. (2016). Effect of substrate depth and roof layers on green roof temperature and water requirements in a semi-arid climate. *Ecological engineering*, *97*, 624-632.

Romero, C. C., & Dukes, M. D. (2016). Review of Turfgrass Evapotranspiration and Crop Coefficients. *Transactions of the ASABE*, *59*(1), 207–223. https://doi.org/10.13031/trans.59.11180

Shafique, M., Kim, R., & Rafiq, M. (2018). Green roof benefits, opportunities and challenges – A review. *Renewable and Sustainable Energy Reviews*, *90*, 757–773. https://doi.org/10.1016/j.rser.2018.04.006

Teemusk, A., Kull, A., Kanal, A., & Mander, Ü. (2019). Environmental factors affecting greenhouse gas fluxes of green roofs in temperate zone. *Science of The Total Environment*, *694*, 133699. https://doi.org/10.1016/j.scitotenv.2019.133699

Van Mechelen, C., Dutoit, T., & Hermy, M. (2015). Adapting green roof irrigation practices for a sustainable future: A review. *Sustainable Cities and Society*, *19*, 74–90. https://doi.org/10.1016/j.scs.2015.07.007

Vijayaraghavan, K. (2016). Green roofs: A critical review on the role of components, benefits, limitations and trends. *Renewable and Sustainable Energy Reviews*, *57*, 740–752. https://doi.org/10.1016/j.rser.2015.12.119

CHAPTER 4

DIURNAL GREENHOUSE GAS EMISSIONS, SUBSTRATE TEMPERATURES, AND WATER BALANCE FROM GREEN ROOFS IN NORTHEASTERN ITALY[2]

[2] Lugo-Arroyo et al. Will be submitted to *Science of the Total Environment*.

ABSTRACT

Covering building rooftops with vegetation [green roofs (GR)] holds promise as a climate change adaptation strategy in cities through the provision of ecosystem services, such as, lowering building temperatures, reducing stormwater runoff, and reducing greenhouse gas (GHG) emissions. However, there is a need for more studies that quantify these potential ecosystem services and evaluate how they are impacted by design and management practices. This work aims to evaluate three selected ecosystem services (reduction of GHGs, cooling of the microclimate, and stormwater management) and how they are affected by abiotic and biotic components of their design and management—i.e., vegetation type, substrate depth, and irrigation regime. We sought to test this by comparing daytime GHG emissions (i.e., CO_2, CH_4, and N_2O), daily substrate temperatures, and the water balance of 48 GR mesocosms in north-eastern Italy during an entire year. Four plant species (*Sedum* spp., cold season grasses, warm season grasses, or wildflowers), two substrate depths (8 or 14 cm), and two irrigation levels during summer season (1 or 2 L m^{-2} day^{-1}) were evaluated, for a total of 16 treatments with 3 replicates. We found that plant species significantly impacted CO_2 emissions in all seasons and treatments, with the GRs serving as small CO_2 sources in the spring season, large sources in a dry summer season, and modest CO_2 sinks in the fall and winter. Deeper substrate depth led to about 30 times higher CO_2 emissions in the spring compared with our shallower substrate treatments. Substrate depth impacted N_2O fluxes only in the summer, where deeper depths were almost two times greater N_2O sinks than shallower substrate treatments. Irrigation level during the summer season most notably affected CO_2 emissions only in the following winter season, although there was a small effect on CH_4 fluxes in the fall and on N_2O fluxes in the summer. For the water balance, we found that both plant species and substrate depth mattered for seasonal

effects. The fall season had the greatest water outputs, and, in all seasons, *Sedum* spp. had the least stormwater retention capacity, with values various orders of magnitude higher than the other plant species treatments. Deeper substrate depth led to higher water retention in all seasons. Substrate temperatures were significantly affected by substrate depth in all seasons. Deeper substrate depths had 2 – 3 ºC less temperature oscillation than the shallower substrate depths. The combined effect of irrigation level and substrate depth was significant only during the summer season. Our results suggest that GRs can aid in capturing CO_2 in the colder months (due to the particular meteorological conditions during the experimental year), providing thermal insulation benefits, and in stormwater management year round.

INTRODUCTION

Blue-green roofs, defined as vegetated rooftops with an additional layer for the temporary storage of rainwater, are a potential strategy for coupling urban climate change adaptation with sustainable development (Andanæs et al., 2018; Manso et al., 2021). Increasing rates of urbanization and the current climate change crisis are accelerating greenhouse gas (GHG) emissions—namely, carbon dioxide (CO_2), methane (CH_4), and nitrous oxide (N_2O)—increasing temperatures, and water scarcity (Van Mechelen et al., 2015; Teemusk et al., 2019; Han & Zhu, 2020). Blue-green roofs (abbreviated as GRs throughout this work) provide an abundance of ecosystem services, including carbon sequestration and capture of GHGs, thermal benefits, and increased stormwater management that aid in mitigating these issues in urban environments (Oberndorfer et al., 2007; Shafique et al., 2018; Manso et al., 2021; Halim et al., 2022). In particular, the aforementioned ecosystem services can aid in closing nutrient, energy, and water cycles in cities while providing ancillary benefits such as improving landscape connectivity, increasing biodiversity, improving water quality, and increasing the longevity of conventional roof membranes (Oberndorfer et al., 2007).

The thermal benefits of GRs are well-researched. GRs can provide both increased comfort and reduced energy costs by cooling the microclimate. The cooling effect of GRs is attributed to the combined effect of plant evapotranspiration, shading by the plant canopy, thermal insulation of the substrate-drainage layers, and an increased albedo when compared to conventional rooftops that leads to an overall reduction in absorbed solar radiation (Jim & Peng, 2012; Shafique et al., 2018). When GRs are upscaled, these thermal benefits can translate into a reduction of the Urban Heat Island (UHI) effect in cities (Sanchez & Reames, 2019). Although these thermal benefits have been documented in both cold and hot regions, studies have found that the effects are more marked in hotter regions and those with high seasonal variability (Shafique et al., 2018). Factors that affect GR's thermal benefits, particularly in terms of energy savings include the GRs' substrate characteristics, meteorological parameters, plant type, and design insulation (Shafique et al., 2018).

On the other hand, less quantified ecosystem services of GRs include carbon sequestration and capture of GHGs. GRs can influence CO_2 emissions both indirectly and directly. Directly, vegetated rooftops capture carbon through photosynthesis and store carbon and other nutrients in the substrate layer as organic matter (Shafique et al., 2020). Indirectly, vegetated rooftops reduce the building temperature and associated energy costs which, consequently, reduces the burning of fossil fuels (Shafique et al., 2020). However, GRs can function as either a sink or source of GHGs besides CO_2. Whether GRs are a source or sink of GHGs depends on the accumulation and decomposition of organic matter in the system, substrate depth, irrigation, vegetation characteristics (Halim et al., 2022) and meteorological conditions (Lugo-Arroyo et al., 2023). For both CH_4 and N_2O, the predominant loss pathways occur during anaerobic metabolism (Dusza et al., 2017; Mitchell et al., 2018). Studies have signaled potential losses of CH_4 from extensive GR systems populated with low evapotranspiration plants, such as *Sedum* spp., that lead to higher substrate moisture (Halim et al.,2022). Similarly, these higher substrate moisture conditions can also cause higher N_2O losses through denitrification. However, since most GRs are designed to promote oxic conditions and readily drained, losses from anaerobic pathways are expected to be minor (Mitchell et al., 2018). Aerobic metabolism can also drive N_2O losses during nitrification, where N_2O and CO_2 often increase following fertilization and certain management activities (Dusza et al., 2017; Mitchell et al., 2018; Teemusk et al., 2019).

Stormwater management is another well-known, but less quantified ecosystem service of GR systems. At a building-scale, GRs can reduce the runoff volume at an annual scale and delay the peak runoff flow for an individual rain event (Versini et al., 2020). This is important because delaying peak runoff ultimately results in a reduction of the rainwater that reaches conventional stormwater management infrastructure (Versini et al., 2020). Blue-green roofs specifically serve to both *retain*—or reduce the water flow—and to *detain*—or temporarily store the water (Versini et al., 2020). Together, the vegetation, substrate, and additional water storage layer can capture water from rain events and, thus reduce the incidence of flash flooding in urban areas with impermeable soils (Ouldboukhitine et al., 2012; Shafique et al., 2018). The stormwater management potential of GRs can be measured using a simplified water balance model, which considers water inputs (such as precipitation and irrigation) and the drainage water as outputs (Versini et al., 2020). The factors that can influence water retention capacity of GRs are plant species, substrate characteristics (depth and porosity), antecedent moisture conditions, and rainfall volume (Shafique et al., 2018; Versini et al., 2020).

These potential ecosystem services of GRs are affected by both biotic and abiotic design and management practices, such as substrate depth, plant species choice, and irrigation regime. To quantify the impact design and management practices have on potential ecosystem services, we measured GHG emissions, substrate temperatures, and the water balance of 48 extensive GR mesocosms in northeastern Italy during an entire year. Moreover, given a lack of information of GHG fluxes and water balance from GR systems, this work aims to provide data towards bridging this literature gap, solidifying our understanding of GRs as a potential climate change mitigation strategy, and better guiding the decisions of policymakers.

MATERIALS AND METHODS

This study was conducted in the University of Padova Experimental Farm "L. Toniolo" located in Legnaro, Padova, Italy (45° 21' 5.82" N, 11° 57' 2.44" E). Data was collected for an entire year, starting April 2022 and until April 2023. The experiment consisted of 48 GR mesocosms in a split-plot design experiment, where each treatment had 3 replicates each. Summer irrigation levels were used as the whole plot treatments, plant species and substrate depths as the sublot treatments. The subplots were arranged in a completely randomized 4x2 factorial design. The plant species treatments were either *Sedum* mixture (Se), cold season grasses (CG; 10% *Poa pratensis* 'Nublue Plus' and 90% *Festuca arundinacea* 'Rhambler' by weight), warm season grasses (WG; *Cynodon dactylon* 'Paul 1'), and wildflower mix (WF). Summer irrigation level applied was 1 L m^{-2} day^{-1} or 2 L m^{-2} day^{-1}. The substrate used for all treatments was Volcaflor Extensive™ by Europomice. Irrigation frequency varied depending on rain events (Table 1). Meteorological data were obtained from the local weather station (500 m from experimental site) managed by the Regional Agency for the Prevention and Environmental Protection of Veneto (ARPA Veneto, by its Italian abbreviation) (https://wwwold.arpa.veneto.it/).

Greenhouse gas (GHG) concentration measurements and flux calculations

Greenhouse gas (CO_2, CH_4, and N_2O) fluxes were measured using a portable Fourier Transform Infrared Spectroscopy (FTIR) analyzer by Gasmet Technologies (The Gasmet™ DX4040) with a static non-stationary chamber technique. The portable FTIR was calibrated before and cleaned after each use with N_2 according to the manufacturer's manual. GHG measurements were taken once a week during the entire monitoring period between 8:00 – 14:30.

Table 4.1 Distribution of water inputs (irrigation and rainfall) received per green roof mesocosm and cumulative rainfall for each sampling period (2022 – 2023).

Irrigation level (L m^{-2} day^{-1})	**Season**	**Total irrigation applied (L m^{-2})**	**Cumulative Rainfall (L m^{-2})**	**Total water input (L m^{-2})**
1	Spring	0	115.2	115.2
	Summer	48	225.0	273.0
	Fall	0	200.2	200.2
	Winter	0	68.4	68.4
2	Spring	0	115.2	115.2
	Summer	96	225.0	321.0
	Fall	0	200.2	200.2
	Winter	0	68.4	68.4

A custom-made cylindrical flux chamber was fitted over a PVC collar (200 mm in diameter) to measure the GHG concentrations. The flux chamber had a rubber sheathed aperture for the insertion of the sensor probe and was lined with wind machines to homogenize the air. The concentration data collected was then used to calculate the fluxes following Maucieri et. al. (2016):

$$\text{GHGs (mg m}^{-2}\text{ h}^{-1}) = \frac{V}{A} \times \frac{dc}{dt} \quad (1)$$

Here, *V* and *A* are the volume and area of the flux chamber, *c* is the concentration measured, and *t* is the time step.

Using the coefficients given in IPCC (2013), the global warming potential of each treatment was calculated as:

$$\text{GWP (CO}_2\text{ eq. mg m}^{-2}\text{ h}^{-1}) = CO_2 + (CH_4 \times 34) + (N_2O \times 298) \quad (2)$$

Substrate temperature measurements

Substrate temperatures were recorded using a handheld soil thermometer three times per day (morning, midday, and evening) once a week. Morning measurements were made at 8:00 – 9:00, midday measurements at 12:00 – 13:00, and evening measurements at 17:00 – 18:00. The handheld soil thermometer was inserted at a depth of about 3 cm from the bottom of the substrate.

Water balance measurements and calculations

The water balance for the GR mesocosms considered only irrigation and rainfall as inputs, and drained water as outputs. Rainfall data was obtained from the ARPAV weather station. Irrigation was applied only during the summer season about 1 – 2 times per week depending on rain events (Table 1). The drainage water collected was weighted after every few rain events, depending on rainfall intensity and duration. With these data, the water balance for each treatment per season was calculated as:

$$H_2O \text{ balance} = \frac{(irrigation + rainfall)}{water\ drained} \quad (3)$$

Statistical analysis

Data analysis was divided into seasons, where spring was designated as March 21 – June 20, summer was June 21 – September 22, fall was September 23 – December 21, and winter was December 22 – March 20. Statistical analysis was done in R 4.2.2 software. Since GHGs data were not normally distributed, non-parametric tests of Kruskal-Wallis was used to evaluate effect of plant species and Mann-Whitney to evaluate effect of substrate depth and irrigation level on GHG fluxes and global warming potential (GWP). For post-hoc comparisons in the case of significance with Kruskal-Wallis test, Dunn's test with Bonferroni adjustment was used. Data were visualized with boxplots. Kruskal-Wallis and Mann-Whitney were also used to analyze the main effects for the water balance of each season.

Since substrate temperature data was normally distributed, 3-way ANOVA was used to study the influence of plant species, substrate depth and irrigation level. Given significance of only substrate depth as a main effect with no other interactions, a coefficient of variability was calculated for each treatment. For the coefficient of variability obtained, a 3-way ANOVA was also done. Spearman's correlation was used to evaluate correlations between GHG emissions and temperatures in each season.

RESULTS

Meteorological data

Meteorological data monitored from April 2022 to April 2023 are represented in Figure 4.1. In spring, average solar radiation was 21.1 MJ m^{-2}, average wind speed was 1.8 m s^{-1}, average minimum temperature was 11.5 ºC, average maximum temperature was 22.6 ºC. In summer, average solar radiation was 22.8 MJ m^{-2}, average wind speed was 1.8 m s^{-1}, average minimum temperature was 18.5 ºC, average maximum temperature was 30.0 ºC. In fall, average solar radiation was 7.5 MJ m^{-2}, average wind speed was 1.3 m s^{-1}, average minimum temperature was 8.1 ºC, average maximum temperature was 16.6 ºC. In winter, average solar radiation was 7.7 MJ m^{-2}, average wind speed was 1.5 m s^{-1}, average minimum temperature was 2.9 ºC, average maximum temperature was 11.2 ºC. The temperature followed expected trends, peaking in summer and at its minimum in the winter. Wind speed stayed relatively constant throughout the entire year. Solar radiation was reduced in fall and winter by over half compared to spring and summer.

The rainfall received by the GRs (Figure 4.1 and Table 4.1) was mainly in the late summer and early autumn, with very few rainfalls received in spring and early summer. This created a very dry growing season, particularly evident during the summer months in 2022 and the spring months in 2023. The long term historical averages (1992 – 2022) for minimum temperatures were 10.8 ºC in spring, 16.7 ºC in summer, 6.7 ºC in fall, and 1.2 ºC in winter. Average historical mean temperatures were 15.9 ºC in spring, 22.4 ºC in summer, 10.7 ºC in fall, and 4.9 ºC in winter. For maximum temperatures, the historical average was calculated with data from the years 2010 – 2022 due to a lack of daily values from 1992 – 2009 for this parameter. Historical maximum temperatures were 21.8 ºC in spring, 29.0 ºC in summer, 15.1 ºC in fall, and 9.7 ºC in winter. Historically, cumulative rainfall was 4.4 mm in spring, 4.4 mm in summer, 4.2 mm in fall, and 3.5 mm in winter.

Greenhouse gas fluxes (GHG) by season

GHG fluxes in spring

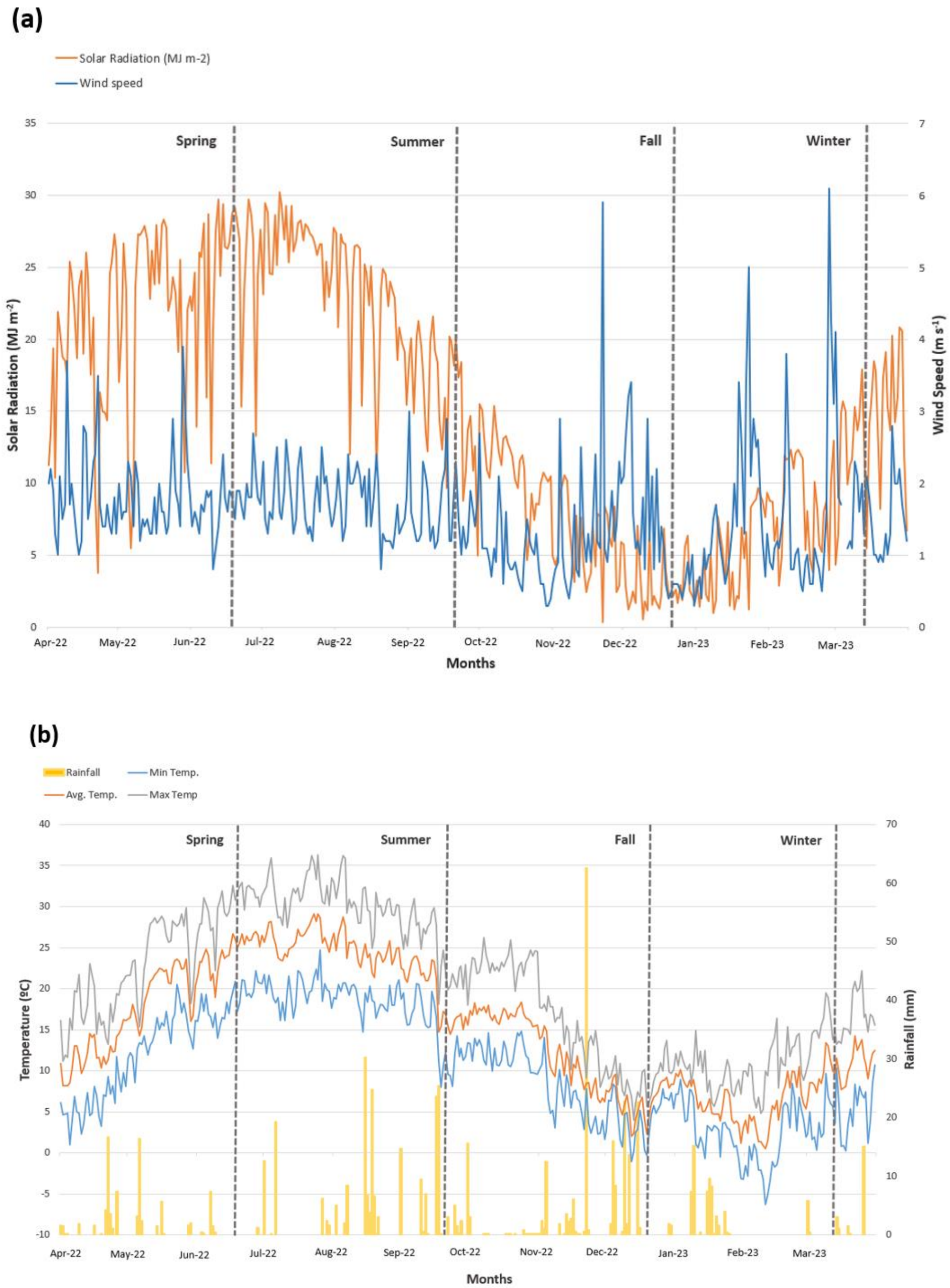

Figure 4.1 (a) Daily solar radiation (MJ m^{-2}) and wind speed (m s^{-1}) from April 2022 to April 2023 and (b) Daily minimum, average, and maximum temperatures (ºC) and rainfall (mm) from April 2022 to April 2023. Gray lines serve as dividers for each season (spring, summer, fall, and winter).

The Kruskal-Wallis test yielded significant results for the effect of plant species on CO_2 ($p = 0.001$) (Figure 4.2) fluxes. In spring, all treatments were net emitters of CO_2, with median values 4 mg m^{-2} h^{-1} (CG), 95 mg m^{-2} h^{-1} (Se), 116 mg m^{-2} h^{-1} (WG), and 275 mg m^{-2} h^{-1} (WF). Here, only WF differed significantly from CG, with no other significant differences among treatments. Plant species was not a significant control for N_2O (overall median value of 0 mg m^{-2} h^{-1}) or CH_4 (overall median value of 0.02 mg m^{-2} h^{-1}) fluxes. The Mann-Whitney test yielded significant results for the effect of substrate depth for CO_2 ($p < 0.001$) (Figure 4.3). Both substrate depths showed positive values, where the median CO_2 values were 10 mg m^{-2} h^{-1} (8 cm depth) and 308 mg m^{-2} h^{-1} (14 cm depth). Spearman's correlation between GHG fluxes and substrate temperature yielded significant results for CO_2 and N_2O but not for CH_4. CO_2 fluxes were positively correlated ($p < 0.0001$) with morning (Spearman $R = 0.290$), midday (Spearman $R = 0.354$), and evening (Spearman $R = 0.186$) temperatures. N_2O showed a negative correlation ($p < 0.05$) with evening (Spearman $R = -0.0912$) temperatures.

GHG fluxes in summer

The Kruskal-Wallis test showed plant species significantly effected CO_2 ($p < 0.0001$) (Figure 4.2). All treatments, in summer, were net emitters of CO_2, with median values of 86.31 mg m^{-2} h^{-1} (WG), 268 mg m^{-2} h^{-1} (Se), 404 mg m^{-2} h^{-1} (CG), and 765 mg m^{-2} h^{-1} (WF). Plant species was not a significant control for CH_4 (overall median value of 0 mg m^{-2} h^{-1}) or N_2O (overall median value of -0.23 mg m^{-2} h^{-1}) fluxes. The Mann-Whitney test yielded significance for substrate depth only for N_2O fluxes ($p < 0.01$) (Figure 4.4). Both substrate depths were a net sink of N_2O with median values of -0.2 mg m^{-2} h^{-1} (8 cm) and -0.3 mg m^{-2} h^{-1} (14 cm). The Mann-Whitney test also yielded significant results for irrigation level as a control for N_2O fluxes ($p < 0.01$) (Figure 4.5).

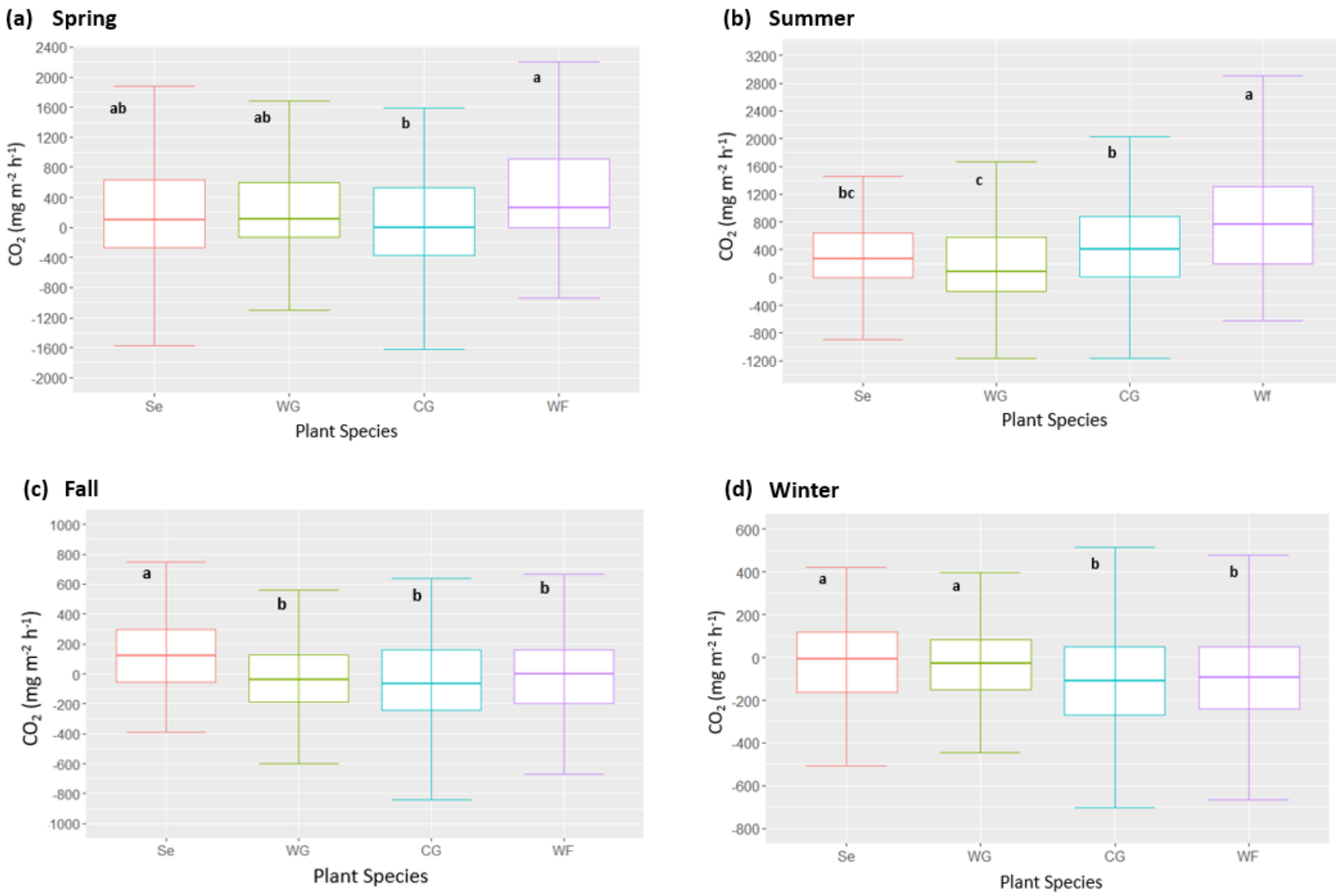

Figure 4.2 Effect of vegetation type (Sedum spp., Se; warm season grasses, WG; cold season grasses, CG; and wildflowers, WF) in green roof mesocosms on CO_2 fluxes during (a) spring, (b) summer, (c) fall, and (d) winter season. Significant differences between treatments are denoted by lowercase letters.

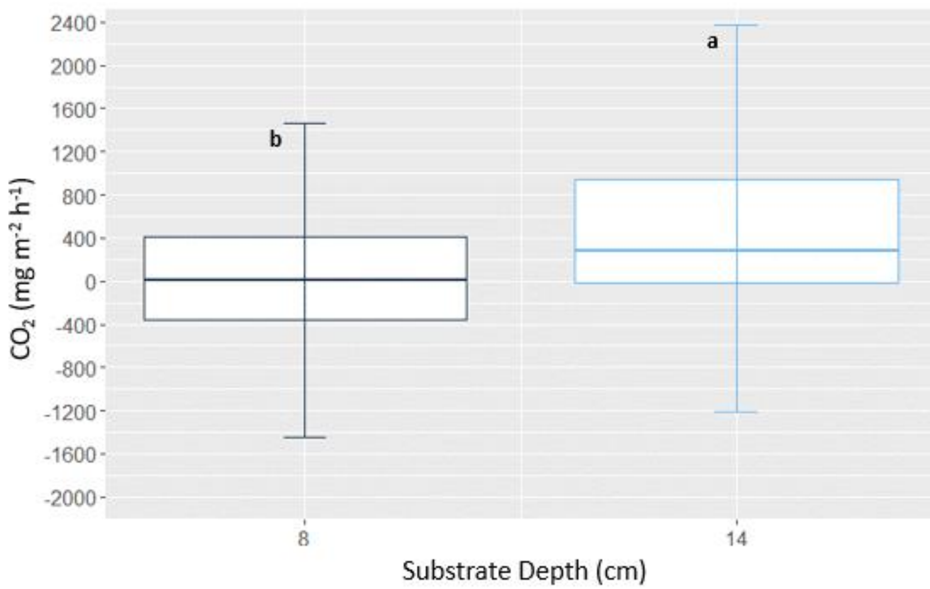

Figure 4.3 Effect of substrate depth (8 or 14 cm) in green roof mesocosms on CO_2 fluxes during the spring season. Significant differences between the treatments are denoted by lowercase letters.

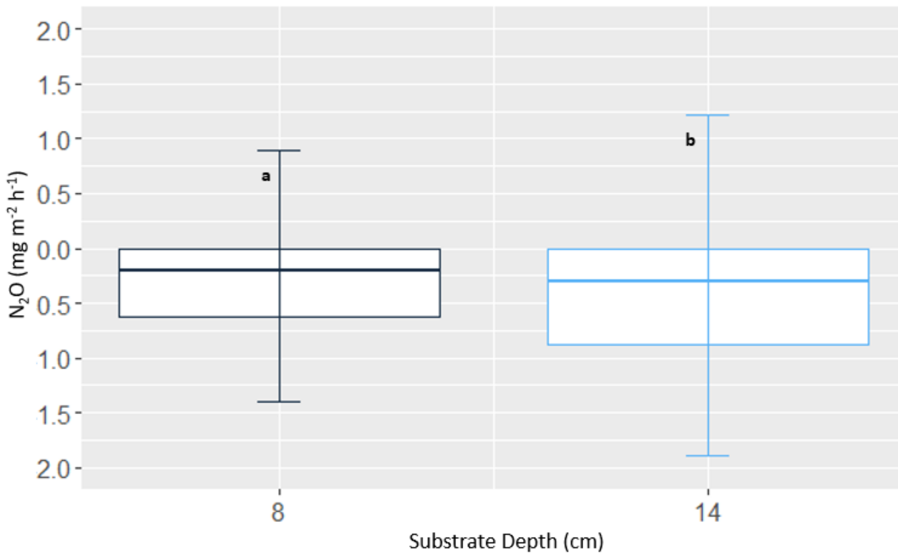

Figure 4.4 Effect of substrate depth (8 or 14 cm) in green roof mesocosms on N_2O fluxes during the summer season. Significant differences between the treatments are denoted by lowercase letters.

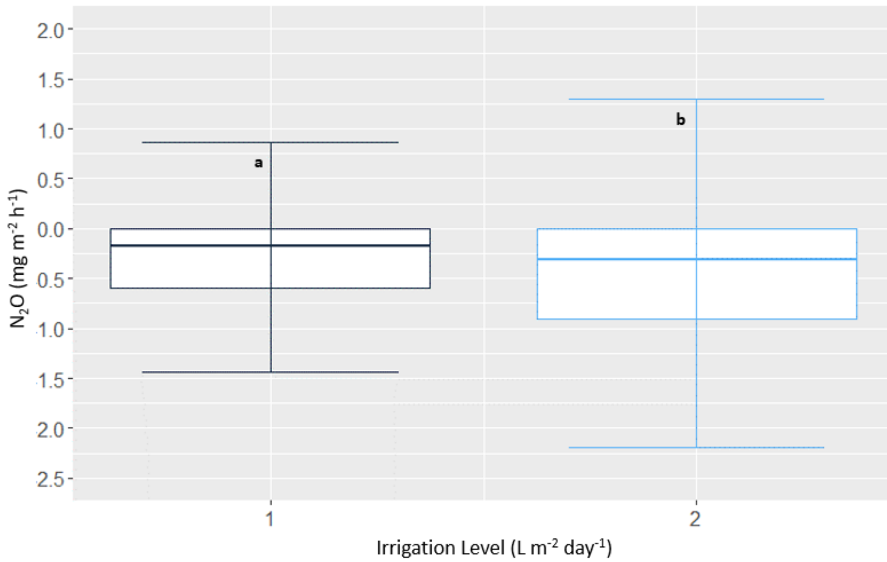

Figure 4.5 Effect of irrigation level (1 or 2 L m^{-2} day^{-1}) in green roof mesocosms on N_2O fluxes during the summer season. Significant differences between the treatments are denoted by lowercase letters.

Both irrigation levels were also a net sink, with median values of -0.18 mg m^{-2} h^{-1} (1 L m^{-2} day^{-1}) and -0.31 mg m^{-2} h^{-1} (2 L m^{-2} day^{-1}). Spearman's correlation yielded significant results for all GHG fluxes in summer. CO_2 fluxes showed a positive correlation ($p < 0.0001$) with morning (Spearman R = 0.187) and midday temperatures (Spearman R = 0.168). CH_4 showed a positive correlation with morning ($p < 0.05$, Spearman R = 0.110), midday ($p = 0.01$, Spearman R = 0.123), and evening ($p < 0.001$, Spearman R = 0.141). N_2O fluxes showed negative correlation for morning ($p < 0.0001$, Spearman R = -0.222), midday ($p < 0.001$, Spearman R = -0.141), and evening ($p < 0.05$, Spearman R = -0.105) temperatures.

GHG fluxes in the fall

Statistical analysis showed that plant species significantly influenced the CO_2 fluxes ($p < 0.0001$) (Figure 4.2). Treatments CG (-65 mg m^{-2} h^{-1}), WG (-35 mg m^{-2} h^{-1}), and WF (-2 mg m^{-2} h^{-1}) were net sinks of CO_2, while Se (123 mg m^{-2} h^{-1}) was a net source. Plant species was not a significant control for CH_4 (overall median value of -0.07 mg m^{-2} h^{-1}) or N_2O (overall median value of -0.03 mg m^{-2} h^{-1}) fluxes. Substrate depth was not a significant control for any GHG flux. However, the Mann-Whitney test yielded significance of irrigation level for CH_4 fluxes ($p = 0.05$), with median values of -0.05 mg m^{-2} h^{-1} (1 L m^{-2} day^{-1}) and -0.09 mg m^{-2} h^{-1} (2 L m^{-2} day^{-1}) (Figure 4.6). Spearman's correlation yielded significant results for CO_2 and N_2O but not CH_4. There was positive correlation between CO_2 fluxes with morning ($p < 0.0001$, Spearman R = 0.233), midday ($p < 0.0001$, Spearman R = 0.197), and evening ($p < 0.05$, Spearman R = 0.111) temperatures. N_2O fluxes yielded negative correlation with midday ($p < 0.01$, Spearman R = -0.135) and evening ($p < 0.0001$, Spearman R = -0.186) temperatures.

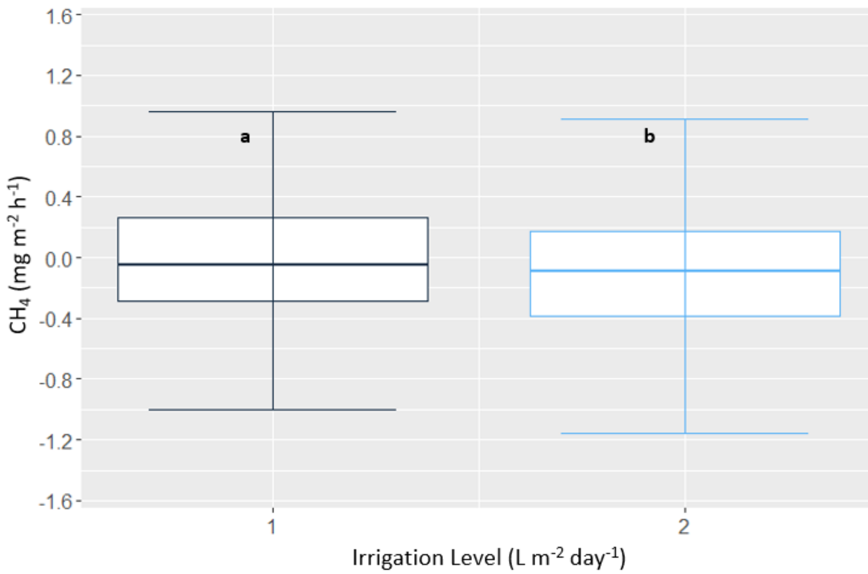

Figure 4.6 Effect of irrigation level (1 or 2 L m^{-2} day^{-1}) in green roof mesocosms on CH_4 fluxes during the fall season. Significant differences between the treatments are denoted by lowercase letters.

GHG fluxes in the winter

The Kruskal-Wallis's test yielded significance ($p < 0.001$) for the effect of plant species on CO_2 fluxes in the winter (Figure 4.2). All treatments were net sinks of CO_2, with median values of -110 mg m^{-2} h^{-1} (CG), -94 mg m^{-2} h^{-1} (WF), -29 mg m^{-2} h^{-1} (WG), and -10 mg m^{-2} h^{-1} (Se). There was no significant effect of plant species for CH_4 (-0.05 mg m^{-2} h^{-1}) or N_2O (0 mg m^{-2} h^{-1}). There was no significant effect of substrate depth. However, Mann-Whitney test yielded significance of irrigation level on CO_2 ($p < 0.01$) fluxes (Figure 4.7). Both irrigation levels had negative values, with median CO_2 fluxes of -83 mg m^{-2} h^{-1} (1 L m^{-2} day^{-1}) and -38 mg m^{-2} h^{-1} (2 L m^{-2} day^{-1}). Spearman's correlation yielded significant results only for CH_4 fluxes, with a positive correlation with only with evening temperatures ($p = 0.01$, Spearman $R = 0.105$).

Yearly GHG fluxes

On a yearly basis, plant species treatments had median CO_2 fluxes of -2 mg m^{-2} h^{-1} (CG), 9 mg m^{-2} h^{-1} (WG), 53 mg m^{-2} h^{-1} (WF), and 74 mg m^{-2} h^{-1} (Se). For substrate depth treatments, median CO_2 fluxes were 6 mg m^{-2} h^{-1} (8 cm) and 61 mg m^{-2} h^{-1} (14 cm). Cumulative N_2O and CH_4 median fluxes were 0 mg m^{-2} h^{-1} and -0.01 mg mg^{-2} h^{-1}, respectively.

Global warming potential (GWP) by season

In the spring, plant species had a significant effect on GWP ($p < 0.0001$) (Figure 4.8). GWP was positive for all treatments with median values 7 mg m^{-2} h^{-1} (CG), 100 mg m^{-2} h^{-1} (Se), 156 mg m^{-2} h^{-1} (WG), and 269 mg m^{-2} h^{-1} (WF).

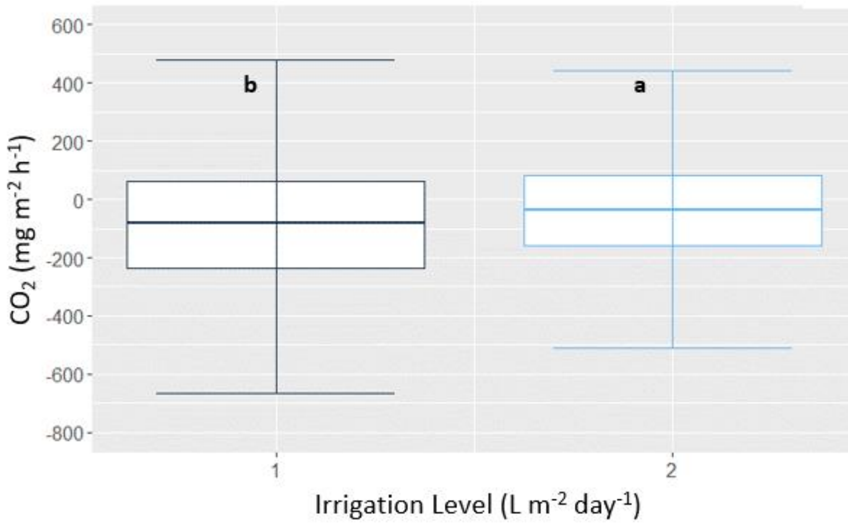

Figure 4.7 Effect of irrigation level (1 or 2 L m^{-2} day^{-1}) in green roof mesocosms on CO_2 during the winter season. Significant differences between the treatments are denoted by lowercase letters.

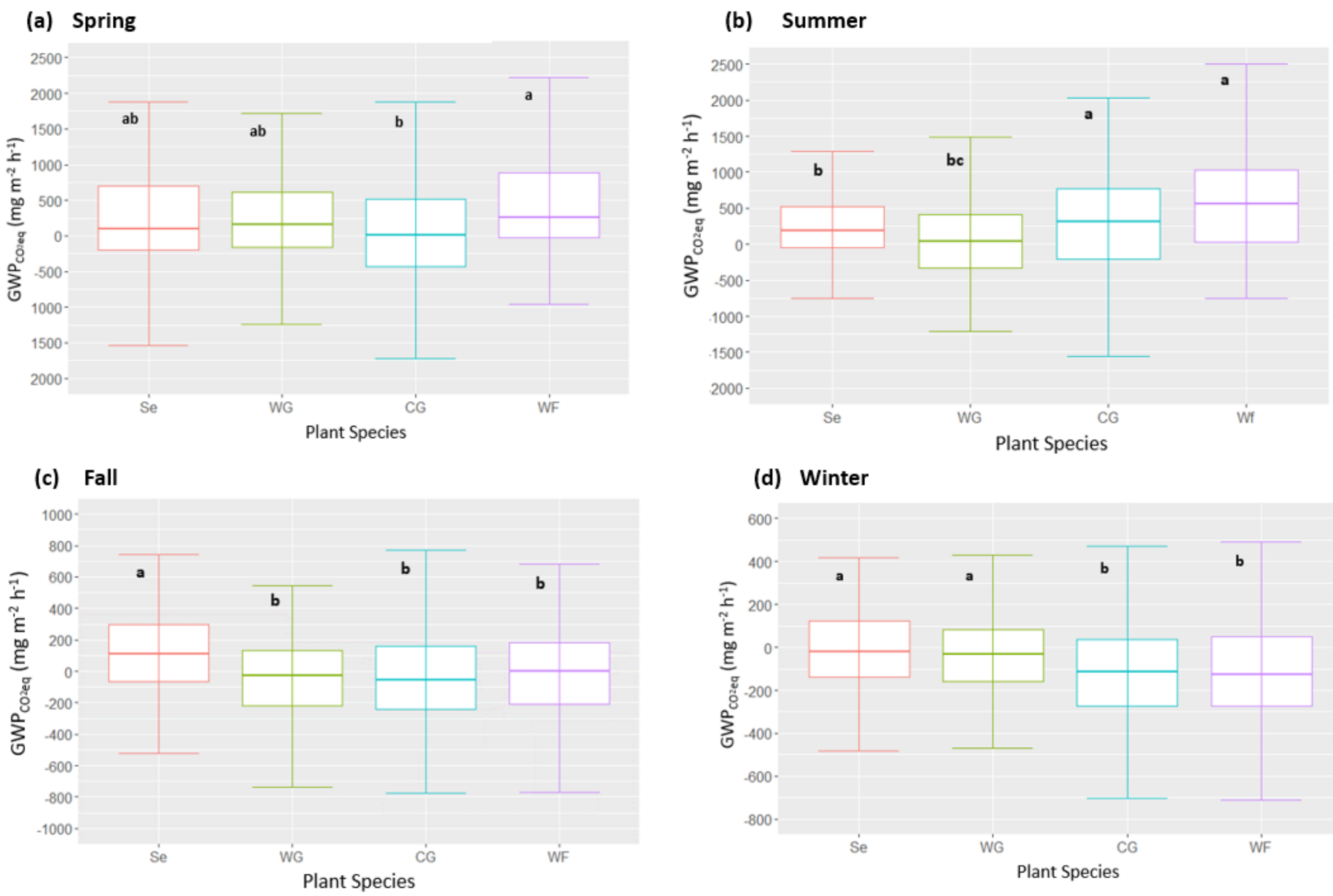

Figure 4.8 Effect of vegetation type (Sedum spp., Se; warm season grasses, WG; cold season grasses, CG; and wildflowers, WF) in green roof mesocosms on GWP during (a) spring, (b) summer, (c) fall, and (d) winter season. Significant differences between treatments are denoted by lowercase letters.

Moreover, depth was also significant for GWP ($p < 0.0001$) in the spring (Figure 4.9) with median values 11 mg m^{-2} h^{-1} (8 cm) and 343 mg m^{-2} h^{-1} (14 cm). Spearman's correlation yielded a significant positive correlation ($p < 0.0001$) for GWP with morning (Spearman R = 0.260), midday (Spearman R = 0.357), and evening (Spearman R = 0.177) temperatures.

Similarly, in the summer, plant species was a significant factor for GWP ($p < 0.0001$) (Figure 4.8), with positive median values of 43 mg m^{-2} h^{-1} (WG), 185 mg m^{-2} h^{-1} (Se), 333 mg m^{-2} h^{-1} (CG), and 587 mg m^{-2} h^{-1} (WF). Spearman's correlation showed a positive correlation between GWP and with morning ($p < 0.001$, Spearman R = 0.125) and midday ($p = 0.0001$, Spearman R = 0.162) temperatures.

Plant species also significantly influenced GWP ($p < 0.0001$) in the fall. GWP median values were negative for treatments CG (-55 mg m^{-2} h^{-1}), WG (-29 mg m^{-2} h^{-1}), and WF (-2 mg m^{-2} h^{-1}) and positive for Se (112 mg m^{-2} h^{-1}) (Figure 4.8). GWP showed a significant positive correlation ($p < 0.0001$) with morning (Spearman R = 0.219) and midday (Spearman R =0.177) temperatures.

Plant species mattered for GWP ($p = 0.0001$) in the winter, yielding negative GWP median values for all treatments—-125 mg m^{-2} h^{-1} (WF), -116 mg m^{-2} h^{-1} (CG), -30 mg m^{-2} h^{-1} (WG), and -22 mg m^{-2} h^{-1} (Se) (Figure 4.8). Irrigation also mattered for GWP ($p = 0.05$) (Figure 4.10), with negative median values of -105 mg m^{-2} h^{-1} (1 L m^{-2} day^{-1}) and -42 mg m^{-2} h^{-1} (2 L m^{-2} day^{-1}). There was no significant correlation between GWP and substrate temperatures.

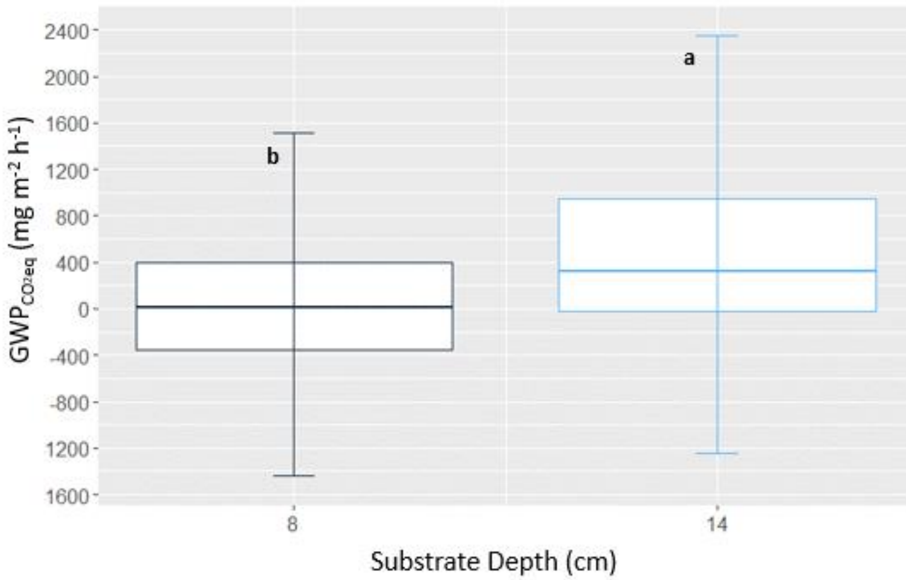

Figure 4.9 Effect of substrate depth (8 or 14 cm) in green roof mesocosms on GWP fluxes during the spring season. Significant differences between the treatments are denoted by lowercase letters.

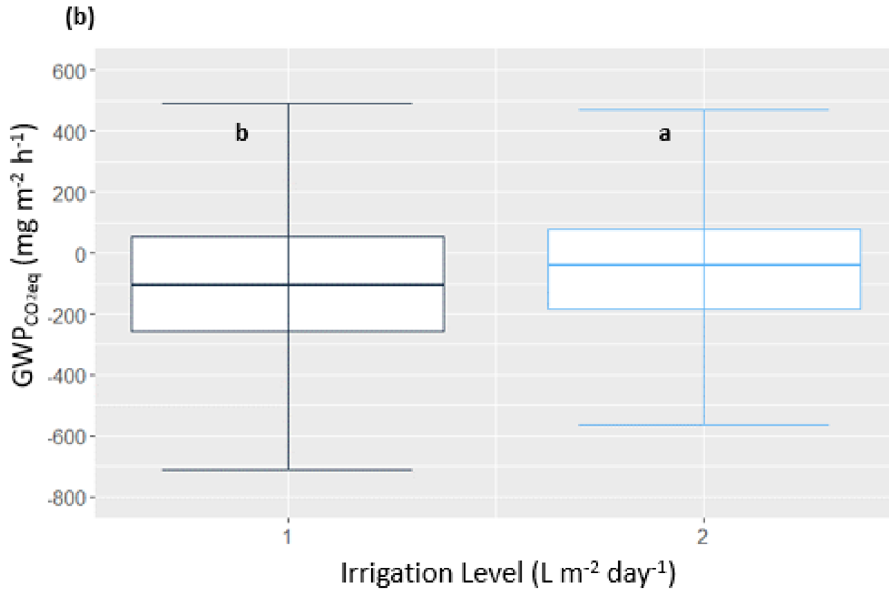

Figure 4.10 Effect of irrigation level (1 or 2 L m^{-2} day^{-1}) in green roof mesocosms on GWP during the winter season. Significant differences between the treatments are denoted by lowercase letters.

Yearly GWP

The yearly GWP median values for plant species treatments were -31 mg m^{-2} h^{-1} (CG), 9 mg m^{-2} h^{-1} (WG), 44 mg m^{-2} h^{-1} (WF), and 51 mg m^{-2} h^{-1} (Se). For substrate depth, median values -4 mg m^{-2} h^{-1} (8 cm) and 47 mg m^{-2} h^{-1}.

Substrate temperatures

For all seasons, the only significant control on substrate temperatures was substrate depth with no significant interactions. During the spring, a significant effect of substrate depth was seen for morning ($p = 0.0001$) and evening temperatures ($p = 0.01$). Spring morning temperatures averaged 15.7 ºC (8 cm) and 17.0 (14 cm), while spring evening temperatures averaged 22.5 ºC (8 cm) and 21.4ºC (14 cm). During the summer, substrate depth was only significant for evening temperatures ($p = 0.0001$). Summer evening temperatures averaged 31.2 ºC (8 cm) and 29.9 ºC (14 cm). In the fall, substrate depth was significant only for morning ($p < 0.01$) temperatures. Fall morning temperatures averaged 10.3 ºC (8 cm) and 11.3 ºC (14 cm). In winter, substrate depth mattered for morning ($p < 0.001$) and evening ($p < 0.05$) temperatures. Winter morning temperatures averaged 4.6 ºC (8 cm) and 5.5 ºC (14 cm), while winter evening temperatures averaged 9.7 ºC (8 cm) and 9.0 ºC (14 cm).

The 3-way ANOVA on the temperatures coefficients of variability of each treatment yielded only significant effects in the summer season for the interaction between substrate depth and irrigation level ($p < 0.05$) (Figure 4.11). Average coefficients of variability were 0.19 (8 cm depth and 1 L m^{-2} day^{-1}), 0.18 (8 cm depth and 2 L m^{-2} day^{-1}), 0.13 (14 cm depth and 1 L m^{-2} day^{-1}), and 0.12 (14 cm depth and 2 L m^{-2} day^{-1}).

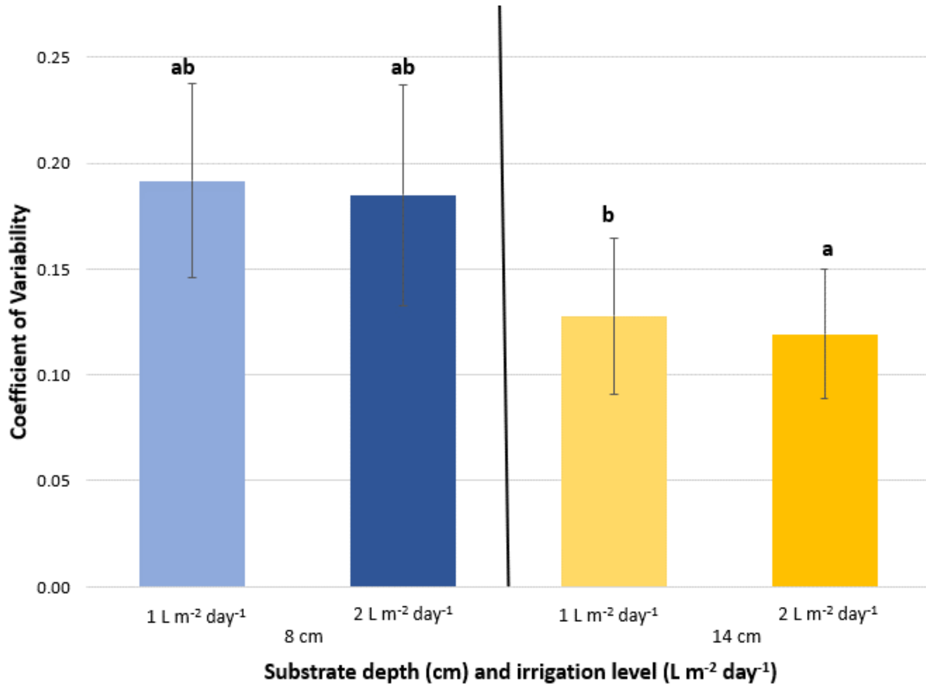

Figure 4.11 Average values of coefficient of variability showing interaction of irrigation level (1 or 2 L m^{-2} day^{-1}) and substrate depth (cm) in green roof mesocosms on GWP during the summer season. Significant differences are denoted by lowercase letters. Errors bars represent the standard deviation of each treatment.

Water balance

The yearly water balance is reported in Table 4.2. For seasonal water balance, plant species was a significant control for spring ($p = 0.01$), summer ($p < 0.001$), fall ($p < 0.001$), and winter ($p < 0.0001$). In spring, summer, and fall, only WF and WG treatments differed significantly. In winter, WF treatments differed significantly from WG and Se treatments, with no other significant differences. In spring, the cumulative water input was 115.2 L m^{-2} whereas the water output median values were 2.87 L m^{-2} (Se), 3.38 L m^{-2} (WF), 3.51 L m^{-2} (CG), and 10.56 L m^{-2} (WG). In summer, with a cumulative water input of 273 L m^{-2} (1 L m^{-2} day^{-1} treatments) and 321 L m^{-2} (2 L m^{-2} day^{-1} treatments). The output median values in summer were 32.25 L m^{-2} (Se), 57.10 L m^{-2} (WF), 73.65 L m^{-2} (WG), and 75.25 L m^{-2} (CG). In fall, the output median values were 136.28 L m^{-2} (WF), 142.88 L m^{-2} (Se), 150.32 L m^{-2} (CG), and 153.69 L m^{-2} (WG) – the input 200.2 L m^{-2}. In winter, a cumulative water input of 68.4 L m^{-2} determined an output median value of 48.86 L m^{-2} (WF), 51.95 L m^{-2} (CG), 54.32 L m^{-2} (Se), and 55.85 L m^{-2} (WG). Substrate depth was a significant control for spring ($p < 0.0001$), summer ($p < 0.0001$), and fall ($p < 0.0001$). Median values were 1.31 L m^{-2} (14 cm) and 8.61 L m^{-2} (8 cm) in spring, 43.81 L m^{-2} (14 cm) and 77.41 L m^{-2} (8 cm) in summer, and 138.60 L m^{-2} (14 cm) and 152.69 L m^{-2} (8 cm) in fall. There was no significant effect of irrigation level for any season.

DISCUSSION

Effect of plant species on GHG and GWP

We found that plant species was a significant control for CO_2 fluxes during all seasons. In the spring and summer, all treatments were net sources of CO_2, meaning that both autotrophic and heterotrophic respiration were higher than photosynthesis.

Table 4.2 Cumulative yearly water balance for the 16 different treatment combinations between plant species (Se, *Sedum* spp.; WG, warm season grasses; CG, cold season grasses; and WF, wildflower mix), substrate depth (8 or 14 cm), and irrigation level (1 or 2 L m^{-2} day^{-1}).

Species	**Substrate Depth (cm)**	**Irrigation Level (L m^{-2} day^{-1})**	**Rain (mm)**	**Irrigation (L m^{-2})**	**Water Output (L m^{-2})**	**Water Drained (%)**
Se	8	1	606	128	259	31.9%
		2		206	295	36.4%
	14	1		128	264	32.6%
		2		206	238	29.3%
WG	8	1	606	128	252	34.4%
		2		206	253	34.5%
	14	1		128	268	36.5%
		2		206	274	37.3%
CG	8	1	606	128	252	34.3%
		2		206	235	32.0%
	14	1		128	263	35.9%
		2		206	270	36.8%
WF	8	1	606	128	247	30.4%
		2		206	285	35.1%
	14	1		128	279	34.4%
		2		206	266	32.8%

In terms of the magnitude of CO_2 emissions, the summer emissions were various orders of magnitude higher than spring emissions for all treatments except WG (warm season grasses). Treatments *Sedum* spp., CG (cold season grasses), and WF (wildflowers) showed an increase in emissions from spring to summer of 181%, over 1000%, and 178% respectively. In contrast, WG showed a decrease of 25% from spring to summer. This decrease of WG emissions can be attributed to the fact that the summer is WG's preferred growing conditions, and thus, allowed the plant to photosynthesize and grow better than in the spring. Moreover, the dramatic increase in CO_2 emissions of the other treatments can be explained by a lack of rainfall and higher than average temperatures, which lead to plant death instead of plant growth. A long-term study looking at GHG fluxes from GRs found that drier conditions decreased the ability of extensive GRs to sequester carbon, while increased rainfall heightened it (Konopka et al., 2021). Konopka et al. (2021) attributed this phenomenon to the reduced availability of substrate water, which directly hinders photosynthesis and carbon assimilation. In the fall and winter, almost all treatments were net sinks of CO_2 (with the exception of Se in the fall), meaning that photosynthesis was higher than autotrophic and heterotrophic respiration. Notably, our fall and winter sampling season received the highest amount of rainfall. In our mesocosms, since the summer season was atypically dry, there was colonization of wild species that established during the stress period in summer and took advantage of the higher water availability at the end of summer and beginning of fall to grow. This occurrence could have also helped to increase CO_2 uptake in the treatments.

Overall, wildflower (WF) treatments showed the highest emissions in both spring and summer and were a relatively small carbon sink in fall and winter. Cold season grasses (CG) performed better in the colder seasons of spring, fall, and winter but very poorly in the summer having the second highest emission median values. The opposite was true for warm season grasses (WG), where these treatments had the lowest emissions in the summer.

Sedum spp. (Se) treatments are particularly noteworthy, given that they are one of the most widely used and studied plants in extensive GR systems. In the case of the Se treatments, CO_2 emission values followed a decreasing trend, where *Sedum* spp. had 56% less emissions in fall than in summer, and a 108% reduction from fall to winter, where it was a net sink. Agra et al. (2017) observed this same trend, where *Sedum* spp. had markedly lower emissions in the winter and cold months and increasingly higher emissions as the seasons progressed into the warmer months. Although some studies cite *Sedum* spp.'s drought resistance mechanism and capacity for crassulacean acid metabolism (CAM) as potentially allowing the plant to uptake enough carbon in the colder months to offset the higher emissions in the hotter months (Konopka et al., 2021), other studies cite the opposite and suggest the use of other grass species as a more effective choice for carbon sequestration (Agra et. al., 2017; Shafique et al., 2018). Our results suggest that *Sedum* spp. and WF are the least effective choices, while WG and CG could potentially be an effective strategy for carbon sequestration depending on the climatic conditions. In agreement with our findings, a literature review on studies examining the carbon sequestration potential of *Sedum* spp. as well as other herbaceous and flowering plants in green infrastructure systems found that GRs populated with these plants typically emit less CO_2 than their natural controls, but *Sedum* spp. consistently had the lowest sequestration rates (Charoenkit & Yiemwattana, 2016).

Additionally, plant species mattered for our calculation of the global warming potential (GWP) in all seasons. GWP fluxes for each season followed the same trend as CO_2 emissions.

GWP was dominated by CO_2 trends because CO_2 fluxes were of the greatest magnitude, while CH_4 and N_2O, even when significant, had zero or very near zero mg m^{-2} day^{-1} magnitudes.

Effect of substrate depth on GHG and GWP

Substrate depth was a significant control for CO_2 fluxes and GWP in the spring and for N_2O in the summer. In spring, substrate depth treatments were both net sources of CO_2, where the deeper substrate depth (14 cm) had a median value about 30 times higher than the shallower substrate depth (8 cm). GWP followed the same trend. Halim et al. (2022) showed a positive relationship between substrate depth and CO_2 efflux because deeper substrates generally have higher aerial mass of organic matter for aerobic decomposition. However, they also highlight that this could potentially be mitigated by promoting greater vegetation growth (Halim et al., 2022). This is particularly relevant to our results given that plant biomass was less than expected due to a lack of rainfall in spring 2023 and heat stress in summer 2022. Potentially, this could have increased the CO_2 efflux from deeper substrate depths treatments. Future measurements of plant biomass and soil organic matter content can better quantify this relationship between carbon cycling, plant growth, and substrate depth.

Our study found that in the summer season, both substrate depths were a net sink of N_2O, with 14 cm treatments that were 1.5 times greater sink than the 8 cm treatments, still with values close to 0. The effect of substrate depth as a control for N_2O emissions is poorly studied. Moreover, previous literature conflicts on whether GRs are a significant sink or source of N_2O. Mitchell et. al. (2018) found that their GR treatments were net emitters, while Teemusk et al. (2019) found that their GRs had highly variable N_2O fluxes in time with no statistical significance. Both of these studies yielded individual negative values of N_2O fluxes, supporting our findings that under some conditions GRs can potentially serve as N_2O sinks. It is widely accepted that substrate depth influences the nitrogen cycling dynamics of GRs, mainly by exerting control on the hydrology of the system (Buffam & Mitchell, 2015). Our summer sampling season was the hottest and driest of the seasons, meaning that the role of substrate moisture control as a regulator for N_2O fluxes could have been more important compared to other seasons. Unfortunately, we have no data on substrate moisture content.

Effect of summer irrigation level on GHG and GWP

Our results show that summer irrigation level was significant for CO_2 and GWP in the winter, CH_4 in the fall, and N_2O in the summer. For CO_2 fluxes and GWP in the winter, the lower irrigation treatment (1 L m^{-2} day^{-1}) was two times a greater sink than the higher irrigation treatment (2 L m^{-2} day^{-1}). Since irrigation was applied only in the summer season, this suggests a delayed effect of irrigation. Similarly, Halim et al. (2022) found that irrigated GRs had higher CO_2 efflux than non-irrigated GRs and, notably, their irrigation treatments were phased out before measurements were taken, showing a similar delayed effect of irrigation on CO_2 fluxes. In the case of N_2O fluxes in the summer, the effect of irrigation was not delayed. A higher irrigation level (2 L m^{-2} day^{-1}) yielded a sink about 1.7 times greater than the lower irrigation level (1 L m^{-2} day^{-1}). Since moisture is assumed to be the main control for N_2O emissions and, given that the effect was only seen in the driest season (i.e., summer), this suggests that a higher irrigation level can favorably impact this ecosystem service and reduce N_2O emissions. In support of this result, Lively et al. (2010) conducted a study on urban lawn systems, which can be considered similar to extensive GRs, and found that higher irrigation levels lead to smaller N_2O emissions.

Effect of substrate depth on substrate temperatures

We found that only substrate depth was a significant control for substrate temperatures in all seasons. The range between evening and morning substrate temperatures was always less in the 14 cm depth treatments than in the 8 cm depth treatments. In spring, fall, and winter the 14 cm depth treatments lessened the temperature oscillation by 2 ºC and, in the summer, by 3 ºC. These results are well supported by literature. Some studies have shown that increasing substrate depth reduces the heat flux entering and exiting the building (Eksi et al., 2017). Moreover, Getter et al. (2011) found that shallower green roofs experience higher temperature fluctuations and, similarly, Nardini et al. (2012) found that deeper substrate depths in extensive GRs decrease the amplitude of daily temperature changes. In the colder months, this thermal insulation can translate to increased heating savings while, in the hotter months, it can translate to increased cooling savings (Eksi et al., 2017). Our results showed that the greatest thermal benefits (i.e., the greatest reduction in thermal oscillation) were obtained during the dry summer season. In support of this, a literature review on GRs found that the hotter and drier a climate is, the more important the effect on urban temperature mitigation (Alexandri & Jones, 2008).

We found that the coefficients of variability were only significantly affected by the interaction between substrate depth and irrigation level treatments in the summer season. The lower level irrigation level and shallower substrate depth treatments yielded the highest variability, while the highest irrigation level and deeper substrate depth yielded the lowest variability. This means that there was higher within treatment variability in the shallower and less irrigated treatments. The importance of substrate depth as a control for variability in substrate temperatures is expected, but the importance of irrigation could have been highlighted during our dry summer season. A review of sustainable irrigation practices for extensive GRs found that in hot, dry summers irrigation was necessary to obtain thermal benefits (Van Mechelen et al., 2015). This could indicate that irrigation becomes important as a control for substrate temperatures beyond a certain threshold. In other words, deeper substrate depth and higher irrigation level highlighted the thermal benefits of our GRs mesocosms and reduced variability among replicates during the hottest season.

Water balance

On a yearly cumulative basis, the percentage of water drained relative to the water inputs received was similar for all treatment combinations, ranging from 29 – 36%. Based on this, our results suggest that all treatments are effective solutions for stormwater management in cities. However, statistical analysis showed some seasonal differences, particularly for the main effects of plant species and substrate depth.

We found that the water balance of GR mesocosms was affected by plant species in all seasons and substrate depth in all seasons except winter. For the effect of plant species, all treatments had the lowest water output in the spring season, increasing in the summer and peaking in the fall, and ultimately lowering again in the winter. Spring water output values were 1 or 2 orders of magnitude less than output values in summer, fall, and winter. This can be explained mainly by the water inputs received. Treatments received little rain and no irrigation in the spring, while in the summer they received little rain but were supplemented with irrigation. On the other hand, higher amounts of rainfall occurred in the fall and winter. A literature review found that GRs retained all small rain events that were less than 10 mm (Li & Yeung, 2014). This, in conjunction with our results, implies that GRs retain less water with more frequent and intense rain events. Warm season grasses (WG) treatments performed the worst and yielded the highest amount of drained water in all seasons. This suggests that WG was the least effective solution for stormwater management. The best solutions were wildflower (WF) and *Sedum* spp. (Se), given that the drained water from these treatments was less than half the amount from WG treatments. Cold season grasses (CG) treatments performed very similarly to WG treatments, except in spring where CG treatments were more similar to WF and Se. Nagase & Dunnett (2012) studied the performance of various plant species in terms of runoff quantity from GRs and found that grasses performed the best and *Sedum* spp. the worst. The reason for the underperformance of *Sedum* spp. relative to other grass species has been shown to be plant height, where mat-forming plants such as *Sedum* spp. have less water storage capacity per unit surface (Nagase & Dunnet, 2012; Shafique et al., 2018). Moreover, Shafique et al. (2018) conducted a literature review that found that grasses held the most amount of water in GRs and stressed that the differences between plant species were attributed to the different water holding and transpiration capacities. Although these measurements were outside the scope of this study, future research incorporating these measurements can provide a better understanding of between treatment variability.

For the effect of substrate depth on the water balance of spring, summer, and fall, the shallower substrate depths (8 cm) had about double the amount of drained water that the deeper substrate depth (14 cm) had in all seasons. Thus, our results show that a deeper substrate depth is a more efficient solution for stormwater management. A literature review highlighted the role a thicker growing medium—i.e., deeper substrate depth—plays in increasing the moisture holding capacity of GRs and, consequently, their stormwater management ability (Shafique et al., 2018). Few studies have looked at the effect of substrate depth on the stormwater management ability of extensive GRs, but it is widely accepted that substrate depth is a pivotal control for the ecosystem services of GRs through its control on water retention and, consequently, the runoff quantity and runoff peaks (Li & Yeung, 2014).

CONCLUSIONS

Green roof ecosystem services were significantly affected by plant species, substrate depth, and summer irrigation level year-round. Regarding controls on GHG fluxes and GWP, plant species were especially important for CO_2 and GWP. We found that mesocosms populated with cold season grasses (CG) and warm season grasses (WG) could be a potential solution for carbon sequestration during the cold months, while mesocosms with *Sedum* spp. and wildflowers (WF) were much less effective. Substrate depth was only important for CO_2 and GWP fluxes in the spring season, substantially increasing efflux. We hypothesize this dramatic increase could be due to a lack of vegetation cover in our mesocosms caused by heat stress during the summer and spring season. For irrigation level, there was a delayed effect on CO_2 and CH_4 in the winter and fall, respectively, but an immediate effect for N_2O in the summer. Notably, a higher irrigation level yielded a higher N_2O sink which suggests that increasing irrigation level can be a management strategy to increase this ecosystem service from GRs. Regarding controls on substrate temperatures, only substrate depth was a significant control. Deeper substrate depth treatments lessened the fluctuations in substrate temperature which, when taken at a building-scale, can result in increased energy savings in both the summer and winter months. In the summer season, the effect of irrigation level as a control was highlighted, especially in its interaction with substrate depth. Higher irrigation level and deeper substrate depth during the hottest and driest season emphasized the thermal benefits of GRs. This is a valuable insight for the implementation of GRs for mitigation of urban temperatures in the context of climate change and increasing temperature extremes worldwide. For the stormwater management potential of the treatments, plant species and substrate depth were the most relevant controls. On a yearly cumulative basis, the water balance of the treatments showed that they were all effective at retaining water, ranging from 29 – 36%. However, seasonal differences showed that wildflower

(WF) and *Sedum* spp. treatments retained the most amount of water in all seasons, while the performance of warm season grasses (WG) and cold season grasses (CG) had greater variability between seasons. Deeper substrate depth treatments were able to retain more water in all seasons.

Ultimately, we did not find a single solution or treatment combination that performed the best for all three ecosystem services. Different treatment combinations were more effective for one given ecosystem service over another. Moreover, these ecosystem services are further affected by local meteorological parameters. This means that when designing and implementing GRs for climate change adaptation in cities, clear and targeted objectives should be defined. In other words, GRs are not a "one-size fits all" solution and careful scientific consideration should guide policymakers in their implementation. There can be trade-offs between ecosystem services that should be evaluated depending on the context and the goal desired. As a case in point, we found that, in northeastern Italy, *Sedum* spp. was one of the least effective solutions for carbon sequestration but one of the most effective species for stormwater retention. All three ecosystem services were significantly affected by both abiotic and biotic design and management parameters year-round, which highlights the need for further research and continuous monitoring on the functioning of these green infrastructures even after implementation.

REFERENCES

Alexandri, E., & Jones, P. (2008). Temperature decreases in an urban canyon due to green walls and green roofs in diverse climates. *Building and Environment*, *43*(4), 480–493. https://doi.org/10.1016/j.buildenv.2006.10.055

Andenæs, E., Kvande, T., Muthanna, T., & Lohne, J. (2018). Performance of Blue-Green Roofs in Cold Climates: A Scoping Review. *Buildings*, *8*(4), 55. https://doi.org/10.3390/buildings8040055

Buffam, I., & Mitchell, M. E. (2015). Nutrient cycling in green roof ecosystems. *Green roof ecosystems*, 107-137.

Charoenkit, S., & Yiemwattana, S. (2016). Living walls and their contribution to improved thermal comfort and carbon emission reduction: A review. *Building and Environment*, *105*, 82–94. https://doi.org/10.1016/j.buildenv.2016.05.031

Dusza, Y., Barot, S., Kraepiel, Y., Lata, J.-C., Abbadie, L., & Raynaud, X. (2017). Multifunctionality is affected by interactions between green roof plant species, substrate depth, and substrate type. *Ecology and Evolution*, *7*(7), 2357–2369. https://doi.org/10.1002/ece3.2691

Eksi, M., Rowe, D. B., Wichman, I. S., & Andresen, J. A. (2017). Effect of substrate depth, vegetation type, and season on green roof thermal properties. *Energy and Buildings*, *145*, 174–187. https://doi.org/10.1016/j.enbuild.2017.04.017

Getter, K. L., Rowe, D. B., Andresen, J. A., & Wichman, I. S. (2011). Seasonal heat flux properties of an extensive green roof in a Midwestern U.S. climate. *Energy and Buildings*, *43*(12), 3548–3557. https://doi.org/10.1016/j.enbuild.2011.09.018

Halim, M. A., Vantellingen, J., Gorgolewski, A. S., Rose, W. K., Drake, J. A. P., Margolis, L., & Thomas, S. C. (2021). Greenhouse gases and green roofs: Carbon dioxide and methane fluxes in relation to substrate characteristics. *Urban Ecosystems*. https://doi.org/10.1007/s11252-021-01166-8

Han, M., & Zhu, B. (2020). Changes in soil greenhouse gas fluxes by land use change from primary forest. *Global Change Biology*, *26*(4), 2656–2667. https://doi.org/10.1111/gcb.14993

Jim, C. Y., & Peng, L. L. H. (2012). Substrate moisture effect on water balance and thermal regime of a tropical extensive green roof. *Ecological Engineering*, *47*, 9–23. https://doi.org/10.1016/j.ecoleng.2012.06.020

Konopka, J., Heusinger, J., & Weber, S. (2021). Extensive Urban Green Roof Shows Consistent Annual Net Uptake of Carbon as Documented by 5 Years of Eddy-Covariance Flux Measurements. *Journal of Geophysical Research: Biogeosciences*, *126*(2). https://doi.org/10.1029/2020JG005879

Li, W. C., & Yeung, K. K. A. (2014). A comprehensive study of green roof performance from environmental perspective. *International Journal of Sustainable Built Environment*, *3*(1), 127–134. https://doi.org/10.1016/j.ijsbe.2014.05.001

Livesley, S. J., Dougherty, B. J., Smith, A. J., Navaud, D., Wylie, L. J., & Arndt, S. K. (2010). Soil-atmosphere exchange of carbon dioxide, methane, and nitrous oxide in urban garden systems: Impact of irrigation, fertilizer, and mulch. *Urban Ecosystems*, *13*(3), 273–293. https://doi.org/10.1007/s11252-009-0119-6

Manso, M., Teotónio, I., Silva, C. M., & Cruz, C. O. (2021). Green roof and green wall benefits and costs: A review of the quantitative evidence. *Renewable and Sustainable Energy Reviews*, *135*, 110111. https://doi.org/10.1016/j.rser.2020.110111

Maucieri, C., Mietto, A., Barbera, A. C., & Borin, M. (2016). Treatment performance and greenhouse gas emission of a pilot hybrid constructed wetland system treating digestate liquid fraction. *Ecological Engineering*, *94*, 406–417. https://doi.org/10.1016/j.ecoleng.2016.05.062

Mitchell, M. E., Hamilton, T. L., Uebel-Niemeier, C., Hopfensperger, K. N., & Buffam, I. (2018). Nitrogen cycling players and processes in green roof ecosystems. *Applied Soil Ecology*, *132*, 114–125. https://doi.org/10.1016/j.apsoil.2018.08.007

Nardini, A., Andri, S., & Crasso, M. (2012). Influence of substrate depth and vegetation type on temperature and water runoff mitigation by extensive green roofs: Shrubs versus herbaceous plants. *Urban Ecosystems*, *15*(3), 697–708. https://doi.org/10.1007/s11252-011-0220-5

Oberndorfer, E., Lundholm, J., Bass, B., Coffman, R. R., Doshi, H., Dunnett, N., Gaffin, S., Köhler, M., Liu, K. K. Y., & Rowe, B. (2007). Green Roofs as Urban Ecosystems: Ecological Structures, Functions, and Services. *BioScience*, *57*(10), 823–833. https://doi.org/10.1641/B571005

Sanchez, L., & Reames, T. G. (2019). Cooling Detroit: A socio-spatial analysis of equity in green roofs as an urban heat island mitigation strategy. *Urban Forestry & Urban Greening*, *44*, 126331. https://doi.org/10.1016/j.ufug.2019.04.014

Shafique, M., Kim, R., & Rafiq, M. (2018). Green roof benefits, opportunities, and challenges – A review. *Renewable and Sustainable Energy Reviews*, *90*, 757–773. https://doi.org/10.1016/j.rser.2018.04.006

Shafique, M., Xue, X., & Luo, X. (2020). An overview of carbon sequestration of green roofs in urban areas. *Urban Forestry & Urban Greening*, *47*, 126515. https://doi.org/10.1016/j.ufug.2019.126515

Teemusk, A., Kull, A., Kanal, A., & Mander, Ü. (2019). Environmental factors affecting greenhouse gas fluxes of green roofs in temperate zone. *Science of The Total Environment*, *694*, 133699. https://doi.org/10.1016/j.scitotenv.2019.133699

Van Mechelen, C., Dutoit, T., & Hermy, M. (2015). Adapting green roof irrigation practices for a sustainable future: A review. *Sustainable Cities and Society*, *19*, 74–90. https://doi.org/10.1016/j.scs.2015.07.007

CHAPTER 5

CONCLUSION

Our studies found that ecosystem services from blue-green roofs (GR) are affected by plant species choice, substrate depth, and summer irrigation regime. In all monitored seasons, all plant species and substrate depth treatments were a significant control for CO_2 fluxes, where GRs mesocosms were a significant CO_2 source during a particular dry-hot summer season. The summer season had hotter than average temperatures and an irregular distribution of rainfall—i.e., June and July received significantly less rainfall than August and September—which resulted in plant stress and death. This dampened the role of photosynthesis while heightening the role of respiration, leading to higher than expected emissions. On a yearly basis, grass treatments (cold and warm season grasses, CG and WG) had lower CO_2 emissions but, considering data only from the hot summer season, drought tolerant *Sedum* spp. had the lowest CO_2 emissions. GRs were a significant carbon sink in fall and winter, which had more frequent rainfall, and were a source once again in spring, which had scant rainfall. Although these atypical meteorological conditions constrain the replicability of our results, in the broader context of climate change and increasing temperatures, it has important implications when implementing GRs for climate change mitigation in cities. Plant species adapted to drought conditions can be a more efficient solution for carbon sequestration in GRs and higher irrigation levels may be needed to allow for adequate plant growth and carbon uptake via photosynthesis to occur. Moreover, our study also showed that, potentially, GRs can also serve as N_2O sinks with higher irrigation levels especially during drought-induced stress conditions, which highlights a potential novel ecosystem service. Overall, our findings suggest that the most important considerations for implementing GRs with the purpose of GHG reduction are plant choice, foremost, and substrate depth.

The thermal benefits of our GRs were consistent during all monitoring seasons, where the deeper substrate depth treatments reduced the jump from minimum to maximum substrate temperatures compared to the shallower substrate depth treatments. Given that the effect of irrigation and plant species was important only during the hottest month in our dry summer season, this can imply that they are important considerations only above a certain threshold temperature or below a threshold substrate moisture content. Given this, the most significant design and management consideration for GRs designed to provide thermal insulation is substrate depth.

The water balance of our GRs indicated that, on a yearly basis, all vegetation treatments were efficient solutions to reduce water outflow. Moreover, deeper substrate depths led to a higher retention of water in all cases. However, there were seasonal differences among the retention of water of the different plant species treatments—where *Sedum* spp. and wildflower (WF) were more consistent across the seasons than warm and cold season grasses (WG and CG). The most important considerations for designing GRs for stormwater management is vegetation—where, plant species with a wider range of growing conditions or stress tolerance mechanisms are more successful than those circumscribed to either hot or cold seasons—and substrate depth.

Ultimately, GRs can be a beneficial solution towards coupling sustainable urban development and climate change adaptation in cities. There is no one singular solution for all three ecosystem services, meaning that there are trade-offs between them. All design and management parameters evaluated significantly affected the selected ecosystem services, meaning that careful consideration of these parameters should be taken when planning and managing a GR system. Moreover, performance of ecosystem services is linked to the meteorological conditions of the site, especially temperature and rainfall, and can be expected to become even more important with the effects of the ongoing climate change crisis.

APPENDIX A

NH_3 FLUX DATA

NH_3 concentration and flux data was measured and calculated for each GR mesocosm during both monitoring periods, in addition to CO_2, CH_4, and N_2O. The raw excel data for the average NH_3 fluxes per mesocosm is shown here (Table A.1).

Table A.1 Flux data for NH_3 (mg m^{-2} h^{-1}) for each of the green roof mesocosms for both monitoring periods (April 2022 – April 2023).

Box	Species	Substrate Depth (cm)	Irrigation Level (L m^{-2})	Date	NH3 (mg m^{-2} h^{-1})
1	Ma	8	1	7/4/2022	-0.256726154
2	Se	14	1	7/4/2022	-0.754774892
3	Se	8	1	7/4/2022	0.682891569
4	Pf	8	1	7/4/2022	-0.083646049
5	Pf	14	1	7/4/2022	0.103250591
6	Mi	8	1	7/4/2022	-0.0667488
7	Ma	14	1	7/4/2022	0.125795815
8	Pf	8	1	7/4/2022	-0.231053538
9	Pf	14	1	7/4/2022	0.182322247
10	Mi	14	1	7/4/2022	-0.121944923
11	Ma	8	1	7/4/2022	-0.074497262
12	Se	14	1	7/4/2022	0.233947542
25	Pf	14	1	7/4/2022	0.188693723
26	Mi	8	1	7/4/2022	-0.471349218
27	Ma	14	1	7/4/2022	0.086259988
28	Se	8	1	7/4/2022	0.517559926
29	Mi	14	1	7/4/2022	0.247997465
30	Ma	8	1	7/4/2022	0.319624062
31	Se	14	1	7/4/2022	0.192544615
32	Mi	8	1	7/4/2022	0.249024369
33	Se	8	1	7/4/2022	0.264427938
34	Ma	14	1	7/4/2022	0.204097292
35	Mi	14	1	7/4/2022	0.3504312
36	Pf	8	1	7/4/2022	-0.154035692
1	Ma	8	1	14/04/2022	-0.335027631
2	Se	14	1	14/04/2022	-0.345039951
3	Se	8	1	14/04/2022	-0.043783479
4	Pf	8	1	14/04/2022	-0.833846548
5	Pf	14	1	14/04/2022	-1.062076098
6	Mi	8	1	14/04/2022	-0.111745893
7	Ma	14	1	14/04/2022	-0.251591631
8	Pf	8	1	14/04/2022	0.14017248
9	Pf	14	1	14/04/2022	0.002613939
10	Mi	14	1	14/04/2022	0.009148787
11	Ma	8	1	14/04/2022	-0.006534848
12	Se	14	1	14/04/2022	-0.429502855

25	Pf	14	1	14/04/2022	-0.082665822
26	Mi	8	1	14/04/2022	-0.28034496
27	Ma	14	1	14/04/2022	-0.098022713
28	Se	8	1	14/04/2022	0.279397048
29	Mi	14	1	14/04/2022	-0.184936186
30	Ma	8	1	14/04/2022	0.184842831
31	Se	14	1	14/04/2022	0.609211163
32	Mi	8	1	14/04/2022	-0.250284661
33	Se	8	1	14/04/2022	0.152261948
34	Ma	14	1	14/04/2022	-0.141152707
35	Mi	14	1	14/04/2022	-0.392090853
36	Pf	8	1	14/04/2022	-0.171866491
1	Ma	8	1	21/04/2022	-0.230680119
2	Se	14	1	21/04/2022	-0.071883323
3	Se	8	1	21/04/2022	0.422314523
4	Pf	8	1	21/04/2022	-0.217447052
5	Pf	14	1	21/04/2022	0.196395508
6	Mi	8	1	21/04/2022	0.156346228
7	Ma	14	1	21/04/2022	0.123228554
8	Pf	8	1	21/04/2022	0.041332911
9	Pf	14	1	21/04/2022	0.170722892
10	Mi	14	1	21/04/2022	-0.120661292
11	Ma	8	1	21/04/2022	-0.134781231
12	Se	14	1	21/04/2022	0.390223754
13	Ma	14	2	21/04/2022	-0.32020753
14	Pf	8	2	21/04/2022	0.043129994
15	Pf	14	2	21/04/2022	-0.380981612
16	Se	14	2	21/04/2022	0.068289157
17	Ma	8	2	21/04/2022	0.028239877
18	Mi	8	2	21/04/2022	0.512168677
19	Mi	14	2	21/04/2022	0.214366338
20	Se	8	2	21/04/2022	-0.093705046
21	Ma	14	2	21/04/2022	-0.251591631
22	Pf	8	2	21/04/2022	0.023105354
23	Mi	14	2	21/04/2022	-0.038508923
24	Ma	8	2	21/04/2022	0.086003262
25	Pf	14	1	21/04/2022	-0.449270769
26	Mi	8	1	21/04/2022	-0.011552677
27	Ma	14	1	21/04/2022	0.168155631
28	Se	8	1	21/04/2022	0.192544615
29	Mi	14	1	21/04/2022	0.087286892
30	Ma	8	1	21/04/2022	-0.107824985
31	Se	14	1	21/04/2022	-0.002567262

32	Mi	8	1	21/04/2022	-0.002567262
33	Se	8	1	21/04/2022	-0.103974092
34	Ma	14	1	21/04/2022	0.178424677
35	Mi	14	1	21/04/2022	-0.019254462
36	Pf	8	1	21/04/2022	-0.279691475
37	Mi	8	2	21/04/2022	0.169439262
38	Mi	14	2	21/04/2022	0.061614277
39	Pf	8	2	21/04/2022	-0.273413354
40	Se	8	2	21/04/2022	-0.019254462
41	Ma	14	2	21/04/2022	-0.125795815
42	Pf	14	2	21/04/2022	-0.380981612
43	Ma	8	2	21/04/2022	0.062897908
44	Se	14	2	21/04/2022	0.023105354
45	Mi	8	2	21/04/2022	-0.449270769
46	Pf	14	2	21/04/2022	0.102433735
47	Se	8	2	21/04/2022	-0.157886585
48	Se	14	2	21/04/2022	5.52E-18
1	Ma	8	1	29/04/2022	-0.037248631
2	Se	14	1	29/04/2022	0.056199689
3	Se	8	1	29/04/2022	-0.009425261
4	Pf	8	1	29/04/2022	0.21025872
5	Pf	14	1	29/04/2022	0.071556581
6	Mi	8	1	29/04/2022	-0.104230818
7	Ma	14	1	29/04/2022	0.037738745
8	Pf	8	1	29/04/2022	-0.241322585
9	Pf	14	1	29/04/2022	-0.28034496
10	Mi	14	1	29/04/2022	0.125469073
11	Ma	8	1	29/04/2022	0
12	Se	14	1	29/04/2022	1.148849538
13	Ma	14	2	29/04/2022	-0.161737477
14	Pf	8	2	29/04/2022	0.111419151
15	Pf	14	2	29/04/2022	0.038986965
16	Se	14	2	29/04/2022	-0.043129994
17	Ma	8	2	29/04/2022	-0.095408774
18	Mi	8	2	29/04/2022	0.244403298
19	Mi	14	2	29/04/2022	0.167128726
20	Se	8	2	29/04/2022	0.522951175
21	Ma	14	2	29/04/2022	0.028753329
22	Pf	8	2	29/04/2022	0
23	Mi	14	2	29/04/2022	0
24	Ma	8	2	29/04/2022	-0.602022831
25	Pf	14	1	29/04/2022	-0.606900628
26	Mi	8	1	29/04/2022	-0.418720357

27	Ma	14	1	29/04/2022	-0.471092492
28	Se	8	1	29/04/2022	-0.077274572
29	Mi	14	1	29/04/2022	0.0166872
30	Ma	8	1	29/04/2022	0.442409179
31	Se	14	1	29/04/2022	-0.007188332
32	Mi	8	1	29/04/2022	0.111419151
33	Se	8	1	29/04/2022	0.284966031
34	Ma	14	1	29/04/2022	0.310895372
35	Mi	14	1	29/04/2022	0.079071655
36	Pf	8	1	29/04/2022	0.394704792
37	Mi	8	2	29/04/2022	-0.636680862
38	Mi	14	2	29/04/2022	0.722427397
39	Pf	8	2	29/04/2022	-0.643355742
40	Se	8	2	29/04/2022	-0.643355742
41	Ma	14	2	29/04/2022	0.445676603
42	Pf	14	2	29/04/2022	0.481361538
43	Ma	8	2	29/04/2022	0.812538277
44	Se	14	2	29/04/2022	-0.158143311
45	Mi	8	2	29/04/2022	0.077764686
46	Pf	14	2	29/04/2022	-0.082665822
47	Se	8	2	29/04/2022	0.539124923
48	Se	14	2	29/04/2022	-0.648746991
1	Ma	8	1	5/5/2022	-0.285572838
2	Se	14	1	5/5/2022	-0.147788091
3	Se	8	1	5/5/2022	0.091236525
4	Pf	8	1	5/5/2022	-0.007188332
5	Pf	14	1	5/5/2022	-0.096137661
6	Mi	8	1	5/5/2022	-0.001777335
7	Ma	14	1	5/5/2022	-0.102923849
8	Pf	8	1	5/5/2022	0.046210708
9	Pf	14	1	5/5/2022	0.072536808
10	Mi	14	1	5/5/2022	0.046595797
11	Ma	8	1	5/5/2022	-0.055420534
12	Se	14	1	5/5/2022	-0.277856691
13	Ma	14	2	5/5/2022	-0.131522783
14	Pf	8	2	5/5/2022	-0.10841743
15	Pf	14	2	5/5/2022	0.08633539
16	Se	14	2	5/5/2022	0.019604543
17	Ma	8	2	5/5/2022	0.053912492
18	Mi	8	2	5/5/2022	-0.035288177
19	Mi	14	2	5/5/2022	-0.150301494
20	Se	8	2	5/5/2022	-0.139192253
21	Ma	14	2	5/5/2022	0.144420131

22	Pf	8	2	5/5/2022	0.032584473
23	Mi	14	2	5/5/2022	0.312541651
24	Ma	8	2	5/5/2022	0.09538364
25	Pf	14	1	5/5/2022	0.154549145
26	Mi	8	1	5/5/2022	0.083646049
27	Ma	14	1	5/5/2022	0.128205092
28	Se	8	1	5/5/2022	0.224472013
29	Mi	14	1	5/5/2022	-0.002940681
30	Ma	8	1	5/5/2022	0.231484408
31	Se	14	1	5/5/2022	-0.166261602
32	Mi	8	1	5/5/2022	-0.295576182
33	Se	8	1	5/5/2022	0.241286679
34	Ma	14	1	5/5/2022	-0.431299938
35	Mi	14	1	5/5/2022	0.123508619
36	Pf	8	1	5/5/2022	-0.073612847
37	Mi	8	2	5/5/2022	-0.118607483
38	Mi	14	2	5/5/2022	-0.142459677
39	Pf	8	2	5/5/2022	-0.118015038
40	Se	8	2	5/5/2022	0.339158588
41	Ma	14	2	5/5/2022	-0.033327723
42	Pf	14	2	5/5/2022	0.031044116
43	Ma	8	2	5/5/2022	0.076457716
44	Se	14	2	5/5/2022	0.022512909
45	Mi	8	2	5/5/2022	0.069922869
46	Pf	14	2	5/5/2022	0.086259988
47	Se	8	2	5/5/2022	-0.131522783
48	Se	14	2	5/5/2022	0.092367557
1	Ma	8	1	12/5/2022	-0.512168677
2	Se	14	1	12/5/2022	0.06120892
3	Se	8	1	12/5/2022	0.035288177
4	Pf	8	1	12/5/2022	0.261720644
5	Pf	14	1	12/5/2022	-0.196045427
6	Mi	8	1	12/5/2022	0.912264718
7	Ma	14	1	12/5/2022	0.311626054
8	Pf	8	1	12/5/2022	-0.02744636
9	Pf	14	1	12/5/2022	0.25420557
10	Mi	14	1	12/5/2022	-0.619993662
11	Ma	8	1	12/5/2022	0.051625296
12	Se	14	1	12/5/2022	-0.172519975
13	Ma	14	2	12/5/2022	0.021564997
14	Pf	8	2	12/5/2022	0.009802271
15	Pf	14	2	12/5/2022	0.014376665
16	Se	14	2	12/5/2022	-0.06600196

17	Ma	8	2	12/5/2022	-0.179054823
18	Mi	8	2	12/5/2022	0.084827348
19	Mi	14	2	12/5/2022	-0.011848899
20	Se	8	2	12/5/2022	0.265968295
21	Ma	14	2	12/5/2022	-0.049011357
22	Pf	8	2	12/5/2022	0.29406814
23	Mi	14	2	12/5/2022	0.29406814
24	Ma	8	2	12/5/2022	-0.293691129
25	Pf	14	1	12/5/2022	0.56068992
26	Mi	8	1	12/5/2022	-0.702402757
27	Ma	14	1	12/5/2022	-0.106027902
28	Se	8	1	12/5/2022	0.37248631
29	Mi	14	1	12/5/2022	0.039535828
30	Ma	8	1	12/5/2022	0.254158892
31	Se	14	1	12/5/2022	0.219500862
32	Mi	8	1	12/5/2022	-0.368402031
33	Se	8	1	12/5/2022	0.22806618
34	Ma	14	1	12/5/2022	0.14017248
35	Mi	14	1	12/5/2022	-0.128409754
36	Pf	8	1	12/5/2022	0.071229838
37	Mi	8	2	12/5/2022	-0.339812073
38	Mi	14	2	12/5/2022	-0.04297919
39	Pf	8	2	12/5/2022	-0.371996197
40	Se	8	2	12/5/2022	-0.005391249
41	Ma	14	2	12/5/2022	-0.130696951
42	Pf	14	2	12/5/2022	-0.400749526
43	Ma	8	2	12/5/2022	-0.237214966
44	Se	14	2	12/5/2022	0.041332911
45	Mi	8	2	12/5/2022	0.190164064
46	Pf	14	2	12/5/2022	0.609724615
47	Se	8	2	12/5/2022	0.269889204
48	Se	14	2	12/5/2022	-0.227412695
1	Ma	8	1	19/05/2022	-0.086947108
2	Se	14	1	19/05/2022	0.183302474
3	Se	8	1	19/05/2022	-0.113216234
4	Pf	8	1	19/05/2022	0.7008624
5	Pf	14	1	19/05/2022	-0.546313255
6	Mi	8	1	19/05/2022	0.580457834
7	Ma	14	1	19/05/2022	-1.100071569
8	Pf	8	1	19/05/2022	0.43243097
9	Pf	14	1	19/05/2022	-0.753467923
10	Mi	14	1	19/05/2022	-0.497955383
11	Ma	8	1	19/05/2022	2.487162978

12	Se	14	1	19/05/2022	-0.743992394
13	Ma	14	2	19/05/2022	-0.118934225
14	Pf	8	2	19/05/2022	0.047050902
15	Pf	14	2	19/05/2022	-0.16353456
16	Se	14	2	19/05/2022	-0.445676603
17	Ma	8	2	19/05/2022	0.531936591
18	Mi	8	2	19/05/2022	1.173005136
19	Mi	14	2	19/05/2022	-1.288508566
20	Se	8	2	19/05/2022	-0.048357872
21	Ma	14	2	19/05/2022	2.230016727
22	Pf	8	2	19/05/2022	0.000980227
23	Mi	14	2	19/05/2022	-0.26662178
24	Ma	8	2	19/05/2022	-0.064694991
25	Pf	14	1	19/05/2022	0.309355015
26	Mi	8	1	19/05/2022	-0.28034496
27	Ma	14	1	19/05/2022	0.172519975
28	Se	8	1	19/05/2022	-0.113706347
29	Mi	14	1	19/05/2022	-0.003850892
30	Ma	8	1	19/05/2022	0.246200382
31	Se	14	1	19/05/2022	-0.742195311
32	Mi	8	1	19/05/2022	-0.916512369
33	Se	8	1	19/05/2022	-0.431299938
34	Ma	14	1	19/05/2022	-0.01372318
35	Mi	14	1	19/05/2022	0.02744636
36	Pf	8	1	19/05/2022	-0.358763131
37	Mi	8	2	19/05/2022	0.079071655
38	Mi	14	2	19/05/2022	0.705996923
39	Pf	8	2	19/05/2022	-0.251591631
40	Se	8	2	19/05/2022	0.09344832
41	Ma	14	2	19/05/2022	-0.544516172
42	Pf	14	2	19/05/2022	-0.65283127
43	Ma	8	2	19/05/2022	0.921903618
44	Se	14	2	19/05/2022	0.351901541
45	Mi	8	2	19/05/2022	0.095408774
46	Pf	14	2	19/05/2022	-0.02058477
47	Se	8	2	19/05/2022	0.305830865
48	Se	14	2	19/05/2022	0.212709288
1	Ma	8	1	26/05/2022	-0.284265869
2	Se	14	1	26/05/2022	-0.241135875
3	Se	8	1	26/05/2022	-0.777880246
4	Pf	8	1	26/05/2022	-0.380981612
5	Pf	14	1	26/05/2022	0.594321046
6	Mi	8	1	26/05/2022	-0.029406814

7	Ma	14	1	26/05/2022	0.875179458
8	Pf	8	1	26/05/2022	0.693020583
9	Pf	14	1	26/05/2022	0.715239065
10	Mi	14	1	26/05/2022	0.043129994
11	Ma	8	1	26/05/2022	-0.07008624
12	Se	14	1	26/05/2022	0.046397418
13	Ma	14	2	26/05/2022	0.33393071
14	Pf	8	2	26/05/2022	-0.039535828
15	Pf	14	2	26/05/2022	0.262374129
16	Se	14	2	26/05/2022	-0.07008624
17	Ma	8	2	26/05/2022	0.381238338
18	Mi	8	2	26/05/2022	0.292972234
19	Mi	14	2	26/05/2022	0.132984148
20	Se	8	2	26/05/2022	0.485212431
21	Ma	14	2	26/05/2022	-1.096734129
22	Pf	8	2	26/05/2022	-0.662633542
23	Mi	14	2	26/05/2022	0.945265698
24	Ma	8	2	26/05/2022	0.618196578
25	Pf	14	1	26/05/2022	0.080868738
26	Mi	8	1	26/05/2022	-0.258779963
27	Ma	14	1	26/05/2022	0.376103815
28	Se	8	1	26/05/2022	-0.585849083
29	Mi	14	1	26/05/2022	0.149157895
30	Ma	8	1	26/05/2022	-0.435150831
31	Se	14	1	26/05/2022	0.722684123
32	Mi	8	1	26/05/2022	0.246200382
33	Se	8	1	26/05/2022	-0.350267829
34	Ma	14	1	26/05/2022	-0.806120123
35	Mi	14	1	26/05/2022	-0.376103815
36	Pf	8	1	26/05/2022	0.258779963
37	Mi	8	2	26/05/2022	1.045902351
38	Mi	14	2	26/05/2022	-0.177141046
39	Pf	8	2	26/05/2022	0.300112874
40	Se	8	2	26/05/2022	-0.7008624
41	Ma	14	2	26/05/2022	0.305830865
42	Pf	14	2	26/05/2022	0.987112062
43	Ma	8	2	26/05/2022	-0.316286622
44	Se	14	2	26/05/2022	0.075734215
45	Mi	8	2	26/05/2022	0.512168677
46	Pf	14	2	26/05/2022	0.472632849
47	Se	8	2	26/05/2022	-0.506777428
48	Se	14	2	26/05/2022	0.706253649
1	Ma	8	1	1/6/2022	-0.451557966

2	Se	14	1	1/6/2022	-0.141199385
3	Se	8	1	1/6/2022	-0.240809132
4	Pf	8	1	1/6/2022	0.007163198
5	Pf	14	1	1/6/2022	-0.274953711
6	Mi	8	1	1/6/2022	0.273156628
7	Ma	14	1	1/6/2022	0.838210892
8	Pf	8	1	1/6/2022	-0.308071385
9	Pf	14	1	1/6/2022	0.51396576
10	Mi	14	1	1/6/2022	-0.309355015
11	Ma	8	1	1/6/2022	-0.166872
12	Se	14	1	1/6/2022	-0.150954978
13	Ma	14	2	1/6/2022	0.147360812
14	Pf	8	2	1/6/2022	0.032347495
15	Pf	14	2	1/6/2022	-0.021821723
16	Se	14	2	1/6/2022	-0.115013317
17	Ma	8	2	1/6/2022	-0.007188332
18	Mi	8	2	1/6/2022	0.094101805
19	Mi	14	2	1/6/2022	-1.038714018
20	Se	8	2	1/6/2022	0.186126462
21	Ma	14	2	1/6/2022	1.754723262
22	Pf	8	2	1/6/2022	-0.452864935
23	Mi	14	2	1/6/2022	0.598428665
24	Ma	8	2	1/6/2022	-0.202813662
25	Pf	14	1	1/6/2022	-0.985828431
26	Mi	8	1	1/6/2022	0.821523692
27	Ma	14	1	1/6/2022	0.154035692
28	Se	8	1	1/6/2022	-0.576350215
29	Mi	14	1	1/6/2022	-1.039740923
30	Ma	8	1	1/6/2022	-0.327325846
31	Se	14	1	1/6/2022	-0.064181538
32	Mi	8	1	1/6/2022	-0.238755323
33	Se	8	1	1/6/2022	-0.405627323
34	Ma	14	1	1/6/2022	0.204867471
35	Mi	14	1	1/6/2022	1.173495249
36	Pf	8	1	1/6/2022	0.971708492
37	Mi	8	2	1/6/2022	0.238755323
38	Mi	14	2	1/6/2022	0.190490806
39	Pf	8	2	1/6/2022	0.007701785
40	Se	8	2	1/6/2022	-0.319880788
41	Ma	14	2	1/6/2022	-0.154035692
42	Pf	14	2	1/6/2022	0.071883323
43	Ma	8	2	1/6/2022	0.201530031
44	Se	14	2	1/6/2022	0.071883323

45	Mi	8	2	1/6/2022	0.304220492
46	Pf	14	2	1/6/2022	0.015403569
47	Se	8	2	1/6/2022	-0.654651692
48	Se	14	2	1/6/2022	0.071883323
1	Ma	8	1	15/06/2022	-12.70409372
2	Se	14	1	15/06/2022	-1.001138645
3	Se	8	1	15/06/2022	4.952247508
4	Pf	8	1	15/06/2022	-0.729615729
5	Pf	14	1	15/06/2022	-1.309303385
6	Mi	8	1	15/06/2022	2.699475508
7	Ma	14	1	15/06/2022	-2.071780062
8	Pf	8	1	15/06/2022	16.31623071
9	Pf	14	1	15/06/2022	1.999896738
10	Mi	14	1	15/06/2022	-1.473608123
11	Ma	8	1	15/06/2022	-2.012733046
12	Se	14	1	15/06/2022	0.659786215
13	Ma	14	2	15/06/2022	-2.600635938
14	Pf	8	2	15/06/2022	0.115013317
15	Pf	14	2	15/06/2022	-0.937050462
16	Se	14	2	15/06/2022	-0.962723077
17	Ma	8	2	15/06/2022	-1.515967938
18	Mi	8	2	15/06/2022	-1.320856062
19	Mi	14	2	15/06/2022	-1.313667729
20	Se	8	2	15/06/2022	-0.311922277
21	Ma	14	2	15/06/2022	-2.131340529
22	Pf	8	2	15/06/2022	-0.621464002
23	Mi	14	2	15/06/2022	0.354025366
24	Ma	8	2	15/06/2022	-0.190490806
25	Pf	14	1	15/06/2022	0.2002464
26	Mi	8	1	15/06/2022	0.502156357
27	Ma	14	1	15/06/2022	-0.24029568
28	Se	8	1	15/06/2022	-0.034658031
29	Mi	14	1	15/06/2022	-0.569932062
30	Ma	8	1	15/06/2022	-1.486444431
31	Se	14	1	15/06/2022	-0.209488542
32	Mi	8	1	15/06/2022	3.219345969
33	Se	8	1	15/06/2022	6.585025846
34	Ma	14	1	15/06/2022	-1.106489723
35	Mi	14	1	15/06/2022	1.447935508
36	Pf	8	1	15/06/2022	-1.200778238
37	Mi	8	2	15/06/2022	0.003080714
38	Mi	14	2	15/06/2022	-0.862599877
39	Pf	8	2	15/06/2022	0.188693723

40	Se	8	2	15/06/2022	0.138632123
41	Ma	14	2	15/06/2022	0.019254462
42	Pf	14	2	15/06/2022	-1.216881969
43	Ma	8	2	15/06/2022	0.311922277
44	Se	14	2	15/06/2022	-3.057608492
45	Mi	8	2	15/06/2022	-0.364551138
46	Pf	14	2	15/06/2022	-0.762476677
47	Se	8	2	15/06/2022	-1.471040862
48	Se	14	2	15/06/2022	5.516718304
1	Ma	8	1	23/06/2022	-0.916512369
2	Se	14	1	23/06/2022	0.15945028
3	Se	8	1	23/06/2022	0.398952443
4	Pf	8	1	23/06/2022	0.482645169
5	Pf	14	1	23/06/2022	-0.436691188
6	Mi	8	1	23/06/2022	0.328609477
7	Ma	14	1	23/06/2022	-1.560895015
8	Pf	8	1	23/06/2022	-0.158143311
9	Pf	14	1	23/06/2022	0.154035692
10	Mi	14	1	23/06/2022	-0.491630585
11	Ma	8	1	23/06/2022	-0.409478215
12	Se	14	1	23/06/2022	0.111419151
13	Ma	14	2	23/06/2022	-0.449270769
14	Pf	8	2	23/06/2022	0.245056783
15	Pf	14	2	23/06/2022	-0.230680119
16	Se	14	2	23/06/2022	0.391507385
17	Ma	8	2	23/06/2022	0.311712228
18	Mi	8	2	23/06/2022	-0.604590092
19	Mi	14	2	23/06/2022	1.583486917
20	Se	8	2	23/06/2022	0.837440714
21	Ma	14	2	23/06/2022	0.854898092
22	Pf	8	2	23/06/2022	0.1168104
23	Mi	14	2	23/06/2022	-0.134781231
24	Ma	8	2	23/06/2022	0.287533292
25	Pf	14	1	23/06/2022	0.138632123
26	Mi	8	1	23/06/2022	0.078301477
28	Se	8	1	23/06/2022	-0.723967754
29	Mi	14	1	23/06/2022	-0.089340702
30	Ma	8	1	23/06/2022	-0.354282092
31	Se	14	1	23/06/2022	0.008985415
32	Mi	8	1	23/06/2022	-0.147874265
33	Se	8	1	23/06/2022	0.539124923
34	Ma	14	1	23/06/2022	1.099814843
35	Mi	14	1	23/06/2022	-0.041076185

36	Pf	8	1	23/06/2022	-0.203070388
37	Mi	8	2	23/06/2022	0.006161428
38	Mi	14	2	23/06/2022	0.735520431
39	Pf	8	2	23/06/2022	0.839494523
40	Se	8	2	23/06/2022	0.495994929
41	Ma	14	2	23/06/2022	0.566851348
42	Pf	14	2	23/06/2022	0.495994929
43	Ma	8	2	23/06/2022	-0.154035692
44	Se	14	2	23/06/2022	0.422057797
45	Mi	8	2	23/06/2022	0.677757046
46	Pf	14	2	23/06/2022	0.754774892
47	Se	8	2	23/06/2022	0.268278831
48	Se	14	2	23/06/2022	0.296518708
1	Ma	8	1	30/06/2022	-0.122201649
2	Se	14	1	30/06/2022	-0.202454604
3	Se	8	1	30/06/2022	0.245173477
4	Pf	8	1	30/06/2022	0.112959508
5	Pf	14	1	30/06/2022	-0.025672615
6	Mi	8	1	30/06/2022	-0.313205908
7	Ma	14	1	30/06/2022	-0.046210708
8	Pf	8	1	30/06/2022	-2.227099385
9	Pf	14	1	30/06/2022	-0.730385908
10	Mi	14	1	30/06/2022	-0.295235077
11	Ma	8	1	30/06/2022	0.386372862
12	Se	14	1	30/06/2022	2.8701984
13	Ma	14	2	30/06/2022	0.061614277
14	Pf	8	2	30/06/2022	-0.252875262
15	Pf	14	2	30/06/2022	0.839494523
16	Se	14	2	30/06/2022	1.170671262
17	Ma	8	2	30/06/2022	0.424881785
18	Mi	8	2	30/06/2022	0.322191323
19	Mi	14	2	30/06/2022	1.119326031
20	Se	8	2	30/06/2022	3.093550154
21	Ma	14	2	30/06/2022	0.365834769
22	Pf	8	2	30/06/2022	0.191260985
23	Mi	14	2	30/06/2022	0.912661477
24	Ma	8	2	30/06/2022	0.260577046
25	Pf	14	1	30/06/2022	-2.145717194
26	Mi	8	1	30/06/2022	-0.142483015
27	Ma	14	1	30/06/2022	-0.628465625
28	Se	8	1	30/06/2022	-1.759857785
29	Mi	14	1	30/06/2022	-1.623536197
30	Ma	8	1	30/06/2022	-0.2002464

31	Se	14	1	30/06/2022	-0.8009856
32	Mi	8	1	30/06/2022	-0.616142769
33	Se	8	1	30/06/2022	-2.529266068
34	Ma	14	1	30/06/2022	0.385089231
35	Mi	14	1	30/06/2022	-1.5519096
36	Pf	8	1	30/06/2022	-0.921903618
37	Mi	8	2	30/06/2022	1.250769822
38	Mi	14	2	30/06/2022	3.4542504
39	Pf	8	2	30/06/2022	-0.357362806
40	Se	8	2	30/06/2022	3.319469169
41	Ma	14	2	30/06/2022	1.934688295
42	Pf	14	2	30/06/2022	2.44300608
43	Ma	8	2	30/06/2022	-3.731514646
44	Se	14	2	30/06/2022	8.907113908
45	Mi	8	2	30/06/2022	2.229666646
46	Pf	14	2	30/06/2022	3.647565194
47	Se	8	2	30/06/2022	3.030652246
48	Se	14	2	30/06/2022	0.4505544
1	Ma	8	1	7/7/2022	-0.039792554
2	Se	14	1	7/7/2022	0.428732677
3	Se	8	1	7/7/2022	0.3170568
4	Pf	8	1	7/7/2022	0.125795815
5	Pf	14	1	7/7/2022	0.423598154
6	Mi	8	1	7/7/2022	0.336311262
7	Ma	14	1	7/7/2022	-0.566081169
8	Pf	8	1	7/7/2022	-0.254158892
9	Pf	14	1	7/7/2022	-1.455637292
10	Mi	14	1	7/7/2022	-0.824090954
11	Ma	8	1	7/7/2022	-0.035941662
12	Se	14	1	7/7/2022	-0.398952443
13	Ma	14	2	7/7/2022	-0.378671077
14	Pf	8	2	7/7/2022	0.820240062
15	Pf	14	2	7/7/2022	0.388940123
16	Se	14	2	7/7/2022	0.015403569
17	Ma	8	2	7/7/2022	-1.210463815
18	Mi	8	2	7/7/2022	1.089802523
19	Mi	14	2	7/7/2022	1.736752431
20	Se	8	2	7/7/2022	3.668616738
21	Ma	14	2	7/7/2022	-0.666204369
22	Pf	8	2	7/7/2022	0.164304738
23	Mi	14	2	7/7/2022	-0.065465169
24	Ma	8	2	7/7/2022	-0.065465169
25	Pf	14	1	7/7/2022	0.366604948

26	Mi	8	1	7/7/2022	-4.399259372
27	Ma	14	1	7/7/2022	3.012938142
28	Se	8	1	7/7/2022	-0.345039951
29	Mi	14	1	7/7/2022	-0.046210708
30	Ma	8	1	7/7/2022	0.166358548
31	Se	14	1	7/7/2022	-0.720116862
32	Mi	8	1	7/7/2022	0.473659754
33	Se	8	1	7/7/2022	-1.424830154
34	Ma	14	1	7/7/2022	-0.1168104
35	Mi	14	1	7/7/2022	-0.326042215
36	Pf	8	1	7/7/2022	0.003850892
37	Mi	8	2	7/7/2022	1.455637292
38	Mi	14	2	7/7/2022	0.659272763
39	Pf	8	2	7/7/2022	-0.283425674
40	Se	8	2	7/7/2022	0.118607483
41	Ma	14	2	7/7/2022	-0.157116406
42	Pf	14	2	7/7/2022	0.465187791
43	Ma	8	2	7/7/2022	-2.306684492
44	Se	14	2	7/7/2022	2.221194683
45	Mi	8	2	7/7/2022	0.847196308
46	Pf	14	2	7/7/2022	-0.111675877
47	Se	8	2	7/7/2022	0.204097292
48	Se	14	2	7/7/2022	-0.186126462
1	Ma	8	1	21/07/2022	0.161737477
2	Se	14	1	21/07/2022	-0.465281146
3	Se	8	1	21/07/2022	0.615582639
4	Pf	8	1	21/07/2022	-0.775686404
5	Pf	14	1	21/07/2022	-0.909324037
6	Mi	8	1	21/07/2022	0.203233759
7	Ma	14	1	21/07/2022	0.230026634
8	Pf	8	1	21/07/2022	0.805093218
9	Pf	14	1	21/07/2022	-0.07008624
10	Mi	14	1	21/07/2022	1.656583855
11	Ma	8	1	21/07/2022	-0.426725545
12	Se	14	1	21/07/2022	0.387189717
13	Ma	14	2	21/07/2022	-0.175133914
14	Pf	8	2	21/07/2022	-1.423214395
15	Pf	14	2	21/07/2022	0.400749526
16	Se	14	2	21/07/2022	1.74937869
17	Ma	8	2	21/07/2022	0.207154667
18	Mi	8	2	21/07/2022	0.059303742
19	Mi	14	2	21/07/2022	0.709847815
20	Se	8	2	21/07/2022	-0.620157033

21	Ma	14	2	21/07/2022	-0.054892719
22	Pf	8	2	21/07/2022	-0.206664554
23	Mi	14	2	21/07/2022	1.319058978
24	Ma	8	2	21/07/2022	0.151608463
25	Pf	14	1	21/07/2022	0.025672615
26	Mi	8	1	21/07/2022	-0.422314523
27	Ma	14	1	21/07/2022	0.118280741
28	Se	8	1	21/07/2022	0.115526769
29	Mi	14	1	21/07/2022	1.085951631
30	Ma	8	1	21/07/2022	-0.262374129
31	Se	14	1	21/07/2022	0.358132985
32	Mi	8	1	21/07/2022	0.754774892
33	Se	8	1	21/07/2022	-0.204097292
34	Ma	14	1	21/07/2022	1.062076098
35	Mi	14	1	21/07/2022	0.172519975
36	Pf	8	1	21/07/2022	-0.186243155
37	Mi	8	2	21/07/2022	0.199476222
38	Mi	14	2	21/07/2022	3.020896652
39	Pf	8	2	21/07/2022	-0.211799077
40	Se	8	2	21/07/2022	-0.183302474
41	Ma	14	2	21/07/2022	-0.947319508
42	Pf	14	2	21/07/2022	2.313102646
43	Ma	8	2	21/07/2022	0.763760308
44	Se	14	2	21/07/2022	-0.039792554
45	Mi	8	2	21/07/2022	3.646795015
46	Pf	14	2	21/07/2022	0.603306462
47	Se	8	2	21/07/2022	0.100636652
48	Se	14	2	21/07/2022	0.328702832
1	Ma	8	1	28/07/2022	-0.301909957
2	Se	14	1	28/07/2022	-0.125544475
3	Se	8	1	28/07/2022	0.283612384
4	Pf	8	1	28/07/2022	0.395358277
5	Pf	14	1	28/07/2022	-0.445676603
6	Mi	8	1	28/07/2022	0.321677871
7	Ma	14	1	28/07/2022	0.118607483
8	Pf	8	1	28/07/2022	0.686485735
9	Pf	14	1	28/07/2022	-0.166638613
10	Mi	14	1	28/07/2022	0.316940106
11	Ma	8	1	28/07/2022	0.096715744
12	Se	14	1	28/07/2022	-0.123508619
13	Ma	14	2	28/07/2022	0.073517035
14	Pf	8	2	28/07/2022	0.116973771
15	Pf	14	2	28/07/2022	0.006534848

16	Se	14	2	28/07/2022	-0.267765378
17	Ma	8	2	28/07/2022	0.107824985
18	Mi	8	2	28/07/2022	0.198659366
19	Mi	14	2	28/07/2022	0.183302474
20	Se	8	2	28/07/2022	0.375590363
21	Ma	14	2	28/07/2022	0.576863668
22	Pf	8	2	28/07/2022	0.255185797
23	Mi	14	2	28/07/2022	0.057833401
24	Ma	8	2	28/07/2022	0.288186777
25	Pf	14	1	28/07/2022	-0.331176738
26	Mi	8	1	28/07/2022	0.277077536
27	Ma	14	1	28/07/2022	-0.091137785
28	Se	8	1	28/07/2022	-2.264324677
29	Mi	14	1	28/07/2022	3.492759323
30	Ma	8	1	28/07/2022	0.086259988
31	Se	14	1	28/07/2022	0.138375397
32	Mi	8	1	28/07/2022	0.4004928
33	Se	8	1	28/07/2022	-0.035941662
34	Ma	14	1	28/07/2022	0.2669952
35	Mi	14	1	28/07/2022	0.37379328
36	Pf	8	1	28/07/2022	0.160103765
37	Mi	8	2	28/07/2022	-0.177141046
38	Mi	14	2	28/07/2022	0.048777969
39	Pf	8	2	28/07/2022	-0.154549145
40	Se	8	2	28/07/2022	1.133702695
41	Ma	14	2	28/07/2022	-4.25745318
42	Pf	14	2	28/07/2022	2.157153177
43	Ma	8	2	28/07/2022	-0.075734215
44	Se	14	2	28/07/2022	0.313205908
45	Mi	8	2	28/07/2022	-0.549393969
46	Pf	14	2	28/07/2022	0.810647839
47	Se	8	2	28/07/2022	-0.041332911
48	Se	14	2	28/07/2022	0.115666802
1	Ma	8	1	4/8/2022	0.216956939
2	Se	14	1	4/8/2022	-0.16075725
3	Se	8	1	4/8/2022	0.830252382
4	Pf	8	1	4/8/2022	0.651851043
5	Pf	14	1	4/8/2022	0.056199689
6	Mi	8	1	4/8/2022	-2.470989231
7	Ma	14	1	4/8/2022	0.222838302
8	Pf	8	1	4/8/2022	0.571472418
9	Pf	14	1	4/8/2022	0.16353456
10	Mi	14	1	4/8/2022	2.248921108

11	Ma	8	1	4/8/2022	-0.035941662
12	Se	14	1	4/8/2022	0.64041506
13	Ma	14	2	4/8/2022	-0.089854154
14	Pf	8	2	4/8/2022	0.128560559
15	Pf	14	2	4/8/2022	0.683545054
16	Se	14	2	4/8/2022	0.526055228
17	Ma	8	2	4/8/2022	-0.102433735
18	Mi	8	2	4/8/2022	2.972375409
19	Mi	14	2	4/8/2022	1.874847763
20	Se	8	2	4/8/2022	-1.248972738
21	Ma	14	2	4/8/2022	1.042308185
22	Pf	8	2	4/8/2022	-0.016173748
23	Mi	14	2	4/8/2022	4.519663938
24	Ma	8	2	4/8/2022	-0.796107803
25	Pf	14	1	4/8/2022	-0.115526769
26	Mi	8	1	4/8/2022	-2.699475508
27	Ma	14	1	4/8/2022	2.048674708
28	Se	8	1	4/8/2022	0.6007392
29	Mi	14	1	4/8/2022	3.111520985
30	Ma	8	1	4/8/2022	0.748356738
31	Se	14	1	4/8/2022	-0.698295138
32	Mi	8	1	4/8/2022	0.827941846
33	Se	8	1	4/8/2022	0.518586831
34	Ma	14	1	4/8/2022	3.108953723
35	Mi	14	1	4/8/2022	0.627695446
36	Pf	8	1	4/8/2022	-0.088057071
37	Mi	8	2	4/8/2022	1.721348862
38	Mi	14	2	4/8/2022	10.33579495
39	Pf	8	2	4/8/2022	0.138632123
40	Se	8	2	4/8/2022	2.201426769
41	Ma	14	2	4/8/2022	0.050318326
42	Pf	14	2	4/8/2022	0.812538277
43	Ma	8	2	4/8/2022	3.590315262
44	Se	14	2	4/8/2022	2.685355569
45	Mi	8	2	4/8/2022	1.243838215
46	Pf	14	2	4/8/2022	1.609672985
47	Se	8	2	4/8/2022	1.102638831
48	Se	14	2	4/8/2022	-0.4338672
1	Ma	8	1	25/08/2022	0.017644088
2	Se	14	1	25/08/2022	0.221531332
3	Se	8	1	25/08/2022	0.737784289
4	Pf	8	1	25/08/2022	0.080680233
5	Pf	14	1	25/08/2022	-0.130696951

6	Mi	8	1	25/08/2022	0.555788784
7	Ma	14	1	25/08/2022	0.370199114
8	Pf	8	1	25/08/2022	0.650544074
9	Pf	14	1	25/08/2022	0.104557561
10	Mi	14	1	25/08/2022	-0.200192541
11	Ma	8	1	25/08/2022	-0.090180896
12	Se	14	1	25/08/2022	-0.168925809
13	Ma	14	2	25/08/2022	0
14	Pf	8	2	25/08/2022	-0.083319306
15	Pf	14	2	25/08/2022	-0.395358277
16	Se	14	2	25/08/2022	-0.226105725
17	Ma	8	2	25/08/2022	-0.100042129
18	Mi	8	2	25/08/2022	-0.101943622
19	Mi	14	2	25/08/2022	-0.411532025
20	Se	8	2	25/08/2022	-0.244403298
21	Ma	14	2	25/08/2022	0.073463176
22	Pf	8	2	25/08/2022	-0.079398398
23	Mi	14	2	25/08/2022	0.033769363
24	Ma	8	2	25/08/2022	-0.495994929
25	Pf	14	1	25/08/2022	0.138632123
26	Mi	8	1	25/08/2022	-0.042359815
27	Ma	14	1	25/08/2022	0.566081169
28	Se	8	1	25/08/2022	-0.635397231
29	Mi	14	1	25/08/2022	0.435150831
30	Ma	8	1	25/08/2022	-0.388940123
31	Se	14	1	25/08/2022	-0.146380585
32	Mi	8	1	25/08/2022	0.295235077
33	Se	8	1	25/08/2022	1.083641095
34	Ma	14	1	25/08/2022	0.321677871
35	Mi	14	1	25/08/2022	0.809667612
36	Pf	8	1	25/08/2022	0.8273117
37	Mi	8	2	25/08/2022	-2.87353584
38	Mi	14	2	25/08/2022	3.879132185
39	Pf	8	2	25/08/2022	-0.203070388
40	Se	8	2	25/08/2022	-0.264171212
41	Ma	14	2	25/08/2022	0.744505846
42	Pf	14	2	25/08/2022	0.593037415
43	Ma	8	2	25/08/2022	0.679040677
44	Se	14	2	25/08/2022	1.259918608
45	Mi	8	2	25/08/2022	0.307301206
46	Pf	14	2	25/08/2022	0.061100825
47	Se	8	2	25/08/2022	0.023525451
48	Se	14	2	25/08/2022	0.247017237

1	Ma	8	1	15/09/2022	-1.597116742
2	Se	14	1	15/09/2022	-0.197930479
3	Se	8	1	15/09/2022	-0.327395862
4	Pf	8	1	15/09/2022	-0.088220442
5	Pf	14	1	15/09/2022	-0.706253649
6	Mi	8	1	15/09/2022	0.005881363
7	Ma	14	1	15/09/2022	0.190490806
8	Pf	8	1	15/09/2022	1.0416547
9	Pf	14	1	15/09/2022	-1.186074831
10	Mi	14	1	15/09/2022	-0.071254972
11	Ma	8	1	15/09/2022	-0.224472013
12	Se	14	1	15/09/2022	0.458256185
13	Ma	14	2	15/09/2022	-0.271824524
14	Pf	8	2	15/09/2022	-0.250938146
15	Pf	14	2	15/09/2022	-0.852144121
16	Se	14	2	15/09/2022	0.469038683
17	Ma	8	2	15/09/2022	1.7617949
18	Mi	8	2	15/09/2022	-1.159935441
19	Mi	14	2	15/09/2022	0.393561194
20	Se	8	2	15/09/2022	-0.141806192
21	Ma	14	2	15/09/2022	-0.305378453
22	Pf	8	2	15/09/2022	0.047704387
23	Mi	14	2	15/09/2022	-0.04360395
24	Ma	8	2	15/09/2022	-0.165588369
25	Pf	14	1	15/09/2022	0.750853984
26	Mi	8	1	15/09/2022	0.390130399
27	Ma	14	1	15/09/2022	-0.506777428
28	Se	8	1	15/09/2022	-0.169439262
29	Mi	14	1	15/09/2022	-0.033327723
30	Ma	8	1	15/09/2022	0.121548164
31	Se	14	1	15/09/2022	-0.297084223
32	Mi	8	1	15/09/2022	-0.097042486
33	Se	8	1	15/09/2022	0.13873984
34	Ma	14	1	15/09/2022	-0.274463597
35	Mi	14	1	15/09/2022	-0.217158011
36	Pf	8	1	15/09/2022	-0.14017248
37	Mi	8	2	15/09/2022	-0.170861129
38	Mi	14	2	15/09/2022	0.047050902
39	Pf	8	2	15/09/2022	0.020911512
40	Se	8	2	15/09/2022	0.058813628
41	Ma	14	2	15/09/2022	0.333277225
42	Pf	14	2	15/09/2022	0.078418171
43	Ma	8	2	15/09/2022	0.040286258

44	Se	14	2	15/09/2022	0.375879404
45	Mi	8	2	15/09/2022	0.010782498
46	Pf	14	2	15/09/2022	-0.278610712
47	Se	8	2	15/09/2022	-0.104884303
48	Se	14	2	15/09/2022	0.053535482
1	Ma	8	1	22/09/2022	0.016337119
2	Se	14	1	22/09/2022	-0.30648435
3	Se	8	1	22/09/2022	0.001960454
4	Pf	8	1	22/09/2022	-0.272524686
5	Pf	14	1	22/09/2022	-0.130043466
6	Mi	8	1	22/09/2022	-0.190490806
7	Ma	14	1	22/09/2022	-0.041332911
8	Pf	8	1	22/09/2022	0.09344832
9	Pf	14	1	22/09/2022	-0.014703407
10	Mi	14	1	22/09/2022	0
11	Ma	8	1	22/09/2022	0
12	Se	14	1	22/09/2022	-0.166638613
13	Ma	14	2	22/09/2022	0.050971811
14	Pf	8	2	22/09/2022	-0.192778003
15	Pf	14	2	22/09/2022	0.094101805
16	Se	14	2	22/09/2022	0.220877847
17	Ma	8	2	22/09/2022	0.211729061
18	Mi	8	2	22/09/2022	-0.139845738
19	Mi	14	2	22/09/2022	-0.177747853
20	Se	8	2	22/09/2022	-0.016337119
21	Ma	14	2	22/09/2022	0
22	Pf	8	2	22/09/2022	-0.005881363
23	Mi	14	2	22/09/2022	0
24	Ma	8	2	22/09/2022	0.151935206
25	Pf	14	1	22/09/2022	-0.214669742
26	Mi	8	1	22/09/2022	-0.084462905
27	Ma	14	1	22/09/2022	-1.053417425
28	Se	8	1	22/09/2022	0.4004928
29	Mi	14	1	22/09/2022	-0.115013317
30	Ma	8	1	22/09/2022	0.010782498
31	Se	14	1	22/09/2022	-0.437332105
32	Mi	8	1	22/09/2022	-0.60741408
33	Se	8	1	22/09/2022	-0.209115122
34	Ma	14	1	22/09/2022	0.41365585
35	Mi	14	1	22/09/2022	-0.784181706
36	Pf	8	1	22/09/2022	-0.017644088
37	Mi	8	2	22/09/2022	-0.49060368
38	Mi	14	2	22/09/2022	0.977613194

39	Pf	8	2	22/09/2022	-1.150786654
40	Se	8	2	22/09/2022	0.048777969
41	Ma	14	2	22/09/2022	-0.106027902
42	Pf	14	2	22/09/2022	-0.407937858
43	Ma	8	2	22/09/2022	0
44	Se	14	2	22/09/2022	0.904422901
45	Mi	8	2	22/09/2022	-0.007841817
46	Pf	14	2	22/09/2022	-0.400586155
47	Se	8	2	22/09/2022	-0.127429527
48	Se	14	2	22/09/2022	0.019604543
1	Ma	8	1	28/09/2022	0.414636077
2	Se	14	1	28/09/2022	-0.507757655
3	Se	8	1	28/09/2022	-0.170559521
4	Pf	8	1	28/09/2022	-0.13461786
5	Pf	14	1	28/09/2022	-0.036268404
6	Mi	8	1	28/09/2022	0.019767914
7	Ma	14	1	28/09/2022	0.481618265
8	Pf	8	1	28/09/2022	-0.222184817
9	Pf	14	1	28/09/2022	0.143766646
10	Mi	14	1	28/09/2022	0.271359545
11	Ma	8	1	28/09/2022	-0.143766646
12	Se	14	1	28/09/2022	0.084462905
13	Ma	14	2	28/09/2022	0.013069695
14	Pf	8	2	28/09/2022	0.177094369
15	Pf	14	2	28/09/2022	-0.131350436
16	Se	14	2	28/09/2022	-0.082339079
17	Ma	8	2	28/09/2022	0.005881363
18	Mi	8	2	28/09/2022	0.030060299
19	Mi	14	2	28/09/2022	-0.188857094
20	Se	8	2	28/09/2022	0.015683634
21	Ma	14	2	28/09/2022	0.080868738
22	Pf	8	2	28/09/2022	0.012579582
23	Mi	14	2	28/09/2022	0.109108615
24	Ma	8	2	28/09/2022	0.079071655
25	Pf	14	1	28/09/2022	0.107824985
26	Mi	8	1	28/09/2022	0.208461637
27	Ma	14	1	28/09/2022	0
28	Se	8	1	28/09/2022	-0.026956246
29	Mi	14	1	28/09/2022	-0.348634117
30	Ma	8	1	28/09/2022	0.089527411
31	Se	14	1	28/09/2022	-0.005134523
32	Mi	8	1	28/09/2022	0.07008624
33	Se	8	1	28/09/2022	-0.108478469

34	Ma	14	1	28/09/2022	1.126771089
35	Mi	14	1	28/09/2022	0.275117082
36	Pf	8	1	28/09/2022	0.086259988
37	Mi	8	2	28/09/2022	0.002567262
38	Mi	14	2	28/09/2022	-0.009802271
39	Pf	8	2	28/09/2022	0.053912492
40	Se	8	2	28/09/2022	-0.138375397
41	Ma	14	2	28/09/2022	0.017970831
42	Pf	14	2	28/09/2022	-0.021564997
43	Ma	8	2	28/09/2022	-0.062897908
44	Se	14	2	28/09/2022	-0.222838302
45	Mi	8	2	28/09/2022	0.061100825
46	Pf	14	2	28/09/2022	0.232640573
47	Se	8	2	28/09/2022	0.020258027
48	Se	14	2	28/09/2022	-0.064694991
1	Ma	8	1	6/10/2022	-0.303216926
2	Se	14	1	6/10/2022	0.201926789
3	Se	8	1	6/10/2022	-0.192778003
4	Pf	8	1	6/10/2022	0
5	Pf	14	1	6/10/2022	-0.133964375
6	Mi	8	1	6/10/2022	0.049991584
7	Ma	14	1	6/10/2022	-0.02744636
8	Pf	8	1	6/10/2022	0.047050902
9	Pf	14	1	6/10/2022	-0.18558967
10	Mi	14	1	6/10/2022	-0.066655445
11	Ma	8	1	6/10/2022	0.011762726
12	Se	14	1	6/10/2022	0.095245403
13	Ma	14	2	6/10/2022	0
14	Pf	8	2	6/10/2022	0
15	Pf	14	2	6/10/2022	-0.000980227
16	Se	14	2	6/10/2022	-0.103904076
17	Ma	8	2	6/10/2022	0.147687555
18	Mi	8	2	6/10/2022	-0.038368891
19	Mi	14	2	6/10/2022	0.030387041
20	Se	8	2	6/10/2022	0
21	Ma	14	2	6/10/2022	-0.18134202
22	Pf	8	2	6/10/2022	0.099983168
23	Mi	14	2	6/10/2022	0.017970831
24	Ma	8	2	6/10/2022	-0.046070675
25	Pf	14	1	6/10/2022	-0.119377662
26	Mi	8	1	6/10/2022	-0.142483015
27	Ma	14	1	6/10/2022	-0.289587102
28	Se	8	1	6/10/2022	-0.3838056

29	Mi	14	1	6/10/2022	-0.974019028
30	Ma	8	1	6/10/2022	-0.752207631
31	Se	14	1	6/10/2022	1.215598338
32	Mi	8	1	6/10/2022	-0.087286892
33	Se	8	1	6/10/2022	1.455637292
34	Ma	14	1	6/10/2022	0.316286622
35	Mi	14	1	6/10/2022	0.21025872
36	Pf	8	1	6/10/2022	0.165331643
37	Mi	8	2	6/10/2022	0.053912492
38	Mi	14	2	6/10/2022	-0.628465625
39	Pf	8	2	6/10/2022	0.175857415
40	Se	8	2	6/10/2022	-0.215649969
41	Ma	14	2	6/10/2022	-0.943468615
42	Pf	14	2	6/10/2022	1.288765292
43	Ma	8	2	6/10/2022	-0.731669538
44	Se	14	2	6/10/2022	0.426165415
45	Mi	8	2	6/10/2022	0.8844216
46	Pf	14	2	6/10/2022	-0.124512185
47	Se	8	2	6/10/2022	-0.016337119
48	Se	14	2	6/10/2022	0.041332911
1	Ma	8	1	13/10/2022	-0.341772527
2	Se	14	1	13/10/2022	0.154549145
3	Se	8	1	13/10/2022	-0.003594166
4	Pf	8	1	13/10/2022	0.079071655
5	Pf	14	1	13/10/2022	0.032347495
6	Mi	8	1	13/10/2022	-0.011109241
7	Ma	14	1	13/10/2022	0.168599067
8	Pf	8	1	13/10/2022	-0.171539748
9	Pf	14	1	13/10/2022	0.108984393
10	Mi	14	1	13/10/2022	-0.058813628
11	Ma	8	1	13/10/2022	-0.047050902
12	Se	14	1	13/10/2022	-0.04116954
13	Ma	14	2	13/10/2022	0.564797538
14	Pf	8	2	13/10/2022	-0.123998732
15	Pf	14	2	13/10/2022	0.030807138
16	Se	14	2	13/10/2022	-0.052932265
17	Ma	8	2	13/10/2022	-0.002613939
18	Mi	8	2	13/10/2022	-0.13502408
19	Mi	14	2	13/10/2022	-0.215649969
20	Se	8	2	13/10/2022	-0.035941662
21	Ma	14	2	13/10/2022	-0.133964375
22	Pf	8	2	13/10/2022	-0.082339079
23	Mi	14	2	13/10/2022	-0.037738745

24	Ma	8	2	13/10/2022	-3.847554868
25	Pf	14	1	13/10/2022	-1.604538462
26	Mi	8	1	13/10/2022	0.643355742
27	Ma	14	1	13/10/2022	0.496648414
28	Se	8	1	13/10/2022	0.291384185
29	Mi	14	1	13/10/2022	0.684688652
30	Ma	8	1	13/10/2022	-1.159118585
31	Se	14	1	13/10/2022	-1.423289797
32	Mi	8	1	13/10/2022	0.593037415
33	Se	8	1	13/10/2022	-0.209115122
34	Ma	14	1	13/10/2022	-0.030060299
35	Mi	14	1	13/10/2022	-0.379674643
36	Pf	8	1	13/10/2022	-0.351574798
37	Mi	8	2	13/10/2022	-0.499589095
38	Mi	14	2	13/10/2022	0.335027631
39	Pf	8	2	13/10/2022	-0.65413824
40	Se	8	2	13/10/2022	0.201273305
41	Ma	14	2	13/10/2022	0.709847815
42	Pf	14	2	13/10/2022	-0.708564185
43	Ma	8	2	13/10/2022	-0.396641908
44	Se	14	2	13/10/2022	-0.094988677
45	Mi	8	2	13/10/2022	0.375753734
46	Pf	14	2	13/10/2022	-0.910304264
47	Se	8	2	13/10/2022	0.005227878
48	Se	14	2	13/10/2022	0
1	Ma	8	1	21/10/2022	-0.079071655
2	Se	14	1	21/10/2022	-0.069316062
3	Se	8	1	21/10/2022	-0.337594892
4	Pf	8	1	21/10/2022	-0.003267424
5	Pf	14	1	21/10/2022	0.002613939
6	Mi	8	1	21/10/2022	0.103250591
7	Ma	14	1	21/10/2022	0.203887244
8	Pf	8	1	21/10/2022	0.06730893
9	Pf	14	1	21/10/2022	0.09775342
10	Mi	14	1	21/10/2022	0.045090448
11	Ma	8	1	21/10/2022	-0.079071655
12	Se	14	1	21/10/2022	-0.080868738
13	Ma	14	2	21/10/2022	0.349147569
14	Pf	8	2	21/10/2022	-0.029523508
15	Pf	14	2	21/10/2022	-0.141969563
16	Se	14	2	21/10/2022	0.217610423
17	Ma	8	2	21/10/2022	-0.122201649
18	Mi	8	2	21/10/2022	0.081685594

19	Mi	14	2	21/10/2022	0.162717704
20	Se	8	2	21/10/2022	-0.409734942
21	Ma	14	2	21/10/2022	-0.165331643
22	Pf	8	2	21/10/2022	-0.181015277
23	Mi	14	2	21/10/2022	-0.031291866
24	Ma	8	2	21/10/2022	-0.265968295
25	Pf	14	1	21/10/2022	-0.179708308
26	Mi	8	1	21/10/2022	0
27	Ma	14	1	21/10/2022	0.016173748
28	Se	8	1	21/10/2022	0.072536808
29	Mi	14	1	21/10/2022	0.158143311
30	Ma	8	1	21/10/2022	0
31	Se	14	1	21/10/2022	-0.431299938
32	Mi	8	1	21/10/2022	-0.043643446
33	Se	8	1	21/10/2022	-0.481361538
34	Ma	14	1	21/10/2022	-0.05227878
35	Mi	14	1	21/10/2022	0.013069695
36	Pf	8	1	21/10/2022	-0.075477489
37	Mi	8	2	21/10/2022	0
38	Mi	14	2	21/10/2022	0
39	Pf	8	2	21/10/2022	0
40	Se	8	2	21/10/2022	0
41	Ma	14	2	21/10/2022	0.057763385
42	Pf	14	2	21/10/2022	0
43	Ma	8	2	21/10/2022	0
44	Se	14	2	21/10/2022	0.035941662
45	Mi	8	2	21/10/2022	0
46	Pf	14	2	21/10/2022	-0.005227878
47	Se	8	2	21/10/2022	-0.04116954
48	Se	14	2	21/10/2022	-0.032347495
1	Ma	8	1	28/10/2022	-0.188693723
2	Se	14	1	28/10/2022	-0.010269046
3	Se	8	1	28/10/2022	0.051345231
4	Pf	8	1	28/10/2022	0.001960454
5	Pf	14	1	28/10/2022	-0.165331643
6	Mi	8	1	28/10/2022	0.037738745
7	Ma	14	1	28/10/2022	0.003267424
8	Pf	8	1	28/10/2022	-0.09475529
9	Pf	14	1	28/10/2022	-0.08103211
10	Mi	14	1	28/10/2022	-0.080868738
11	Ma	8	1	28/10/2022	0.193431488
12	Se	14	1	28/10/2022	-0.09344832
13	Ma	14	2	28/10/2022	0.030550412

14	Pf	8	2	28/10/2022	0.247997465
15	Pf	14	2	28/10/2022	0.364551138
16	Se	14	2	28/10/2022	0.230680119
17	Ma	8	2	28/10/2022	0.170722892
18	Mi	8	2	28/10/2022	-0.122201649
19	Mi	14	2	28/10/2022	-0.063388021
20	Se	8	2	28/10/2022	-0.113216234
21	Ma	14	2	28/10/2022	-0.233947542
22	Pf	8	2	28/10/2022	-0.010782498
23	Mi	14	2	28/10/2022	0.069922869
24	Ma	8	2	28/10/2022	0.006534848
25	Pf	14	1	28/10/2022	-0.345039951
26	Mi	8	1	28/10/2022	1.001232
27	Ma	14	1	28/10/2022	-0.412045477
28	Se	8	1	28/10/2022	0.150954978
29	Mi	14	1	28/10/2022	0.0667488
30	Ma	8	1	28/10/2022	0.500616
31	Se	14	1	28/10/2022	2.476123754
32	Mi	8	1	28/10/2022	-0.055196123
33	Se	8	1	28/10/2022	-0.042359815
34	Ma	14	1	28/10/2022	0.402546609
35	Mi	14	1	28/10/2022	-0.198659366
36	Pf	8	1	28/10/2022	0.217610423
37	Mi	8	2	28/10/2022	-0.562230277
38	Mi	14	2	28/10/2022	0.086259988
39	Pf	8	2	28/10/2022	-0.137348492
40	Se	8	2	28/10/2022	0.474943385
41	Ma	14	2	28/10/2022	-0.612291877
42	Pf	14	2	28/10/2022	-1.170671262
43	Ma	8	2	28/10/2022	1.205329292
44	Se	14	2	28/10/2022	0.889556123
45	Mi	8	2	28/10/2022	0.120404566
46	Pf	14	2	28/10/2022	7230.855214
47	Se	8	2	28/10/2022	0.168599067
48	Se	14	2	28/10/2022	0.368402031
1	Ma	8	1	11/11/2022	0
2	Se	14	1	11/11/2022	0
3	Se	8	1	11/11/2022	0
4	Pf	8	1	11/11/2022	0
5	Pf	14	1	11/11/2022	0
6	Mi	8	1	11/11/2022	-0.152752062
7	Ma	14	1	11/11/2022	-0.158143311
8	Pf	8	1	11/11/2022	-0.139915754

9	Pf	14	1	11/11/2022	0.025159163
10	Mi	14	1	11/11/2022	-0.449270769
11	Ma	8	1	11/11/2022	0.138375397
12	Se	14	1	11/11/2022	-0.137231799
13	Ma	14	2	11/11/2022	0
14	Pf	8	2	11/11/2022	0
15	Pf	14	2	11/11/2022	0
16	Se	14	2	11/11/2022	0
17	Ma	8	2	11/11/2022	0
18	Mi	8	2	11/11/2022	0
19	Mi	14	2	11/11/2022	0
20	Se	8	2	11/11/2022	-0.026956246
21	Ma	14	2	11/11/2022	0.005391249
22	Pf	8	2	11/11/2022	0.073680406
23	Mi	14	2	11/11/2022	0.093705046
24	Ma	8	2	11/11/2022	-0.271359545
25	Pf	14	1	11/11/2022	-1.746764751
26	Mi	8	1	11/11/2022	-0.381238338
27	Ma	14	1	11/11/2022	-0.464674338
28	Se	8	1	11/11/2022	-0.704456566
29	Mi	14	1	11/11/2022	-0.088057071
30	Ma	8	1	11/11/2022	-0.166872
31	Se	14	1	11/11/2022	0.261860677
32	Mi	8	1	11/11/2022	0.023105354
33	Se	8	1	11/11/2022	0
34	Ma	14	1	11/11/2022	-0.110392246
35	Mi	14	1	11/11/2022	0.010782498
36	Pf	8	1	11/11/2022	-6.90E-19
37	Mi	8	2	11/11/2022	-0.837954166
38	Mi	14	2	11/11/2022	-0.321677871
39	Pf	8	2	11/11/2022	0.333744
40	Se	8	2	11/11/2022	0.487779692
41	Ma	14	2	11/11/2022	1.183507569
42	Pf	14	2	11/11/2022	-0.021821723
43	Ma	8	2	11/11/2022	0.128363077
44	Se	14	2	11/11/2022	0.069922869
45	Mi	8	2	11/11/2022	0.061614277
46	Pf	14	2	11/11/2022	0.032347495
47	Se	8	2	11/11/2022	-0.186126462
48	Se	14	2	11/11/2022	0.047704387
1	Ma	8	1	18/11/2022	0
2	Se	14	1	18/11/2022	0
3	Se	8	1	18/11/2022	0

4	Pf	8	1	18/11/2022	0
5	Pf	14	1	18/11/2022	0
6	Mi	8	1	18/11/2022	0
7	Ma	14	1	18/11/2022	0.005391249
8	Pf	8	1	18/11/2022	0.079071655
9	Pf	14	1	18/11/2022	-0.183302474
10	Mi	14	1	18/11/2022	-0.469038683
11	Ma	8	1	18/11/2022	0.2336208
12	Se	14	1	18/11/2022	0.312692455
13	Ma	14	2	18/11/2022	0
14	Pf	8	2	18/11/2022	0
15	Pf	14	2	18/11/2022	0
16	Se	14	2	18/11/2022	0
17	Ma	8	2	18/11/2022	0
18	Mi	8	2	18/11/2022	0
19	Mi	14	2	18/11/2022	-0.156346228
20	Se	8	2	18/11/2022	0.066492074
21	Ma	14	2	18/11/2022	-0.023525451
22	Pf	8	2	18/11/2022	0.618850063
23	Mi	14	2	18/11/2022	-0.001797083
24	Ma	8	2	18/11/2022	0.159940394
25	Pf	14	1	18/11/2022	0.691876985
26	Mi	8	1	18/11/2022	0.048777969
27	Ma	14	1	18/11/2022	0.053527403
28	Se	8	1	18/11/2022	-0.260577046
29	Mi	14	1	18/11/2022	-0.082152369
30	Ma	8	1	18/11/2022	-0.111675877
31	Se	14	1	18/11/2022	-0.499075643
32	Mi	8	1	18/11/2022	0.012579582
33	Se	8	1	18/11/2022	0.527572246
34	Ma	14	1	18/11/2022	-0.172519975
35	Mi	14	1	18/11/2022	-0.367258432
36	Pf	8	1	18/11/2022	0.181505391
37	Mi	8	2	18/11/2022	-0.015403569
38	Mi	14	2	18/11/2022	0.373536554
39	Pf	8	2	18/11/2022	-0.398952443
40	Se	8	2	18/11/2022	-0.243889846
41	Ma	14	2	18/11/2022	-0.064181538
42	Pf	14	2	18/11/2022	0.065465169
43	Ma	8	2	18/11/2022	0.495994929
44	Se	14	2	18/11/2022	0.556769011
45	Mi	8	2	18/11/2022	0.305504123
46	Pf	14	2	18/11/2022	-0.079071655

47	Se	8	2	18/11/2022	0.176114142
48	Se	14	2	18/11/2022	0.160103765
1	Ma	8	1	25/11/2022	0
2	Se	14	1	25/11/2022	0
3	Se	8	1	25/11/2022	0
4	Pf	8	1	25/11/2022	0
5	Pf	14	1	25/11/2022	0
6	Mi	8	1	25/11/2022	0
7	Ma	14	1	25/11/2022	-0.010782498
8	Pf	8	1	25/11/2022	-0.014376665
9	Pf	14	1	25/11/2022	-0.035941662
10	Mi	14	1	25/11/2022	-0.053912492
11	Ma	8	1	25/11/2022	-0.240809132
12	Se	14	1	25/11/2022	-0.09344832
13	Ma	14	2	25/11/2022	0
14	Pf	8	2	25/11/2022	0
15	Pf	14	2	25/11/2022	0
16	Se	14	2	25/11/2022	0
17	Ma	8	2	25/11/2022	0
18	Mi	8	2	25/11/2022	0.010782498
19	Mi	14	2	25/11/2022	0.154549145
20	Se	8	2	25/11/2022	-0.084462905
21	Ma	14	2	25/11/2022	0.032347495
22	Pf	8	2	25/11/2022	0.080868738
23	Mi	14	2	25/11/2022	-0.195111877
24	Ma	8	2	25/11/2022	0.163021108
25	Pf	14	1	25/11/2022	-0.388169945
26	Mi	8	1	25/11/2022	0.016173748
27	Ma	14	1	25/11/2022	0.469038683
28	Se	8	1	25/11/2022	-0.269562462
29	Mi	14	1	25/11/2022	0.106027902
30	Ma	8	1	25/11/2022	0.156602954
31	Se	14	1	25/11/2022	0.028753329
32	Mi	8	1	25/11/2022	-0.291127458
33	Se	8	1	25/11/2022	-0.294721625
34	Ma	14	1	25/11/2022	-0.370199114
35	Mi	14	1	25/11/2022	0.057506658
36	Pf	8	1	25/11/2022	0.431299938
37	Mi	8	2	25/11/2022	0.138632123
38	Mi	14	2	25/11/2022	0.157886585
39	Pf	8	2	25/11/2022	-0.014376665
40	Se	8	2	25/11/2022	-0.098839569
41	Ma	14	2	25/11/2022	0.195882055

42	Pf	14	2	25/11/2022	0.091651237
43	Ma	8	2	25/11/2022	-0.204867471
44	Se	14	2	25/11/2022	0.107824985
45	Mi	8	2	25/11/2022	0.005391249
46	Pf	14	2	25/11/2022	0.258779963
47	Se	8	2	25/11/2022	-0.075477489
48	Se	14	2	25/11/2022	-0.155319323
1	Ma	8	1	6/12/2022	0
2	Se	14	1	6/12/2022	0
3	Se	8	1	6/12/2022	0
4	Pf	8	1	6/12/2022	-0.003920909
5	Pf	14	1	6/12/2022	-0.017773349
6	Mi	8	1	6/12/2022	0
7	Ma	14	1	6/12/2022	-0.004574393
8	Pf	8	1	6/12/2022	0.059467113
9	Pf	14	1	6/12/2022	0.064041506
10	Mi	14	1	6/12/2022	-0.083319306
11	Ma	8	1	6/12/2022	0.205093677
12	Se	14	1	6/12/2022	-0.047395598
13	Ma	14	2	6/12/2022	0
14	Pf	8	2	6/12/2022	0
15	Pf	14	2	6/12/2022	0
16	Se	14	2	6/12/2022	0
17	Ma	8	2	6/12/2022	0
18	Mi	8	2	6/12/2022	-0.015683634
19	Mi	14	2	6/12/2022	-0.003267424
20	Se	8	2	6/12/2022	0.009802271
21	Ma	14	2	6/12/2022	0.02058477
22	Pf	8	2	6/12/2022	0.043129994
23	Mi	14	2	6/12/2022	-0.05165043
24	Ma	8	2	6/12/2022	0.015403569
25	Pf	14	1	6/12/2022	-0.222184817
26	Mi	8	1	6/12/2022	-0.111745893
27	Ma	14	1	6/12/2022	-0.068289157
28	Se	8	1	6/12/2022	0.058813628
29	Mi	14	1	6/12/2022	0.021866605
30	Ma	8	1	6/12/2022	0.11958771
31	Se	14	1	6/12/2022	0.067635672
32	Mi	8	1	6/12/2022	-0.003770104
33	Se	8	1	6/12/2022	0.069746931
34	Ma	14	1	6/12/2022	-0.001508042
35	Mi	14	1	6/12/2022	-0.381238338
36	Pf	8	1	6/12/2022	0.00473956

37	Mi	8	2	6/12/2022	0.014376665
38	Mi	14	2	6/12/2022	-0.05227878
39	Pf	8	2	6/12/2022	-0.170559521
40	Se	8	2	6/12/2022	0.109785439
41	Ma	14	2	6/12/2022	-0.182473051
42	Pf	14	2	6/12/2022	0.045618263
43	Ma	8	2	6/12/2022	0.121774371
44	Se	14	2	6/12/2022	-0.006786188
45	Mi	8	2	6/12/2022	-0.055689827
46	Pf	14	2	6/12/2022	0.024505678
47	Se	8	2	6/12/2022	0.025259699
48	Se	14	2	6/12/2022	0.022243616
1	Ma	8	1	16/12/2022	0
2	Se	14	1	16/12/2022	0
3	Se	8	1	16/12/2022	0
4	Pf	8	1	16/12/2022	0
5	Pf	14	1	16/12/2022	0.00236978
6	Mi	8	1	16/12/2022	-0.009425261
7	Ma	14	1	16/12/2022	0
8	Pf	8	1	16/12/2022	-0.032799908
9	Pf	14	1	16/12/2022	0.062081052
10	Mi	14	1	16/12/2022	0.050950267
11	Ma	8	1	16/12/2022	0.118934225
12	Se	14	1	16/12/2022	0.134781231
13	Ma	14	2	16/12/2022	-0.022871966
14	Pf	8	2	16/12/2022	0
15	Pf	14	2	16/12/2022	0
16	Se	14	2	16/12/2022	0
17	Ma	8	2	16/12/2022	0
18	Mi	8	2	16/12/2022	-0.015834438
19	Mi	14	2	16/12/2022	-0.00037701
20	Se	8	2	16/12/2022	0.012441344
21	Ma	14	2	16/12/2022	0.000980227
22	Pf	8	2	16/12/2022	0.032045887
23	Mi	14	2	16/12/2022	0.067635672
24	Ma	8	2	16/12/2022	0.021866605
25	Pf	14	1	16/12/2022	0.033553929
26	Mi	8	1	16/12/2022	0.090180896
27	Ma	14	1	16/12/2022	0.14017248
28	Se	8	1	16/12/2022	-0.147360812
29	Mi	14	1	16/12/2022	-0.020258027
30	Ma	8	1	16/12/2022	-0.150954978
31	Se	14	1	16/12/2022	-0.028753329

32	Mi	8	1	16/12/2022	0.055546204
33	Se	8	1	16/12/2022	-0.029406814
34	Ma	14	1	16/12/2022	0.053912492
35	Mi	14	1	16/12/2022	0.013572376
36	Pf	8	1	16/12/2022	-0.27348337
37	Mi	8	2	16/12/2022	0.127592898
38	Mi	14	2	16/12/2022	0.201273305
39	Pf	8	2	16/12/2022	0.047704387
40	Se	8	2	16/12/2022	-0.256819509
41	Ma	14	2	16/12/2022	0.389967028
42	Pf	14	2	16/12/2022	-0.01372318
43	Ma	8	2	16/12/2022	0.081358852
44	Se	14	2	16/12/2022	-0.059793855
45	Mi	8	2	16/12/2022	-0.062734537
46	Pf	14	2	16/12/2022	-0.105211046
47	Se	8	2	16/12/2022	-0.087089411
48	Se	14	2	16/12/2022	0.013949386
1	Ma	8	1	23/12/2022	-0.028753329
2	Se	14	1	23/12/2022	-0.132213969
3	Se	8	1	23/12/2022	-0.038228858
4	Pf	8	1	23/12/2022	-0.341445785
5	Pf	14	1	23/12/2022	-0.111745893
6	Mi	8	1	23/12/2022	-0.190164064
7	Ma	14	1	23/12/2022	-0.179708308
8	Pf	8	1	23/12/2022	-0.102923849
9	Pf	14	1	23/12/2022	0.248977692
10	Mi	14	1	23/12/2022	0.062081052
11	Ma	8	1	23/12/2022	0.038228858
12	Se	14	1	23/12/2022	-3.31E-17
13	Ma	14	2	23/12/2022	-0.071883323
14	Pf	8	2	23/12/2022	-0.240809132
15	Pf	14	2	23/12/2022	0.345039951
16	Se	14	2	23/12/2022	-0.033981207
17	Ma	8	2	23/12/2022	0.062734537
18	Mi	8	2	23/12/2022	0.058813628
19	Mi	14	2	23/12/2022	-0.059303742
20	Se	8	2	23/12/2022	-0.059467113
21	Ma	14	2	23/12/2022	0.416923274
22	Pf	8	2	23/12/2022	0.079398398
23	Mi	14	2	23/12/2022	0.12969159
24	Ma	8	2	23/12/2022	-1.81E-17
25	Pf	14	1	23/12/2022	-0.033327723
26	Mi	8	1	23/12/2022	-0.04116954

27	Ma	14	1	23/12/2022	0.186243155
28	Se	8	1	23/12/2022	-0.154222402
29	Mi	14	1	23/12/2022	0.328049347
30	Ma	8	1	23/12/2022	0.50710417
31	Se	14	1	23/12/2022	0.263681099
32	Mi	8	1	23/12/2022	0.079071655
33	Se	8	1	23/12/2022	-0.007188332
34	Ma	14	1	23/12/2022	0.314326167
35	Mi	14	1	23/12/2022	-0.153568917
36	Pf	8	1	23/12/2022	0.084073327
37	Mi	8	2	23/12/2022	-0.282142043
38	Mi	14	2	23/12/2022	-0.163697931
39	Pf	8	2	23/12/2022	-0.030387041
40	Se	8	2	23/12/2022	0.219244135
41	Ma	14	2	23/12/2022	-0.201926789
42	Pf	14	2	23/12/2022	-0.014376665
43	Ma	8	2	23/12/2022	0.062799167
44	Se	14	2	23/12/2022	-0.339158588
45	Mi	8	2	23/12/2022	0.22507523
46	Pf	14	2	23/12/2022	0.181505391
47	Se	8	2	23/12/2022	-0.047050902
48	Se	14	2	23/12/2022	-0.113706347
1	Ma	8	1	9/1/2023	-0.125795815
2	Se	14	1	9/1/2023	-0.174317058
3	Se	8	1	9/1/2023	0.068289157
4	Pf	8	1	9/1/2023	-0.082665822
5	Pf	14	1	9/1/2023	-0.250334929
6	Mi	8	1	9/1/2023	-0.065348476
7	Ma	14	1	9/1/2023	0.088220442
8	Pf	8	1	9/1/2023	-0.202580274
9	Pf	14	1	9/1/2023	-0.158796796
10	Mi	14	1	9/1/2023	0.032347495
11	Ma	8	1	9/1/2023	-0.175460657
12	Se	14	1	9/1/2023	-0.038228858
13	Ma	14	2	9/1/2023	0.044927077
14	Pf	8	2	9/1/2023	0.025159163
15	Pf	14	2	9/1/2023	-0.123508619
16	Se	14	2	9/1/2023	-0.065675218
17	Ma	8	2	9/1/2023	-0.040189312
18	Mi	8	2	9/1/2023	-0.078418171
19	Mi	14	2	9/1/2023	0.172519975
20	Se	8	2	9/1/2023	0.289493747
21	Ma	14	2	9/1/2023	-0.058436618

22	Pf	8	2	9/1/2023	0.203887244
23	Mi	14	2	9/1/2023	0.102597107
24	Ma	8	2	9/1/2023	-0.096715744
28	Se	8	1	9/1/2023	0.242606215
29	Mi	14	1	9/1/2023	-0.070599692
30	Ma	8	1	9/1/2023	-0.413329108
31	Se	14	1	9/1/2023	-0.022545224
32	Mi	8	1	9/1/2023	0.155856114
33	Se	8	1	9/1/2023	-0.047704387
34	Ma	14	1	9/1/2023	0.331316771
35	Mi	14	1	9/1/2023	-0.074497262
36	Pf	8	1	9/1/2023	-0.178401338
40	Se	8	2	9/1/2023	-0.106027902
41	Ma	14	2	9/1/2023	0.062081052
42	Pf	14	2	9/1/2023	-0.1264493
43	Ma	8	2	9/1/2023	0.338178361
44	Se	14	2	9/1/2023	0.130370209
45	Mi	8	2	9/1/2023	-0.428685999
46	Pf	14	2	9/1/2023	-0.086259988
47	Se	8	2	9/1/2023	-0.203887244
48	Se	14	2	9/1/2023	0.098676198
1	Ma	8	1	13/01/2023	-0.138538768
2	Se	14	1	13/01/2023	0.064694991
3	Se	8	1	13/01/2023	0
4	Pf	8	1	13/01/2023	-0.150954978
5	Pf	14	1	13/01/2023	0.010455756
6	Mi	8	1	13/01/2023	0.333277225
7	Ma	14	1	13/01/2023	0.104557561
8	Pf	8	1	13/01/2023	-0.279691475
9	Pf	14	1	13/01/2023	-0.049664841
10	Mi	14	1	13/01/2023	-0.069596126
11	Ma	8	1	13/01/2023	0.018951058
12	Se	14	1	13/01/2023	0.044927077
13	Ma	14	2	13/01/2023	-0.016173748
14	Pf	8	2	13/01/2023	-0.032347495
15	Pf	14	2	13/01/2023	0.033981207
16	Se	14	2	13/01/2023	0.022545224
17	Ma	8	2	13/01/2023	0.129389982
18	Mi	8	2	13/01/2023	-0.015683634
19	Mi	14	2	13/01/2023	-0.145563729
20	Se	8	2	13/01/2023	-0.260740417
21	Ma	14	2	13/01/2023	-0.179708308
22	Pf	8	2	13/01/2023	-0.042476509

23	Mi	14	2	13/01/2023	-0.041332911
24	Ma	8	2	13/01/2023	-0.007841817
25	Pf	14	1	13/01/2023	0.438488271
26	Mi	8	1	13/01/2023	0.021821723
27	Ma	14	1	13/01/2023	-0.423598154
28	Se	8	1	13/01/2023	0.030807138
29	Mi	14	1	13/01/2023	-0.264427938
30	Ma	8	1	13/01/2023	0.253388714
31	Se	14	1	13/01/2023	0.054239235
32	Mi	8	1	13/01/2023	0.011762726
33	Se	8	1	13/01/2023	0.016173748
34	Ma	14	1	13/01/2023	-0.035288177
35	Mi	14	1	13/01/2023	-0.090834381
36	Pf	8	1	13/01/2023	0.008822044
37	Mi	8	2	13/01/2023	0.260577046
38	Mi	14	2	13/01/2023	0.5506776
39	Pf	8	2	13/01/2023	0.291127458
40	Se	8	2	13/01/2023	0.143766646
41	Ma	14	2	13/01/2023	0.005227878
42	Pf	14	2	13/01/2023	0.162717704
43	Ma	8	2	13/01/2023	0.143766646
44	Se	14	2	13/01/2023	-0.136578314
45	Mi	8	2	13/01/2023	-0.036968566
46	Pf	14	2	13/01/2023	0.158143311
47	Se	8	2	13/01/2023	0.043129994
48	Se	14	2	13/01/2023	-0.015683634
1	Ma	8	1	20/01/2023	0.246200382
2	Se	14	1	20/01/2023	-0.026956246
3	Se	8	1	20/01/2023	0.082152369
4	Pf	8	1	20/01/2023	0.019254462
5	Pf	14	1	20/01/2023	-0.265968295
6	Mi	8	1	20/01/2023	-0.097042486
7	Ma	14	1	20/01/2023	-0.076457716
8	Pf	8	1	20/01/2023	-0.198962769
9	Pf	14	1	20/01/2023	-0.161737477
10	Mi	14	1	20/01/2023	0.206664554
11	Ma	8	1	20/01/2023	-0.152752062
12	Se	14	1	20/01/2023	0.423598154
13	Ma	14	2	20/01/2023	-0.071883323
14	Pf	8	2	20/01/2023	-0.178424677
15	Pf	14	2	20/01/2023	-6.90E-19
16	Se	14	2	20/01/2023	0.003850892
17	Ma	8	2	20/01/2023	0.037225292

18	Mi	8	2	20/01/2023	0.094988677
19	Mi	14	2	20/01/2023	0.044110221
20	Se	8	2	20/01/2023	-0.478024098
21	Ma	14	2	20/01/2023	0.374820185
22	Pf	8	2	20/01/2023	0.188693723
23	Mi	14	2	20/01/2023	0.043643446
24	Ma	8	2	20/01/2023	-0.113216234
25	Pf	14	1	20/01/2023	-0.001797083
26	Mi	8	1	20/01/2023	-0.010269046
27	Ma	14	1	20/01/2023	0.062081052
28	Se	8	1	20/01/2023	-0.032347495
29	Mi	14	1	20/01/2023	-0.048777969
30	Ma	8	1	20/01/2023	0.284966031
31	Se	14	1	20/01/2023	0.314489538
32	Mi	8	1	20/01/2023	0.217447052
33	Se	8	1	20/01/2023	0.050318326
34	Ma	14	1	20/01/2023	0.208461637
35	Mi	14	1	20/01/2023	0.209768606
36	Pf	8	1	20/01/2023	-0.132657405
37	Mi	8	2	20/01/2023	-0.249794548
38	Mi	14	2	20/01/2023	0.145563729
39	Pf	8	2	20/01/2023	-0.147360812
40	Se	8	2	20/01/2023	0.041076185
41	Ma	14	2	20/01/2023	0.236188062
42	Pf	14	2	20/01/2023	0.190490806
43	Ma	8	2	20/01/2023	-0.059303742
44	Se	14	2	20/01/2023	-0.102433735
45	Mi	8	2	20/01/2023	-0.044436963
46	Pf	14	2	20/01/2023	0.278547877
47	Se	8	2	20/01/2023	0.037738745
48	Se	14	2	20/01/2023	0.263354356
1	Ma	8	1	27/01/2023	0.07008624
2	Se	14	1	27/01/2023	-0.309098289
3	Se	8	1	27/01/2023	-0.188693723
4	Pf	8	1	27/01/2023	0.077764686
5	Pf	14	1	27/01/2023	-0.071229838
6	Mi	8	1	27/01/2023	-0.044927077
7	Ma	14	1	27/01/2023	0.208461637
8	Pf	8	1	27/01/2023	0.068289157
9	Pf	14	1	27/01/2023	-0.246200382
10	Mi	14	1	27/01/2023	-0.239012049
11	Ma	8	1	27/01/2023	0.172519975
12	Se	14	1	27/01/2023	0.011552677

13	Ma	14	2	27/01/2023	0.156346228
14	Pf	8	2	27/01/2023	-0.050318326
15	Pf	14	2	27/01/2023	-0.167128726
16	Se	14	2	27/01/2023	0.066492074
17	Ma	8	2	27/01/2023	0.152261948
18	Mi	8	2	27/01/2023	0.123998732
19	Mi	14	2	27/01/2023	0.209768606
20	Se	8	2	27/01/2023	-0.190490806
21	Ma	14	2	27/01/2023	0.084462905
22	Pf	8	2	27/01/2023	-0.21025872
23	Mi	14	2	27/01/2023	-0.346837034
24	Ma	8	2	27/01/2023	0.106518015
25	Pf	14	1	27/01/2023	-0.123228554
26	Mi	8	1	27/01/2023	-0.115013317
27	Ma	14	1	27/01/2023	0.043129994
28	Se	8	1	27/01/2023	-0.017644088
29	Mi	14	1	27/01/2023	-0.053912492
30	Ma	8	1	27/01/2023	0.134781231
31	Se	14	1	27/01/2023	0.102433735
32	Mi	8	1	27/01/2023	-0.1168104
33	Se	8	1	27/01/2023	-0.316286622
34	Ma	14	1	27/01/2023	-0.231333603
35	Mi	14	1	27/01/2023	0.131350436
36	Pf	8	1	27/01/2023	-0.158796796
37	Mi	8	2	27/01/2023	0.034144578
38	Mi	14	2	27/01/2023	-0.149157895
39	Pf	8	2	27/01/2023	0.16353456
40	Se	8	2	27/01/2023	0.021564997
41	Ma	14	2	27/01/2023	-0.113216234
42	Pf	14	2	27/01/2023	-0.221041218
43	Ma	8	2	27/01/2023	0.053912492
44	Se	14	2	27/01/2023	-0.066492074
45	Mi	8	2	27/01/2023	-0.005391249
46	Pf	14	2	27/01/2023	0.071883323
47	Se	8	2	27/01/2023	0.086259988
48	Se	14	2	27/01/2023	0.030713783
1	Ma	8	1	3/2/2023	0.064694991
2	Se	14	1	3/2/2023	-0.177911225
3	Se	8	1	3/2/2023	0.032347495
4	Pf	8	1	3/2/2023	0.016663861
5	Pf	14	1	3/2/2023	0
6	Mi	8	1	3/2/2023	-0.057506658
7	Ma	14	1	3/2/2023	-0.150301494

8	Pf	8	1	3/2/2023	-0.07008624
9	Pf	14	1	3/2/2023	-0.190490806
10	Mi	14	1	3/2/2023	0.177911225
11	Ma	8	1	3/2/2023	0.127079446
12	Se	14	1	3/2/2023	-0.163021108
13	Ma	14	2	3/2/2023	0.277264246
14	Pf	8	2	3/2/2023	-0.021821723
15	Pf	14	2	3/2/2023	0.062897908
16	Se	14	2	3/2/2023	0.239012049
17	Ma	8	2	3/2/2023	0.080868738
18	Mi	8	2	3/2/2023	0.003920909
19	Mi	14	2	3/2/2023	0.014376665
20	Se	8	2	3/2/2023	0.134781231
21	Ma	14	2	3/2/2023	0.034658031
22	Pf	8	2	3/2/2023	0.080868738
23	Mi	14	2	3/2/2023	0.014376665
24	Ma	8	2	3/2/2023	-0.068289157
25	Pf	14	1	3/2/2023	-0.335027631
26	Mi	8	1	3/2/2023	-0.145563729
27	Ma	14	1	3/2/2023	-0.119377662
28	Se	8	1	3/2/2023	-0.247997465
29	Mi	14	1	3/2/2023	-0.21025872
30	Ma	8	1	3/2/2023	-0.047494338
31	Se	14	1	3/2/2023	-0.315773169
32	Mi	8	1	3/2/2023	-0.039535828
33	Se	8	1	3/2/2023	0.18689664
34	Ma	14	1	3/2/2023	0.017970831
35	Mi	14	1	3/2/2023	-0.282142043
36	Pf	8	1	3/2/2023	-0.197679138
37	Mi	8	2	3/2/2023	-0.011552677
38	Mi	14	2	3/2/2023	-0.147360812
39	Pf	8	2	3/2/2023	0.28034496
40	Se	8	2	3/2/2023	0.073190293
41	Ma	14	2	3/2/2023	0.391507385
42	Pf	14	2	3/2/2023	-0.204867471
43	Ma	8	2	3/2/2023	0.044927077
44	Se	14	2	3/2/2023	0.118094031
45	Mi	8	2	3/2/2023	0.462107077
46	Pf	14	2	3/2/2023	-0.014376665
47	Se	8	2	3/2/2023	-0.16353456
48	Se	14	2	3/2/2023	0.046210708
1	Ma	8	1	10/2/2023	0.005655157
2	Se	14	1	10/2/2023	0.028426587

3	Se	8	1	10/2/2023	-0.32045887
4	Pf	8	1	10/2/2023	0.089200669
5	Pf	14	1	10/2/2023	0.039101368
6	Mi	8	1	10/2/2023	-0.227412695
7	Ma	14	1	10/2/2023	-0.118607483
8	Pf	8	1	10/2/2023	0.036595146
9	Pf	14	1	10/2/2023	0.136477778
10	Mi	14	1	10/2/2023	-0.014703407
11	Ma	8	1	10/2/2023	0.004901136
12	Se	14	1	10/2/2023	0.223491786
13	Ma	14	2	10/2/2023	-0.055872947
14	Pf	8	2	10/2/2023	-0.116119214
15	Pf	14	2	10/2/2023	-0.085279761
16	Se	14	2	10/2/2023	-0.048634346
17	Ma	8	2	10/2/2023	-0.046372284
18	Mi	8	2	10/2/2023	0.074648066
19	Mi	14	2	10/2/2023	0.087240215
20	Se	8	2	10/2/2023	0.027252469
21	Ma	14	2	10/2/2023	-0.101900535
22	Pf	8	2	10/2/2023	-0.193104745
23	Mi	14	2	10/2/2023	0.007841817
24	Ma	8	2	10/2/2023	-0.359743358
25	Pf	14	1	10/2/2023	0.144093389
26	Mi	8	1	10/2/2023	0.018096501
27	Ma	14	1	10/2/2023	0.089200669
28	Se	8	1	10/2/2023	-0.029406814
29	Mi	14	1	10/2/2023	0.083319306
30	Ma	8	1	10/2/2023	0.059190638
31	Se	14	1	10/2/2023	-0.223491786
32	Mi	8	1	10/2/2023	0.296682079
33	Se	8	1	10/2/2023	0.047126304
34	Ma	14	1	10/2/2023	0.162922367
35	Mi	14	1	10/2/2023	0.057467162
36	Pf	8	1	10/2/2023	-0.191144291
37	Mi	8	2	10/2/2023	-0.077111201
38	Mi	14	2	10/2/2023	-0.102546839
39	Pf	8	2	10/2/2023	0.267677409
40	Se	8	2	10/2/2023	-0.1264493
41	Ma	14	2	10/2/2023	0.014703407
42	Pf	14	2	10/2/2023	0.059793855
43	Ma	8	2	10/2/2023	-0.007841817
44	Se	14	2	10/2/2023	-0.122528392
45	Mi	8	2	10/2/2023	-0.029622249

46	Pf	14	2	10/2/2023	-0.227714303
47	Se	8	2	10/2/2023	-0.056928576
48	Se	14	2	10/2/2023	-0.031399583
1	Ma	8	1	17/02/2023	-0.041094137
2	Se	14	1	17/02/2023	0.150954978
3	Se	8	1	17/02/2023	0.129745449
4	Pf	8	1	17/02/2023	-0.167769644
5	Pf	14	1	17/02/2023	0.040516055
6	Mi	8	1	17/02/2023	0.00867124
7	Ma	14	1	17/02/2023	0.116873235
8	Pf	8	1	17/02/2023	0.139192253
9	Pf	14	1	17/02/2023	-0.071556581
10	Mi	14	1	17/02/2023	-0.017644088
11	Ma	8	1	17/02/2023	-0.208788379
12	Se	14	1	17/02/2023	0.025485905
13	Ma	14	2	17/02/2023	0.086913472
14	Pf	8	2	17/02/2023	0.003393094
15	Pf	14	2	17/02/2023	0.054666513
16	Se	14	2	17/02/2023	-0.102923849
17	Ma	8	2	17/02/2023	-0.010782498
18	Mi	8	2	17/02/2023	0.075477489
19	Mi	14	2	17/02/2023	0.015683634
20	Se	8	2	17/02/2023	-0.091161123
21	Ma	14	2	17/02/2023	-0.113052863
22	Pf	8	2	17/02/2023	0.103904076
23	Mi	14	2	17/02/2023	-0.127429527
24	Ma	8	2	17/02/2023	0.075477489
25	Pf	14	1	17/02/2023	0.043129994
26	Mi	8	1	17/02/2023	-0.078418171
27	Ma	14	1	17/02/2023	-0.297008821
28	Se	8	1	17/02/2023	0.033327723
29	Mi	14	1	17/02/2023	0.015683634
30	Ma	8	1	17/02/2023	0.273156628
31	Se	14	1	17/02/2023	0.073894045
32	Mi	8	1	17/02/2023	-0.052932265
33	Se	8	1	17/02/2023	-0.154875887
34	Ma	14	1	17/02/2023	0.038228858
35	Mi	14	1	17/02/2023	-0.456132359
36	Pf	8	1	17/02/2023	-0.083319306
37	Mi	8	2	17/02/2023	0.067635672
38	Mi	14	2	17/02/2023	-0.011109241
39	Pf	8	2	17/02/2023	-0.015457428
40	Se	8	2	17/02/2023	-0.177747853

41	Ma	14	2	17/02/2023	-0.264007841
42	Pf	14	2	17/02/2023	-0.103904076
43	Ma	8	2	17/02/2023	-0.097268692
44	Se	14	2	17/02/2023	0.06730893
45	Mi	8	2	17/02/2023	0.156836341
46	Pf	14	2	17/02/2023	-0.24029568
47	Se	8	2	17/02/2023	-0.105257723
48	Se	14	2	17/02/2023	-0.088974463
1	Ma	8	1	24/02/2023	0.123282412
2	Se	14	1	24/02/2023	-0.068615899
3	Se	8	1	24/02/2023	0.014376665
4	Pf	8	1	24/02/2023	-0.013069695
5	Pf	14	1	24/02/2023	-0.096891682
6	Mi	8	1	24/02/2023	-0.036595146
7	Ma	14	1	24/02/2023	0.033176918
8	Pf	8	1	24/02/2023	-0.135271344
9	Pf	14	1	24/02/2023	0.024832421
10	Mi	14	1	24/02/2023	0.077111201
11	Ma	8	1	24/02/2023	0.02058477
12	Se	14	1	24/02/2023	-0.317593591
13	Ma	14	2	24/02/2023	-0.038455064
14	Pf	8	2	24/02/2023	0.1071715
15	Pf	14	2	24/02/2023	-0.090180896
16	Se	14	2	24/02/2023	-0.125469073
17	Ma	8	2	24/02/2023	-0.059793855
18	Mi	8	2	24/02/2023	-0.107824985
19	Mi	14	2	24/02/2023	0.066655445
20	Se	8	2	24/02/2023	0.068615899
21	Ma	14	2	24/02/2023	0.028753329
22	Pf	8	2	24/02/2023	0.061427567
23	Mi	14	2	24/02/2023	0.272129723
24	Ma	8	2	24/02/2023	0.072536808
25	Pf	14	1	24/02/2023	0.197679138
26	Mi	8	1	24/02/2023	-0.149157895
27	Ma	14	1	24/02/2023	-0.369872371
28	Se	8	1	24/02/2023	-0.098839569
29	Mi	14	1	24/02/2023	-0.206501183
30	Ma	8	1	24/02/2023	0.210515446
31	Se	14	1	24/02/2023	-0.123508619
32	Mi	8	1	24/02/2023	0.001960454
33	Se	8	1	24/02/2023	0.09344832
34	Ma	14	1	24/02/2023	-0.235254512
35	Mi	14	1	24/02/2023	-0.099329683

36	Pf	8	1	24/02/2023	0.025159163
37	Mi	8	2	24/02/2023	-0.271359545
38	Mi	14	2	24/02/2023	0.214366338
39	Pf	8	2	24/02/2023	0.244403298
40	Se	8	2	24/02/2023	-0.066492074
41	Ma	14	2	24/02/2023	0.236234739
42	Pf	14	2	24/02/2023	-0.246200382
43	Ma	8	2	24/02/2023	0.247740738
44	Se	14	2	24/02/2023	-0.323474954
45	Mi	8	2	24/02/2023	-0.340162154
46	Pf	14	2	24/02/2023	0.116647029
47	Se	8	2	24/02/2023	0.024832421
48	Se	14	2	24/02/2023	-0.131187065
1	Ma	8	1	3/3/2023	-0.206407828
2	Se	14	1	3/3/2023	-0.004574393
3	Se	8	1	3/3/2023	0.191144291
4	Pf	8	1	3/3/2023	-0.16075725
5	Pf	14	1	3/3/2023	0.322494727
6	Mi	8	1	3/3/2023	-0.030060299
7	Ma	14	1	3/3/2023	0.040516055
8	Pf	8	1	3/3/2023	0.182322247
9	Pf	14	1	3/3/2023	0.250284661
10	Mi	14	1	3/3/2023	-0.195391942
11	Ma	8	1	3/3/2023	-0.321677871
12	Se	14	1	3/3/2023	-0.548110338
13	Ma	14	2	3/3/2023	0.016990604
14	Pf	8	2	3/3/2023	0.075804232
15	Pf	14	2	3/3/2023	-0.180361792
16	Se	14	2	3/3/2023	0.142459677
17	Ma	8	2	3/3/2023	0.14017248
18	Mi	8	2	3/3/2023	0.138538768
19	Mi	14	2	3/3/2023	-0.016990604
20	Se	8	2	3/3/2023	0.033981207
21	Ma	14	2	3/3/2023	0.219570878
22	Pf	8	2	3/3/2023	-0.160103765
23	Mi	14	2	3/3/2023	-0.190164064
24	Ma	8	2	3/3/2023	0.350921314
25	Pf	14	1	3/3/2023	-0.07008624
26	Mi	8	1	3/3/2023	-0.184936186
27	Ma	14	1	3/3/2023	-0.925987898
28	Se	8	1	3/3/2023	-4.039189272
29	Mi	14	1	3/3/2023	-1.459558201
30	Ma	8	1	3/3/2023	0.790063069

31	Se	14	1	3/3/2023	-0.164678158
32	Mi	8	1	3/3/2023	0.291454201
33	Se	8	1	3/3/2023	0.272503143
34	Ma	14	1	3/3/2023	-0.392744338
35	Mi	14	1	3/3/2023	-0.360723585
36	Pf	8	1	3/3/2023	-0.099329683
37	Mi	8	2	3/3/2023	0
38	Mi	14	2	3/3/2023	-0.032674238
39	Pf	8	2	3/3/2023	-0.328049347
40	Se	8	2	3/3/2023	0.384575778
41	Ma	14	2	3/3/2023	2.624068035
42	Pf	14	2	3/3/2023	-0.416269789
43	Ma	8	2	3/3/2023	0.115013317
44	Se	14	2	3/3/2023	0.079071655
45	Mi	8	2	3/3/2023	0.101290137
46	Pf	14	2	3/3/2023	0.239828905
47	Se	8	2	3/3/2023	0.136578314
48	Se	14	2	3/3/2023	-0.052932265
1	Ma	8	1	10/3/2023	0.115666802
2	Se	14	1	10/3/2023	-0.126776043
3	Se	8	1	10/3/2023	0.190164064
4	Pf	8	1	10/3/2023	-0.115013317
5	Pf	14	1	10/3/2023	-0.04116954
6	Mi	8	1	10/3/2023	0.02336208
7	Ma	14	1	10/3/2023	-0.12089468
8	Pf	8	1	10/3/2023	0.007841817
9	Pf	14	1	10/3/2023	-0.059303742
10	Mi	14	1	10/3/2023	0
11	Ma	8	1	10/3/2023	-0.010782498
12	Se	14	1	10/3/2023	-0.005332005
13	Ma	14	2	10/3/2023	-0.055546204
14	Pf	8	2	10/3/2023	0.086259988
15	Pf	14	2	10/3/2023	-0.000653485
16	Se	14	2	10/3/2023	0.104230818
17	Ma	8	2	10/3/2023	0.012579582
18	Mi	8	2	10/3/2023	-0.123508619
19	Mi	14	2	10/3/2023	-0.094101805
20	Se	8	2	10/3/2023	0
21	Ma	14	2	10/3/2023	-0.139845738
22	Pf	8	2	10/3/2023	0
23	Mi	14	2	10/3/2023	0
24	Ma	8	2	10/3/2023	0
25	Pf	14	1	10/3/2023	0.071883323

26	Mi	8	1	10/3/2023	0
27	Ma	14	1	10/3/2023	-0.064694991
28	Se	8	1	10/3/2023	0
29	Mi	14	1	10/3/2023	0
30	Ma	8	1	10/3/2023	0
31	Se	14	1	10/3/2023	0
32	Mi	8	1	10/3/2023	0
33	Se	8	1	10/3/2023	0
34	Ma	14	1	10/3/2023	0
35	Mi	14	1	10/3/2023	0
36	Pf	8	1	10/3/2023	-0.004574393
37	Mi	8	2	10/3/2023	0
38	Mi	14	2	10/3/2023	0.053912492
39	Pf	8	2	10/3/2023	0
40	Se	8	2	10/3/2023	0
41	Ma	14	2	10/3/2023	0
42	Pf	14	2	10/3/2023	0
43	Ma	8	2	10/3/2023	0
44	Se	14	2	10/3/2023	0
45	Mi	8	2	10/3/2023	0
46	Pf	14	2	10/3/2023	-0.075150747
47	Se	8	2	10/3/2023	-0.035941662
48	Se	14	2	10/3/2023	9.41E-20
1	Ma	8	1	17/03/2023	0.226432468
2	Se	14	1	17/03/2023	0.237214966
3	Se	8	1	17/03/2023	-0.292924542
4	Pf	8	1	17/03/2023	-0.016337119
5	Pf	14	1	17/03/2023	-0.076457716
6	Mi	8	1	17/03/2023	-0.010782498
7	Ma	14	1	17/03/2023	0.177747853
8	Pf	8	1	17/03/2023	-0.003594166
9	Pf	14	1	17/03/2023	0.212055803
10	Mi	14	1	17/03/2023	0.274953711
11	Ma	8	1	17/03/2023	-0.057506658
12	Se	14	1	17/03/2023	0.059303742
13	Ma	14	2	17/03/2023	0.162717704
14	Pf	8	2	17/03/2023	-0.064694991
15	Pf	14	2	17/03/2023	-0.197679138
16	Se	14	2	17/03/2023	0.048521243
17	Ma	8	2	17/03/2023	-0.188693723
18	Mi	8	2	17/03/2023	0.237214966
19	Mi	14	2	17/03/2023	-0.010782498
20	Se	8	2	17/03/2023	-0.141969563

21	Ma	14	2	17/03/2023	-0.22675921
22	Pf	8	2	17/03/2023	-0.312692455
23	Mi	14	2	17/03/2023	0.145563729
24	Ma	8	2	17/03/2023	0.270846092
25	Pf	14	1	17/03/2023	-0.953737662
26	Mi	8	1	17/03/2023	-0.195882055
27	Ma	14	1	17/03/2023	-0.767354474
28	Se	8	1	17/03/2023	-0.424111606
29	Mi	14	1	17/03/2023	0.102433735
30	Ma	8	1	17/03/2023	0.244403298
31	Se	14	1	17/03/2023	-0.073166954
32	Mi	8	1	17/03/2023	-0.226105725
33	Se	8	1	17/03/2023	0
34	Ma	14	1	17/03/2023	0.42607206
35	Mi	14	1	17/03/2023	0.260577046
36	Pf	8	1	17/03/2023	-0.199476222
37	Mi	8	2	17/03/2023	0.371996197
38	Mi	14	2	17/03/2023	-0.019767914
39	Pf	8	2	17/03/2023	0.352228283
40	Se	8	2	17/03/2023	0.080378625
41	Ma	14	2	17/03/2023	-0.161737477
42	Pf	14	2	17/03/2023	0.048521243
43	Ma	8	2	17/03/2023	-0.005391249
44	Se	14	2	17/03/2023	0.035677385
45	Mi	8	2	17/03/2023	-0.048521243
46	Pf	14	2	17/03/2023	0.445676603
47	Se	8	2	17/03/2023	-1.482593538
48	Se	14	2	17/03/2023	-0.395358277
1	Ma	8	1	24/03/2023	-0.046210708
2	Se	14	1	24/03/2023	-0.117627256
3	Se	8	1	24/03/2023	0.16353456
4	Pf	8	1	24/03/2023	0.091236525
5	Pf	14	1	24/03/2023	0.067635672
6	Mi	8	1	24/03/2023	-0.210748834
7	Ma	14	1	24/03/2023	0.180361792
8	Pf	8	1	24/03/2023	0.10586453
9	Pf	14	1	24/03/2023	-0.166638613
10	Mi	14	1	24/03/2023	-0.005881363
11	Ma	8	1	24/03/2023	0.109009875
12	Se	14	1	24/03/2023	0.056853174
13	Ma	14	2	24/03/2023	-0.018473511
14	Pf	8	2	24/03/2023	0.107070964
15	Pf	14	2	24/03/2023	0.036268404

16	Se	14	2	24/03/2023	-0.159777023
17	Ma	8	2	24/03/2023	0.258779963
18	Mi	8	2	24/03/2023	0.135650787
19	Mi	14	2	24/03/2023	-0.063714764
20	Se	8	2	24/03/2023	-0.186997176
21	Ma	14	2	24/03/2023	-0.059567649
22	Pf	8	2	24/03/2023	0.001960454
23	Mi	14	2	24/03/2023	-0.032799908
24	Ma	8	2	24/03/2023	-0.448480843
25	Pf	14	1	24/03/2023	-0.071883323
26	Mi	8	1	24/03/2023	0.09214135
27	Ma	14	1	24/03/2023	0.134291117
28	Se	8	1	24/03/2023	0.523441289
29	Mi	14	1	24/03/2023	-0.488806597
30	Ma	8	1	24/03/2023	0.18820361
31	Se	14	1	24/03/2023	0.155856114
32	Mi	8	1	24/03/2023	-0.328806959
33	Se	8	1	24/03/2023	0.115666802
34	Ma	14	1	24/03/2023	0.14703407
35	Mi	14	1	24/03/2023	-0.186027721
36	Pf	8	1	24/03/2023	-0.207808152
37	Mi	8	2	24/03/2023	0.329356317
38	Mi	14	2	24/03/2023	0.172519975
39	Pf	8	2	24/03/2023	-0.069596126
40	Se	8	2	24/03/2023	0.221531332
41	Ma	14	2	24/03/2023	0.377387446
42	Pf	14	2	24/03/2023	0.056853174
43	Ma	8	2	24/03/2023	0.012742953
44	Se	14	2	24/03/2023	-0.129389982
45	Mi	8	2	24/03/2023	0.024505678
46	Pf	14	2	24/03/2023	0.352228283
47	Se	8	2	24/03/2023	0.500616
48	Se	14	2	24/03/2023	0.282305414
12	Se	14	1	31/03/2023	-0.162064219
24	Ma	8	2	31/03/2023	0.405160548
25	Pf	14	1	31/03/2023	0.086259988
26	Mi	8	1	31/03/2023	0.484885688
27	Ma	14	1	31/03/2023	0.024832421
28	Se	8	1	31/03/2023	-0.103904076
29	Mi	14	1	31/03/2023	0
30	Ma	8	1	31/03/2023	0
31	Se	14	1	31/03/2023	0.271196173
32	Mi	8	1	31/03/2023	-0.149974751

33	Se	8	1	31/03/2023	-0.149648009
34	Ma	14	1	31/03/2023	-0.046070675
35	Mi	14	1	31/03/2023	-0.01372318
36	Pf	8	1	31/03/2023	0.01372318
37	Mi	8	2	31/03/2023	0.260891222
38	Mi	14	2	31/03/2023	-0.331316771
39	Pf	8	2	31/03/2023	0.158796796
40	Se	8	2	31/03/2023	0
41	Ma	14	2	31/03/2023	0.069922869
42	Pf	14	2	31/03/2023	0.049664841
43	Ma	8	2	31/03/2023	0.148994524
44	Se	14	2	31/03/2023	-0.169579294
45	Mi	8	2	31/03/2023	0.14703407
46	Pf	14	2	31/03/2023	0.129389982
47	Se	8	2	31/03/2023	0.107824985
48	Se	14	2	31/03/2023	-0.049664841
1	Ma	8	1	17/04/2023	-0.168599067
2	Se	14	1	17/04/2023	0.181668762
3	Se	8	1	17/04/2023	0.058813628
4	Pf	8	1	17/04/2023	-0.849856924
5	Pf	14	1	17/04/2023	0
6	Mi	8	1	17/04/2023	-0.168599067
7	Ma	14	1	17/04/2023	-0.021564997
8	Pf	8	1	17/04/2023	0.008495302
9	Pf	14	1	17/04/2023	-0.579640978
10	Mi	14	1	17/04/2023	0.085368202
11	Ma	8	1	17/04/2023	-0.140499222
12	Se	14	1	17/04/2023	-0.091161123
13	Ma	14	2	17/04/2023	0.214996484
14	Pf	8	2	17/04/2023	-0.17448043
15	Pf	14	2	17/04/2023	0.071556581
16	Se	14	2	17/04/2023	-0.60185946
17	Ma	8	2	17/04/2023	0
18	Mi	8	2	17/04/2023	0.176440884
19	Mi	14	2	17/04/2023	-0.275770567
20	Se	8	2	17/04/2023	-0.085279761
21	Ma	14	2	17/04/2023	-0.01372318
22	Pf	8	2	17/04/2023	-0.202171846
23	Mi	14	2	17/04/2023	0.030914856
24	Ma	8	2	17/04/2023	0.066655445
33	Se	8	1	17/04/2023	0.131350436
34	Ma	14	1	17/04/2023	0.152915433
35	Mi	14	1	17/04/2023	-0.198659366

36	Pf	8	1	17/04/2023	-0.013069695
45	Mi	8	2	17/04/2023	0.018951058
46	Pf	14	2	17/04/2023	-0.345693436
47	Se	8	2	17/04/2023	-0.071556581
48	Se	14	2	17/04/2023	-0.238521936